Master's Thesis

The Function of HSF2 in Epithelial-Mesenchymal Transition

Jenny Pessa, 38845

jpessa@abo.fi

Instructors:

Prof. Lea Sistonen

M.Sc. Mikael Puustinen

Study Program in Cell Biology

Faculty of Science and Engineering

Åbo Akademi University

2020

Åbo Akademi University / Åbo Akademi
Faculty of Science and Engineering / Fakulteten för naturvetenskaper och teknik
Jenny Pessa, 2020 **Matriculation number: 38845**

The Function of HSF2 in Epithelial-Mesenchymal Transition
Master's Thesis, 104 p.
Keywords: HSF2, EMT, TGFβ signaling pathway, cancer, cell invasion

Funktionen av HSF2 i Epitel-Mesenkymal Övergång
Pro gradu-avhandling, 104 s.
Nyckelord: HSF2, EMT, TGFβ-signalräckan, cancer, cellinvasion

---

In western society, cancer is amongst the leading cause of death with millions of new cases diagnosed annually. A key force driving carcinogenesis is metastasis, which is achieved by a mechanism inducing cellular motility called epithelial-mesenchymal transition (EMT). During normal conditions, EMT is an important cellular program required for embryonal development and wound healing, but unfortunately in cancer, this process is subverted in order to improve the invasion capacity of the cancerous cells. One of the main inducers of EMT is the transforming growth factor beta (TGFβ) signaling pathway, and sustained activation of this pathway has previously been linked to cancer progression. In the field of cancer research, one key topic involves characterizing the crosstalk between different signaling pathways, which together can relay a survival advantage to the cell. One important survival pathway, that counteracts proteotoxic stress, is called the heat shock response (HSR). A key regulatory protein in this pathway is the transcription factor HSF2, which can be active in normal and pathological conditions. Unpublished results from the Sistonen laboratory have shown that the TGFβ signaling pathway can reduce the expression of HSF2 in breast cancer cells, which might be important for the progression of EMT. First, luciferase assay was used to determine which part of the HSF2 promoter regulates HSF2 expression during EMT. Second, wound healing assay was used to elucidate whether HSF2 influences cellular invasion capacity upon EMT. Finally, western blot was utilized to establish if HSF1 impacts HSF2 protein expression during EMT. The results revealed that the 5'UTR of HSF2 is required for the downregulation of HSF2 during EMT, and it is likely that HSF2 inhibits the cellular invasion capacity both during control conditions and upon EMT stimuli. Also, the gene expression of HSF2 during EMT was shown not to be affected by HSF1, another HSF family member, which has previously been indicated to affect the expression of HSF2. Taken together, the results from my thesis provide the first evidence that HSF2 exhibits a functional role in EMT and cell invasion, thus raising the possibility that HSF2 displays a tumor-suppressing function in breast cancer development.

I västvärlden är cancer fortfarande den främsta dödsorsaken och flera miljoner nya cancerfall diagnostiseras årligen. Epitel-mesenkymal övergång (EMT) är ett av de huvudsakliga process som bidrar till cancercellernas förmåga att metastasera. EMT är en normal cellulär process som sker vid embryonalutveckling och sårläkning. Vid EMT erhåller cellerna distinkta egenskaper som främjar cellvandring genom förändringar i signalräckor som styr cellrörelser. En av de huvudsakliga signalräckorna som styr EMT är transformerande tillväxtfaktor beta (TGFβ), och ökad aktivering av denna signalräcka har tidigare anknutits till cancerutveckling. Ett nyckeltema inom cancerforskning involverar karakterisering av samverkan mellan de olika signalräckorna som tillsammans kan stöda cellens överlevnadsförmåga. En av dessa signalräckor är värmechockresponsen (HSR), som regleras av värmechockfaktorer så som HSF2. HSF2 har tidigare visats kunna hämma cancerformation och opublicerade resultat från Sistonens laboratorium har visat att uttrycket av HSF2 påverkas av TGFβ-signalräckan, därmed är det möjligt att HSF2 har en viktig roll i EMT och cancerutveckling. I denna studie undersöktes HSF2s funktion vid EMT. Detta gjordes genom att utreda vilken del av HSF2-promotorn reglerar HSF2-genuttrycket vid EMT. För detta ändamål utnyttjades kloning- och luciferasmetoder för att bestämma HSF2 promotoraktiviteten. Därtill studerades hur HSF2 påverkar cellernas invasionsförmåga vid EMT genom att mäta cellernas migrationshastighet och slutligen användes western blot för att bestämma om HSF1 kan styra uttrycket av HSF2 vid EMT. Resultaten visade att 5'UTR av HSF2 är viktig för nedregleringen av HSF2-genuttrycket vid EMT och att HSF2 kan hämma migrationsförmågan i cellerna under EMT. Dessutom bekräftades att genuttrycket av HSF2 inte styrs av HSF1 vid EMT. Sammanlagt ger min avhandling de första bevisen på att HSF2 uppvisar en viktigt regulatorisk funktion under EMT och cellinvasion, samt antyder att HSF2 kan ha en tumörhämmande effekt i bröstcancerutvecklingen.

Table of Contents

Forewords

I would like to pay my special regards to Lea Sistonen for giving me the opportunity to accomplish my master's thesis study in an inspirational environment. I would also like to thank all the other members of Sistonen laboratory, who have helped me during the practical work of this thesis, especially Alejandro, who kindly assisted me with the wound healing assays and the statistical analysis. Foremost I wish to express my deepest gratitude to Mikael for being a supreme practical instructor, for his patience, and the excessive amount of work and time he has spent helping me out both during the practical work and the writing process. Finally, I wish to acknowledge the support of my family, especially my mother, and my dearest friends who kept me going during the most stressful times of my studies.

Abbreviations

AFT1	Activating transcription factor 1
Ago	Argonaute
AKT	Alpha serine/threonine-protein kinase
APC/C	E3-ubiquityn ligase anaphase-promoting complex/cyclosome
ATP	Adenosine triphosphate
BMP	Bone morphogenetic protein
BSA	Bovine serum albumin
CAF	Cancer-associated fibroblast
CMV	Cytomegalovirus
CRC	Colorectal cancer
CSC	Cancer stem cell
DBD	DNA-binding domain
DMEM	Dulbecco's Modified Eagle Medium
E-cadherin	Epithelial cadherin
ECL	Enhanced chemiluminescence
ECM	Extracellular matrix
EMT	Epithelial-mesenchymal transition
EMT-TF	Epithelial-mesenchymal transition-involved transcription factor
ER	Estrogen receptor
ESCC	Esophageal squamous cell carcinoma
FBS	Fetal bovine serum
HCC	Hepatocellular carcinoma
HER2	Human epidermal growth factor receptor 2
HIF-1α	Hypoxia-inducible factor-1-aplha
HR-A	Heptad repeat A
HR-B	Heptad repeat B
HR-C	Heptad repeat C
HRP	Horseradish peroxidase
HSE	Heat shock element
HSF	Heat shock factor

HSF1-CaSig	HSF1 cancer signature
HSP	Heat shock protein
HSR	Heat shock response
LGL	Lethal giant larvae protein
LIF	Leukemia inhibitory factor
MET	Mesenchymal-epithelial transition
miR	MicroRNA
MM	Multiple myeloma
MMP	Matrix metalloproteinase
NaN_3	Sodium azide
N-cadherin	Neural cadherin
ONPG	O-nitrophenyl-β-D-galactopyranoside
PATJ	PALS1-associated tight junction protein
PBS	Phosphate-buffered saline
PCR	Polymerase chain reaction
P_i	Inorganic phosphate
pI	Isoelectric point
PI3K	Phosphoinositide 3-kinase
Pol II	RNA polymerase II
PR	Progesterone receptor
PTM	Post-translational modification
RD	Regulatory domain
RISC	RNA-induced silencing complex
RNAi	RNA interference
Scr	Scrambled control shRNA
SDS	Sodium dodecyl sulphate
SDS-PAGE	Sodium dodecyl sulphate polyacrylamide gel electrophoresis
shRNA	Short hairpin RNA
siRNA	Small interfering RNA
SOC	Super optimal broth with catabolite repression medium
T4 PNK	T4 polynucleotide kinase
TAD	Transactivation domain
TBE	Tris-Borate-EDTA

TF	Transcription factor
TGFβ	Transforming growth factor beta
TGFβR1	Transforming growth factor beta receptor type 1
TGFβR2	Transforming growth factor beta receptor type 2
UTR	Untranslated region
VEGF	Vascular endothelial growth factor
XV	StemXvivo
ZEB	Zinc-finger E-box-binding homeobox factor

1 Introduction

The cells that build up a multicellular organism maintain a complex signaling network to maintain intracellular homeostasis. This network is modulated in response to both extracellular and intracellular cues that help the cell to adjust to changes in the environment. Although cells have coping mechanisms that protect them against various stresses, some of the cells may occasionally break free from the normally strictly controlled signaling networks and begin to divide uncontrollably. Malignant transformation is enabled by a variety of mechanisms including accumulation of mutations in genes regulating the activities of key signaling pathways. An important process contributing to the migration capacity of cells is epithelial-mesenchymal transition (EMT). This cellular program is normally involved in developmental processes, tissue establishment, and wound healing, however, it can also be hijacked by cancer cells to improve their invasion abilities and allow metastasis. One of the essential pathways that induce EMT is the transforming growth factor β (TGFβ) signaling pathway. The activity of this pathway is downregulated in the early stages of cancer, but is shifted to an increased activity as the cancer progression proceeds. The TGFβ signaling pathway has also been shown to modulate the activity of a transcription factor called heat shock factor 2 (HSF2). HSF2 belongs to the family of heat shock factors (HSFs), which are the key factors modulating the activity of a pathway that is activated in response to proteotoxic stress. The heat shock response (HSR) is one of the major pathways that HSFs induce, however, they are also involved in modulating developmental processes and pathologies such as cancer.

An impaired function of HSFs has been linked to the formation of numerous types of cancers. Recently, HSF2 was discovered to function as a tumor suppressor in prostate cancer and the disease progression was correlated with a decreased expression of HSF2. Additionally, unpublished results from the Sistonen laboratory have indicated that HSF2 expression is modulated by TGFβ signaling. Owing to these discoveries, the main objective of this thesis was to elucidate what regulates HSF2 expression upon EMT and to determine whether the expression of HSF2 impacts cellular invasion capacity during EMT.

2 Overview of Literature

2.1 Epithelial-mesenchymal transition

The capability of cancer cells to invade new tissues and metastasize largely depends on their ability to enhance cellular motility, which is modulated by multiple signaling pathways. Epithelial-mesenchymal transition (EMT) is one of the key processes contributing to the migratory capacity of epithelial cells, and under normal physiological conditions this process is required for cell motility during embryonal development and wound healing of damaged tissues. The EMT process is guided by alterations in several molecular mechanisms, which together allow for a phenotypic switch.

2.1.1 Cellular changes during EMT

EMT is a process where epithelial cells transiently gain a mesenchymal state, and it generally occurs during embryogenesis, tissue morphogenesis, and wound healing (Nieto, 2009; Kalluri & Weinberg, 2009; Thiery et al. 2009; Nieto et al. 2016). Epithelial cells form cell sheets that line the mammalian internal cavities such as the digestive tract. In order to establish a cell sheet, these cells are nonmotile, they display an apical-basal polarity, and are connected to adjacent cells as well as to the underlying basement membrane via junctions consisting of multiprotein adhesion complexes and cytoskeletal components. The epithelial cell polarity is generated by distinct basal, lateral, and apical plasma membrane regions, each displaying a unique set of proteins that convey the distinctive features for each region (Lee & Streuli, 2014). The mechanism contributing to epithelial cell polarity remains unknown. However, it has been suggested that it could be maintained by a positive feedback loop created by the activity of polarity-involved proteins or by directed exocytosis guided by apical and basal determinants (Klunder et al. 2017). In order to enable the formation of a sheet, epithelial cells are connected to each other at the lateral sides and to the underlying basement membrane at the basal side. Several cell-cell junctions are displayed between adjacent epithelial cells including tight junctions, which are indispensable in forming a continuous cell sheet without gaps thus preventing leakage of molecules. Other important junctions include adherens junctions, which connect the neighboring cells together via actin bundles, desmosomes, which connect the neighboring cells via intermediate filaments, and gap junctions, which enable diffusion of small ions and

molecules between the adjacent cells maintaining a similar intracellular ion concentration (Lampe & Lau, 2004). Additionally, hemidesmosomes attach the epithelial cells at their basal region to the underlying basement membrane via intermediate filaments. These junctional complexes together with the apical-basal polarity maintain the integrity of the epithelial cell sheet, however, this integrity is lost when the cells are predisposed to signals inducing EMT, which is followed by major alterations in these integrity-maintaining features.

During EMT, the epithelial cell morphology is lost and a mesenchymal morphology is adopted by the cells. Mesenchymal cells display a spindle-shaped morphology, front-to-back polarity, heavily rearranged cytoskeleton accompanied by stress fiber formation, and an enhanced migratory ability since they are not connected to adjacent cells or to the underlying basement membrane via junctions (Dongre & Weinberg, 2019). The front-to-back polarity enables cellular movement in one direction as a so-called leading edge, usually defined by the formation of membrane protrusions such as lamellipodia or filopodia (Figure 1), which are generated by actin polymerization that extends the protruding front end of the cell in the direction of movement also allowing attachment to nearby a surface (Trepat et al. 2012). At the back end of mesenchymal cells, previously formed adhesions are disrupted and the contraction of stress fibers pulls the rear forward allowing movement. Stress fibers are filament bundles comprised of actin filaments and non-muscle myosin II displaying contractile activity important in morphogenesis and cell adhesion (Kreis & Birchmeier, 1980). Additionally, the induction of EMT results in the disruption of cell-cell and cell-matrix junctions, mainly guided by the alterations in the gene expression pattern, which is a prerequisite to acquire the ability of cellular motility featured by mesenchymal cells. The secretion of proteins that disrupt the underlying membrane and the surrounding extracellular matrix (ECM), such as matrix metalloproteinases (MMPs), serves to further increase cellular motility (Miyoshi et al. 2004; Miyoshi et al. 2005). The ECM is a 3D network rich in glycoproteins and collagen providing structural support for the surrounding cells. MMPs are zinc-containing proteinases that mainly operate to degrade the ECM and ECM-involved proteins, but can additionally degrade a large set of other molecules (Verma & Hansch, 2007). Together these features obtained via EMT account for the mesenchymal state morphology, however the mesenchymal cell still maintain the capacity to return to an epithelial state.

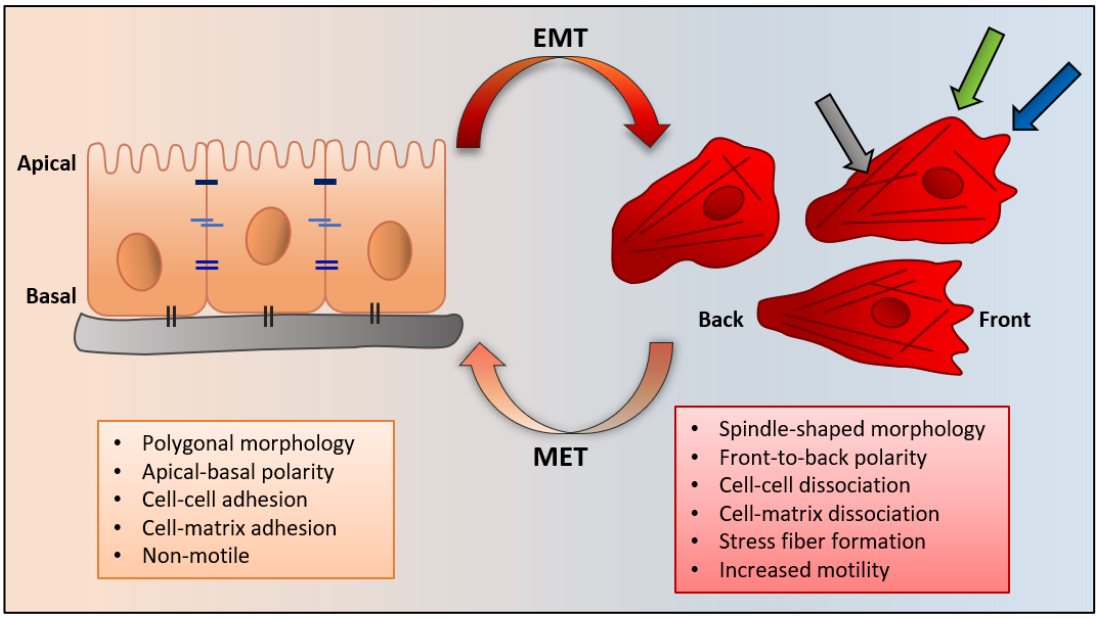

Figure 1. The morphology and characteristic features of epithelial and mesenchymal cells. Epithelial cells (left) display a polygonal morphology, an apical-basal polarity and are attached to adjacent cells as well as to the underlying basement membrane (grey) via junctional adhesion complexes indicated as blue lines between cells and black lines between cells and basement membrane, respectively, enabling the formation of an intact cell sheet. Induction of EMT results in the switch to a mesenchymal cell state (right) that displays a spindle-shaped morphology and an improved motility due to the disruption of cell-cell and cell-matrix adhesions. Mesenchymal cells also display a front-to-back polarity and stress fibers (indicated as a grey arrow), that together enable directional cell movement, which is typically characterized by the formation of lamellipodia and filopodia indicated as a green and blue arrow, respectively. The mesenchymal cells can switch back to the epithelial cell state via the reverse process, mesenchymal-epithelial transition (MET).

Mesenchymal cells are in some cases capable to transit back to an epithelial state through the reverse process called mesenchymal-epithelial transition (MET). MET is utilized by cells especially during developmental stages to generate epithelial tissue via re-establishment of epithelial features (Pei et al. 2019), and is thought to occur directly as a consequence of the shutdown of EMT-involved transcription factors (EMT-TFs), that promote the transition back to the epithelial state (Tsai et al. 2012, Ocana et al. 2012; Schmidt et al. 2015, Beerling et al. 2016). Importantly, MET has also been proposed as an essential mechanism driving the final steps of the so-called invasion-metastasis cascade that promotes the attachment of cancer cells to distantly located tissues, which subsequently advances the formation of new cancer colonies (Nieto et al. 2016; Pattabiraman et al. 2016). Although the process has been identified, no MET-inducing TFs or proteins have been identified to this date.

2.2 The function of EMT during development and wound healing

The EMT program was first identified when profound alterations in the morphology and cellular movement of cultured epithelial cells were observed by Greenburg and Hay in 1982 (Greenburg & Hay, 1982). Since then, further research has been able to identify that EMT contributes to the regulation of many developmental events including gastrulation, where EMT is used to acquire mesenchymal cells to form the mesodermal layer (Oda et al. 1998; Lim & Thiery, 2012; Schafer et al. 2014), and neural crest cell activation, where the improved cellular migration capacity enables the dispersion of these cells throughout the developing embryo (Shoval et al. 2007; Clay & Halloran, 2014; Simoes-Costa & Bronner, 2015). Furthermore, EMT has also been shown to facilitate neural crest development and palatal fusion in the developing mouse embryo via SNAI1 and SNAI2-induced suppression of E-cadherin expression (Aybar et al. 2003; Martinez-Alvarez et al. 2004). EMT is also important for tissue regeneration and wound healing. These processes are facilitated by EMT to allow cells to migrate to the damaged location, enhance proliferation, and following these events, revert back to re-establish the integrity of the epithelial sheet (et al. 2016). One of the TFs regulating EMT that plays an essential role in this process is SNAI2, whose increased expression was demonstrated to result in degradation of desmosomal junctions in human keratinocytes (Savagner et al. 2005).

2.3 EMT in cancer progression and invasion

Early-stage neoplastic cells display an epithelial-like state but during cancer progression, a more-mesenchymal state is gradually adopted. Cancer cells actively undergoing EMT have been implicated to facilitate acquisition of a cancer stem cell (CSC) state and to acquire an increased therapeutic drug resistance. The mechanistical regulation of EMT in cancer progression is still poorly understood, but the importance cannot be undermined as it can plausibly be an integral component in the evolution of all types of malignant carcinomas (Blanco et al. 2002; Gravdal et al. 2007; Prudkin et al. 2009; Rhim et al. 2012; Zhou et al. 2014; Yan et al. 2015; Ye et al. 2015; Mahmood et al. 2017; Roth et al. 2017). The course of events leading to distant metastatic colony-formation is commonly known as the invasion-metastasis cascade. Numerous attempts trying to unravel the most prominently mutated driver genes have consistently failed, though the accessibility of genome-wide sequencing and comprehensive

bioinformatics analyses. This implies that some of the steps involved in the invasion-metastasis cascade might be driven by non-genetic processes, such as EMT (Vogelstein et al. 1989). For instance, it is known that metastasizing carcinoma cells typically display expression patterns that closely resemble those of activated EMT programs. It has been reported that expression of a transcription factor called zinc-finger E-box-binding homeobox factor-1 (ZEB1) is necessary for enabling metastasis in pancreatic adenocarcinoma in a mouse model (Ye et al. 2015), and that SNAI1 is required for dissemination of mouse carcinoma cells (Krebs et al. 2017). The importance of SNAI2 was demonstrated in a further study, where non-metastatic cells obtained increased metastatic abilities in response to induced SNAI2 expression (Guo et al. 2012). These studies provide evidence that the primary carcinoma can evolve invasion and metastasis capabilities via expression of EMT-TFs orchestrating the induction of EMT (Guo et al. 2012), implying that at least a transient expression of EMT is indispensable for metastatic progression of carcinoma cells.

2.4 EMT-inducing transcription factors

The observed alterations in the cellular appearance after an EMT induction are a direct consequence of major modifications in the gene expression pattern affecting cellular attachment, organization of cytoskeletal components, and the expressed polarity. The gene expression pattern is altered so that epithelial-state maintaining genes are suppressed and mesenchymal-state maintaining genes are instead induced (Figure 2). These alterations in gene expression are modulated by associated transcription factors (EMT-TFs) regulating the activity of EMT-involved genes.

The gene expression pattern characteristic of epithelial cells includes several genes encoding proteins that are important for the formation of junctional cell-cell and cell-matrix complexes and genes that are responsible for maintaining the apical-basal polarity. Probably the most important epithelial marker is epithelial cadherin (E-cadherin), which is a calcium-dependent cell adhesion molecule that belongs to the family of classical cadherins and is essential in the establishment of adherens junctions (Brüser & Bogdan, 2017). The loss of E-cadherin expression is seen as one of the key identifiers of induced EMT. Other important epithelial markers, whose downregulation implies an activated EMT process, are for instance occludins and claudins, which together enable the assembly of tight junctions (González-Mariscal et

al. 2003). The tight junction assembly is assisted by PALS1-associated tight junction protein (PATJ) and lethal giant larvae (LGL) protein, that are also important in maintaining the apical-basal polarity in epithelial cells (Aigner et al. 2007; Spaderna et al. 2008). When EMT is activated, the expression of these and many other epithelial state-involved genes are repressed by the action of EMT-TFs such as the zinc-finger E-box-binding homeobox factors ZEB1 and ZEB2, SNAI1 (Snail), SNAI2 (Slug), and the helix-loop-helix factors TWIST1 and TWIST2 (Dongre & Weinberg, 2019). ZEB1 and ZEB2 affect E-cadherin expression by binding to E-box elements located in the promoter region of the E-cadherin gene, *CDH1* (Hill et al. 2013), and by recruiting histone deacetylases, which result in chromatin condensation leading to the transcriptional repression of E-cadherin and thereby the induction of EMT (Singh and Settleman, 2010; Hanrahan et al. 2017). SNAI1, SNAI2, TWIST1, and TWIST2 inhibit E-cadherin expression in much the same way as ZEB transcription factors via repressing the transcriptional activity by binding to the E-box elements in the promoter region (Batlle et al. 2000; Cano et al. 2000; Herranz et al. 2008). ZEB1 and SNAI1 also repress the expression of the apical-basal polarity-maintaining genes (Aigner et al. 2007; Spaderna et al. 2008), inducing the disruption of the epithelial cell sheet integrity. Moreover, SNAI1 and ZEB2 have been shown to induce the expression of MMPs, which, as previously described, are proteinases that function to degrade the ECM and related proteins thereby promoting the invasion capacity of cells (Miyoshi et al. 2004; Miyoshi et al. 2005).

The EMT induction by transcriptional repression of epithelial state-associated genes is not the only function of the EMT-TFs, but they simultaneously induce the transcription of mesenchymal state-involved genes (Figure 2). Thus, EMT-TFs display a dual function in inducing the EMT program. For instance, neural cadherin (N-cadherin) and vimentin expression is upregulated when the EMT program is activated serving as markers indicating the mesenchymal state (Jennbacken et al. 2010; Wang et al. 2016; Loh et al. 2019). N-cadherin is a transmembrane cell adhesion molecule that belongs to the same protein superfamily as E-cadherin (Shapiro et al. 1995). It is generally accepted that a switch in cadherin expression, downregulation of E-cadherin and upregulation of N-cadherin, is associated with EMT and an improved cellular invasion capacity, however, the underlying mechanism remains unclear. N-cadherin expression is frequently induced during EMT and is thereby seen as one of

the most important identifiers of the mesenchymal state (Jennbacken et al. 2010; Wang et al. 2016; Loh et al. 2019). Whereas vimentin is a dynamic protein that belongs to type the III intermediate filament family proteins, providing structural support to the cell and it is also typically expressed in mesenchymal cells (Liu et al. 2015), functioning as an additional example of a marker of EMT. The function of the addressed EMT-TFs, among others, guide the phenotypic changes from the epithelial characteristics to mesenchymal ones, and the activation of these EMT-TFs is in turn modulated by several signaling pathways.

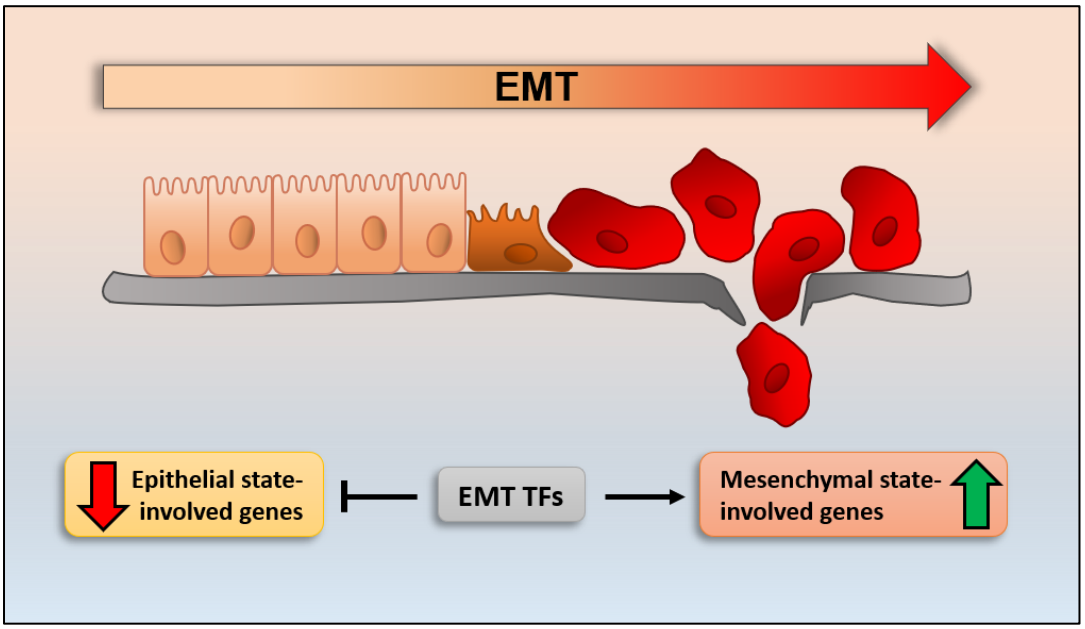

Figure 2. Epithelial-mesenchymal transition. The activation of the EMT process is modulated by transcription factors (EMT-TFs) that regulate the expression of genes involved in EMT. The advancement of EMT is indicated by the switch from an epithelial state-expressing cell (light orange), which is attached to the underlying basement membrane (grey), to the motile mesenchymal state-expressing cell (red) via an intermediate state (brown), displaying partly epithelial and partly mesenchymal features. The mesenchymal cells have acquired a high invasion capacity and are able to invade through the basement membrane.

2.5 Signaling pathways regulating EMT

Multiple intracellular signaling pathways can stimulate the induction of EMT. These pathways are activated by the epithelial cells in response to signaling molecules released by the surrounding microenvironment. Ligand binding to the cognate receptors displayed on the cell surface of epithelial cells trigger a cascade of signaling events that eventually culminate in the activation of the EMT process. The main mechanism of action, in which a certain signaling pathway induces EMT, involves the activation of the major EMT-TFs, which together facilitate acquirement of the

mesenchymal state. TGFβ (Xu et al. 2009), NOTCH (Timmerman et al. 2004), and WNT (Savagner, 2001) are known to be important pathways involved in activating EMT by inducing the expression of EMT-TFs, and the functions of these pathways have also been implicated to regulate EMT during cancer progression (Bierie & Moses, 2006; Su et al. 2012; Liu et al. 2013; Yuan et al. 2014; Ma et al. 2017; Tang et al. 2017; Ramachandran et al. 2018; Zhang et al. 2018).

2.5.1 TGFβ signaling pathway

One of the key signaling pathways activating the EMT process is called transforming growth factor beta (TGFβ) signaling pathway (Bierie et al. 2006; Xu et al. 2009; Lamouille et al. 2014). The TGFβ signaling pathway is involved in several cellular processes including cell differentiation, proliferation, apoptosis, production of the extracellular matrix (ECM), secretion of cytokines, and cancer cell motility (Moses et al. 1990; Heldin et al. 2012, Loomans & Andl, 2014). The pathway activation is mediated by ligand binding to its reciprocal receptor complex constituted of TGFβ receptor type 1 (TGFβR1) and TGFβ receptor type 2 (TGFβR2). One way to induce the pathway is by the so-called canonical pathway mechanism, which relies on SMAD protein activation. The signaling pathway induction is initiated by ligand-binding to its cognate receptor displayed on the cell surface. Multiple ligands belong to the TGFβ ligand family including three types of TGFβ isoforms, multiple bone morphogenetic proteins (BMPs), and two activins (Dongre & Weinberg, 2019). Ligand-binding to the receptor monomer causes TGFβR2 to phosphorylate and activate TGFβR1, which in turn phosphorylates proteins of the R-SMAD family, usually SMAD2 and SMAD3 proteins. Activated R-SMADs form heterotrimers with SMAD4 proteins and the complex is translocated to the nucleus where it functions as a target gene transcription regulator, inducing for example the EMT process (Figure 3) (Cantelli et al. 2017). The transcriptional regulation of genes is orchestrated in cooperation with other transcription factors, co-activators, co-factors, and adaptors, enabling a large set of biological responses to be yielded from a single pathway.

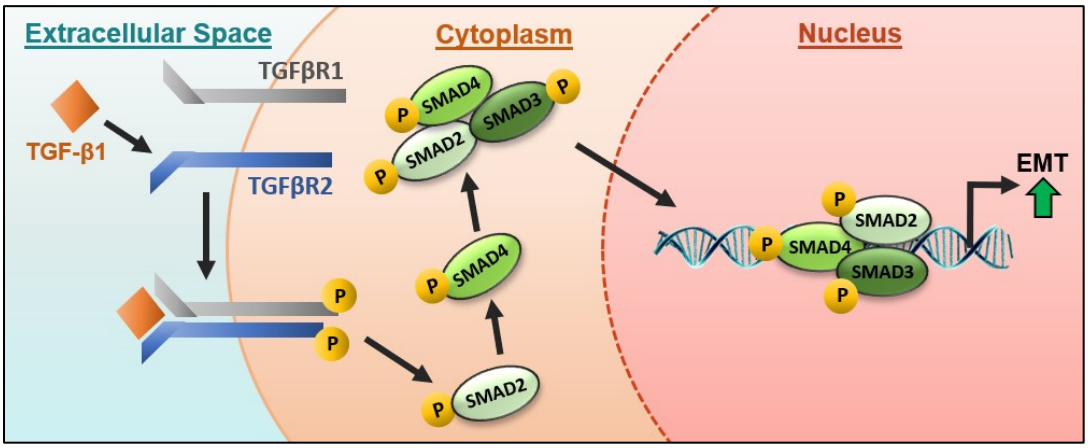

Figure 3. The transforming growth factor-β signaling pathway. The TGFβ signaling pathway is activated by the TGFβ-1 ligand (orange) binding to the TGFβR2 receptor monomer (blue). This binding initiates receptor dimerization, phosphorylation, and activation. The activated receptor dimer phosphorylates proteins of the R-SMAD family (SMAD2 and SMAD3), which stimulates complex formation with SMAD4 proteins. The formed SMAD-complex is subsequently translocated to the nucleus where it binds to DNA and functions as a transcriptional regulator of target gene activity, for instance, stimulating the transcription of EMT-inducing genes.

2.5.2 Other signaling pathways involved in modulating EMT

As described previously for the TFs, the regulation of EMT is not based on the induction of a single component but rather on the interplay between associated signaling pathways that together modulate the initiation as well as the magnitude of EMT-TF expression. An additional pathway modulating the induction of EMT is the WNT signaling pathway, which is activated when one of its 19 identified ligands bind to the cell surface receptors of the Frizzled family. The binding event induces a series of events that eventually lead to the translocation of β-catenin to the nucleus. β-catenin is a transcriptional co-factor that stimulates the transcription of its target genes that are generally involved in cell fate determination, differentiation, proliferation, and tumorigenesis (Clevers, 2006; Lamouille et al. 2014). During the epithelial cell state, β-catenin is sequestered at the cell membrane in adherens junctions, but the disruption of junctional complexes in response to stimulated EMT frees the bound β-catenin and allows it to be directly used for the WNT signaling pathway, which in turn stimulates further advancement of EMT (Balsamo et al. 1998). Additionally, active WNT signaling directly induces the gene transcription of EMT-TFs including ZEB1, TWIST, and SNAI2 by the β-catenin molecule directly binding to their promoter regions and thereby inducing the gene expression (Sanchez-Tillo et al. 2010). The WNT pathway is seen as one of the key activators of the EMT process as the absence

of the WNT ligand has been shown to significantly disrupt the function of the developmental EMT process by for instance impairing mesoderm, and neural crest cell formation (Liu et al. 1999; Garcia-Castro et al. 2002). In addition, WNT signaling has also been implicated to have a role in cancer progression via stimulating EMT and cancer stem cell formation in several carcinomas (Derynck et al. 2014; Gonzalez & Medici, 2014; Batlle & Clevers, 2017; de Sousa et al. 2017; Tammela et al. 2017).

Another signaling pathway, involved in modulating cell fate, proliferation, and differentiation (Kopan, 2002; Osborne & Minter, 2007; Bray, 2016), implicated in the modulation of EMT is NOTCH. The key components in this pathway are the Delta-like or Jagged ligands, which bind to the NOTCH receptors 1-4 (NOTCH1-4) inducing a series of proteolytic cleavages that result in the generation of the functional NOTCH ligand that translocates to the nucleus and regulates target gene transcription by associating with transcriptional activators and binding partners (Kopan, 2002; Osborne & Minter, 2007). The NOTCH pathway has been implicated in EMT activation especially during developmental stages, as NOTCH has been shown to be expressed in the same embryonic regions as EMT is actively expressed, and cells with abolished NOTCH1 have been shown both to fail SNAI1 expression and fail to induce EMT (Timmerman et al. 2004). Furthermore, NOTCH has been shown to cooperate with the TGFβ signaling pathway in order to induce EMT. The interplay between these two pathways have been demonstrated to rely on SMAD proteins, which associate with the active NOTCH ligand and together induce the expression of multiple target genes including those that support adopting the mesenchymal state (Blokziil et al. 2003; Zavadil et al. 2004; Derynck et al. 2014). Also, as for the previously discussed signaling pathways, NOTCH signaling has been indicated to modulate the EMT process in several types of carcinomas (Yuan et al. 2014; Tang et al. 2017). In these cases, NOTCH signaling is abnormally overexpressed causing a continuous EMT stimulation and thereby predisposing the cells to malignant transformation (Natsuizaka et al. 2017).

2.5.3 The TGFβ signaling pathway in cancer

Since the TGFβ pathway is a signaling cascade involved in various fundamental biological processes, its malfunction is inevitably to cause serious diseases such as cancer. The TGFβ pathway has been proposed to display a dual role in tumor

progression functioning as a suppressor in early stage tumorigenesis (Massagué, 2012; Derynck & Miyazono, 2017) and as an inducer during the later stages as the tumor progression advances (Derynck et al. 2001; Massagué, 2008). During the more advanced stages of tumor progression, TGFβ signaling is usually impaired by mutations or deletions in the reciprocal receptors or the SMAD proteins, which are the key proteins in the so-called canonical TGFβ signaling pathway (Massagué, 2008; Derynck & Miyazono, 2017). However, some types of cancers, especially carcinomas, tend to sustain functional TGFβ signaling which is instead hijacked by the cancer cells in order to promote EMT and allow an increased invasion capacity and result in metastatic dissemination (Massagué, 2008; Derynck & Miyazono, 2017).

The interplay between TGFβ signaling and EMT appears to be a crucial cornerstone in cancer progression and have been extensively studied during the recent years. Research regarding TGFβ-induced EMT in cancer has revealed a clear correlation between these two phenomena in several types of cancers including epithelial, lung, liver, prostate, and breast cancers (Franco et al. 2010; Mise et al. 2012; Shiota et al. 2012; Bertran et al. 2013; Pu et al. 2014; Salvo et al. 2014; Thakur et al. 2014; Parvani et al. 2015; Bae et al. 2016; Cantelli et al. 2017). For instance in breast and lung cancer, TGFβ signaling has been shown to modulate integrin expression leading to improved migratory abilities of cells, dissemination, and metastasis (Mise et al. 2012; Salvo et al. 2014; Parvani et al. 2015; Bae et al. 2016). In addition, TGFβ-induced EMT regulates the expression of EMT-TFs, which has also been reported to confer apoptotic resistance resulting in an enhanced survival in hepatocellular carcinoma (Franco et al. 2010). However, the tumor-supporting abilities provided by TGFβ signaling are not strictly restrained to carcinomas, but it has also been implicated that the local invasion of non-epithelial cancer cells can be regulated via TGFβ signaling (Joseph et al. 2014; Mahabir et al. 2014). During the past decade, research has been focusing on identifying additional TFs involved in the context of the TGFβ signaling cascade, EMT, and cancer. Recently, attention towards the role of heat shock factors (HSFs) in these processes have gained an exceeding amount of interest and it has been substantiated that many of the HSF family transcription factors do play a key role in cancer progression. For instance, both HSF1, and just recently, HSF2, have been implicated to function in EMT and thereby in the evolution of cancer.

2.6 The heat shock response

Cells are continuously exposed to various kinds of environmental stresses that predisposes them to disturbances in proteostasis, and they have therefore evolved coping mechanisms including transcriptional programs to re-establish the internal physiological balance and counteract the damage. One such program is the heat shock response (HSR), which is a pathway cells activate upon protein-damaging conditions. The HSR was first described by Ferruccio Ritossa in the 1960s, who identified a pattern indicating increased transcription in regions of chromosome puffs in the salivary glands of *Drosophila melanogaster* larvae (Ritossa, 1962). Further research during the following decade showed that the induced level of transcription in the chromosome puffs encoded heat shock proteins (HSPs), which are molecular chaperones synthesized by cells in response to protein-damaging stress (Tissiéres et al. 1974). Later, HSF1 was identified as the master transcription factor regulating the HSR (Parker & Topol, 1984) and further research was able to characterize additional HSFs (Schuetz et al. 1991; Nakai et al. 1993; Nakai et al. 1997).

The HSR is highly conserved across species and has been identified in nearly all cell and tissue types of multicellular organisms. Mechanistically in eukaryotes, the HSR pathway is initiated by heat shock factors (HSFs). Upon activation, these transcription factors form homo- and heterotrimers that are translocated into the nucleus where they bind to a specific DNA sequence called the heat shock element (HSE) (Åkerfelt et al. 2007), which is located in the promoter region of genes encoding heat shock proteins (HSPs) (Amin et al. 1988). The binding of activated HSF trimers to the HSEs induce target gene transcription resulting in the synthesis of HSPs and other target proteins (Figure 4). The synthesized HSPs are molecular chaperones that bind to proteins stabilizing their conformation and function (Åkerfelt et al. 2010). HSFs are also important in regulating a variety of transcriptional programs driving physiological processes including differentiation and organ development. Furthermore, the importance of these factors have also been implicated in pathological conditions, including many different types of cancers and neurodegenerative diseases such as Huntington's (Gomez-Pastor et al. 2017) and Alzheimer's disease (Campanella et al. 2018).

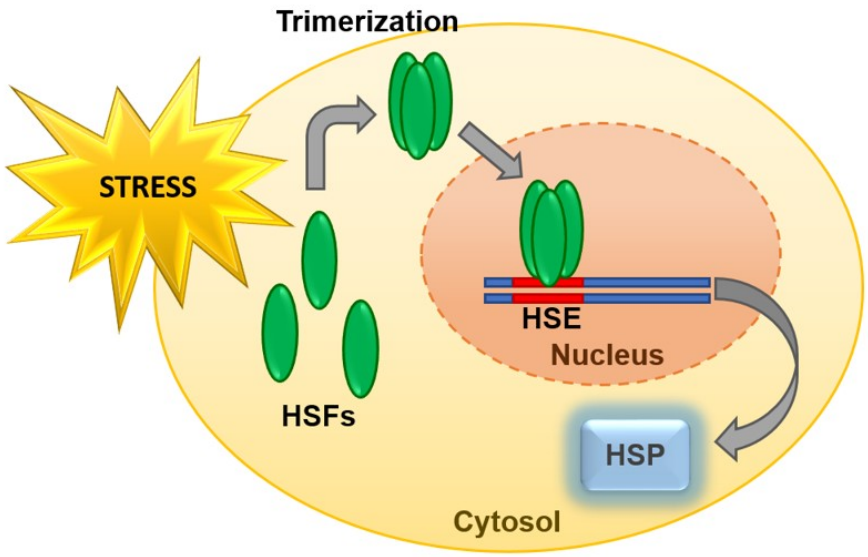

Figure 4. The heat shock response. The heat shock response (HSR) is activated in response to proteotoxic stress, which induces heat shock factor (HSF) trimerization in the cytosol. Trimerized HSFs are translocated to the nucleus where they bind to heat shock elements (HSEs) and stimulate the transcription of target genes. Actively transcribed target genes result in the synthesis of e.g. heat shock proteins (HSPs), which function as molecular chaperons maintaining proper folding and function of proteins, thereby helping the cell to cope against stress.

2.7 Heat shock factors

HSFs are transcription factors modulating the activity of multiple transcriptional programs that allow the cell to adapt to alterations in environmental and intracellular conditions. These programs include, for instance, those activated in response to protein-damaging stress and upon processes involved in development and differentiation (Abane & Mezger, 2010; Joutsen & Sistonen, 2019). The capacity of HSFs to induce a transcriptional program is modulated by several factors such as post-translational modifications (PTMs), which can either have an inducing or an inhibiting effect.

2.7.1 The domain structure of HSFs

Six HSFs have been identified to be encoded by the human genome including HSF1, HSF2, HSF4, HSF5, HSFX, and HSFY (Gomez-Pastor et al. 2018). The members of the HSF family are characterized by domains displaying unique structural and functional features (Figure 5). A common feature for all HSFs, and the most conserved of these domains, is the winged helix-turn-helix DNA-binding domain (DBD) located at the amino-terminal end (Vuister et al. 1994; Åkerfelt et al. 2010). This highly

conserved domain enables HSF-binding to the cis-acting HSEs in the promoter region of the target gene. The HSE comprises inverted pentameric nGAAn repeats, “n” being any possible nucleotide, and the HSF typically requires at least two HSE motifs for successful binding (Jaeger et al. 2014). In difference to many other transcription factors, HSFs function as trimers upon activation. The trimerization process is enabled by a leucine zipper oligomerization domain which is constituted of two heptad repeats, HR-A and HR-B (Sorger and Nelson, 1989; Peteranderl et al. 1999). These heptad repeats are thought to participate in oligomerization via their charged and hydrophobic residues susceptible to inter-molecular leucine zipper formation (Rabindran et al. 1993), and are therefore essential for the trimerization and activation of HSFs. A HR-C domain functions as a repressor to inhibit spontaneous trimerization of HSFs during unstressed conditions (Rabindran et al. 1993). This repressor domain has been shown to be missing from HSF4 resulting in the generation of continuously active HSF4 trimers (Nakai et al. 1997). Furthermore, some HSFs contain an alternative domain rich in acidic and hydrophobic residues called a transactivation domain (TAD). This domain is located at the carboxy-terminal end and is considered essential for the induction of the transcriptional response (Sullivan et al. 2001). In addition, HSF1 contains a regulatory domain (RD), which is responsible for controlling the activation during stress conditions and also for the repression of the TAD during unstressed conditions, is located between the HR-A and HR-B domains (Green et al. 1995).

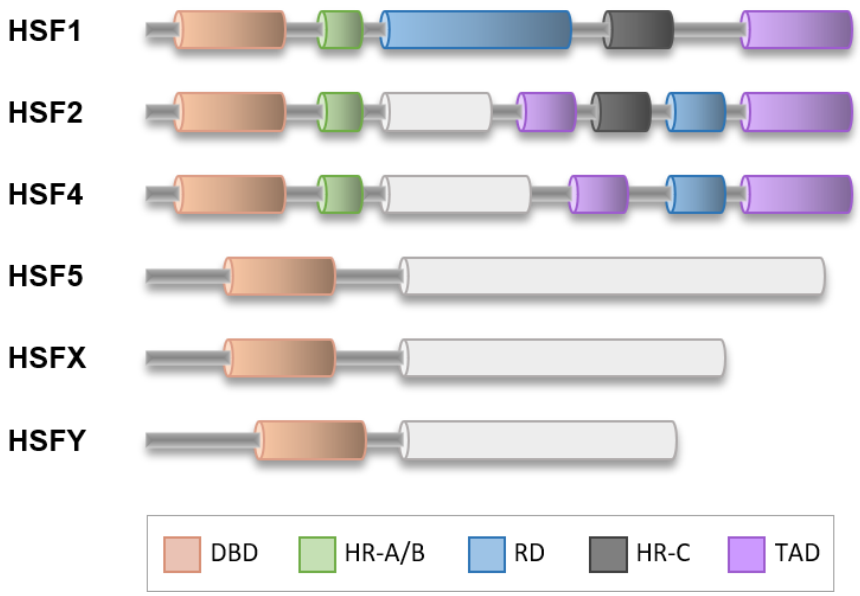

Figure 5. The domain structures of human heat shock factors (HSFs). Six different HSFs are expressed in humans, HSF1, HSF2, HSF4, HSF5, HSFX, and HSFY. All HSFs contain an evolutionarily highly conserved DNA-binding domain (DBD). HSF1, HSF2, and HSF4 also contain a hydrophobic heptad repeat domain (HR-A/B), which is responsible for mediating oligomerization, and a regulatory domain (RD), which is known to modulate stress responsiveness in HSF1. The HR-C domain in HSF1 and HSF2 prevents spontaneous trimerization upon unstressed conditions. The transactivation domain, present in HSF1, HSF2, and HSF4, controls transcriptional activity. The complete domain structure has not yet been validated for HSF5, HSFX, and HSFY.

2.7.2 Trimerization and regulation of HSFs

During normal physiological conditions, HSF1 is present as inert monomers that shuttle between the nucleus and the cytoplasm. Likewise during these conditions the core region of the HSP promoter is pre-loaded with stalled RNA polymerase II (Pol II) and other transcription-associated components that maintain the promoter region in an open state (Fujimoto et al. 2012; Mahat et al. 2016). However, exposure to stress causes the nuclear export of HSF1 to be restricted and thereby results in a rapid accumulation of HSF1 monomers in the nucleoplasm (Budzynski & Sistonen, 2017). Proteotoxic stress is also accompanied by HSF1 monomer-oligomerization and thus the formation of HSF1 trimers. Subsequently, HSF1 trimers bind to HSEs and interact with additional transcription factors and co-activators, which leads to the opening of the chromatin structure and promotes the releasement of the stalled Pol II, which in turn enhances the transcription of target genes (Sarge et al. 1993; Vihervaara et al. 2013; Himanen & Sistonen, 2019). Currently, the major activation mechanism of HSF1 is considered to be the chaperone titration model. According to this model, the activity of HSF1 is regulated by HSP chaperones, such as HSP70/*HSPA1A* and

HSP90/*HSPC* (Le Breton & Mayer, 2016), which are recruited to damaged proteins when the cell is exposed to proteotoxic stress. As a consequence of this recruitment process, HSF1 is dissociated from the chaperone complex, which normally keeps it inert. The chaperone titration model has been supported by studies in different organisms for instance, in mammals the HSR was shown to be activated upon pharmaceutical inhibition of the HSP90/*HSPC* chaperone (Powers & Workman, 2007), whereas in *Caenorhabditis elegans* (*C. elegans*), a robust HSF-1 induction was observed in response to Hsp-70 ablation (Guisbert et al. 2013).

The detailed mechanism of transcriptional attenuation of the HSR remains unknown, but it has been suggested that at least two mechanisms contribute to HSF1 attenuation. First, the chaperone titration model has been proposed to modulate the activity of HSF1 also by promoting attenuation via a negative feedback mechanism created by the HSPs. A second attenuation mechanism is based on decreasing the DNA-binding affinity of HSF1, which is achieved by acetylation of specific residues in the DBD (Westerheide et al. 2009). The attenuation is thought to occur in response to a prolonged exposure to stress. The chaperone titration model has been suggested to regulate HSR activation and attenuation via stress-induced accumulation of HSPs that have been shown to facilitate interaction with HSF1. This interaction impairs the *trans*-activation capacity of HSF1 as well as induces the assembly of transcriptional co-repressors to the HSP promoter inhibiting the function of HSF1 (Gómez et al. 2008). The second HSF1 attenuation mechanism has been shown to be reliant on acetylation of two specific lysine residues in the DBD, lysine 80 and lysine 118 (Westerheide et al. 2009; Raychaudhuri et al. 2014). Acetylation of these residues during stress causes the releasement of DNA-bound HSF1, which is one of the key steps contributing to the attenuation process. The DBD acetylation status is modulated, at least partly, by a transcription factor called activating transcription factor 1 (ATF1), which recruits an acetyl transferase complex called CBP/p300 to the DNA-bound HSF1 (Takii et al. 2015). However, the DBD-acetylation stimulating HSR attenuation can be counteracted by a deacetylase, SIRT1, and histone acetylases, HDAC7 and HDAC9, which can thereby alter the acetylation status of the DBD and prolong the HSR (Westerheide et al. 2009; Zelin & Freeman, 2015).

In contrast to HSF1, HSF2 is typically present as cytosolic dimers already during unstressed conditions. However, HSF2 is similarly activated and trimerized upon

stimulation, which induces its DNA-binding activity and results in transcriptional activation of its target genes (Sistonen et al. 1994; Mathew et al. 1998). During heat shock, the attenuation of HSF2 is mainly modulated via proteosomal degradation, demonstrated by studies showing that HSF2 is susceptible to ubiquitylation and is therefore directed for degradation by the proteasome (Ahlskog et al. 2010).

The oligomerization domains of HSF1 and HSF2 display significant sequence homology (Schuetz et al. 1991). This sequence homology is thought to be a key feature in enabling HSF1 and HSF2 binding to DNA as heterotrimeric complexes (Sandqvist et al. 2009). The transcriptional properties of the trimer has been shown to be affected by the abundance of each transcription factor (Sandqvist et al. 2009). Moreover, heterotrimerization of HSF1 and HSF2 has been shown to modulate a distinct transcriptional program when exposed to alcohol, where the specific transcriptional effect was lost if either transcription factor was ablated (El Fatimy et al. 2014).

2.7.3 Mechanisms modulating the activity of HSFs

One major mechanism contributing to the modulation of HSF activity includes post-translational modifications (PTMs). For instance, HSF1 is susceptible to many PTMs during the HSR including phosphorylation, sumoylation, and acetylation. To this date, 23 serine and threonine residues prone to phosphorylation have been discovered in human HSF1. Most of these residues are located in the RD domain and the majority of them have a repressive effect on the transcriptional activity (Cotto et al. 1996). Phosphorylation of HSF1 has been shown to repress its spontaneous activation during unstressed conditions (Chu et al. 1996; Kline & Morimoto, 1997; Chu et al. 1998) and to modulate its degradation during stress-predisposing conditions via interaction with a ubiquitin ligase (Kourtis et al. 2015). However, HSF1 is also subjected to activating phosphorylations, one of the most important ones being the phosphorylation site on serine 326, which is seen as a hallmark of HSF1 activation (Boellman et al. 2004; Guettouche et al. 2005; Shah et al. 2016). Moreover, HSF1 is frequently sumoylated on lysine 298 (Hong et al. 2001; Hietakangas et al. 2003), though contradictory results were presented by the two original studies, regarding the importance of this sumoylation in the HSR induction, demonstrating that the exact impact of this modification remains unclear and might be dependent on the biological context. Sumoylation has also been demonstrated to negatively modulate the transactivation

capacity of HSF1 during stress conditions (Hietakangas et al. 2006), however the mechanistical details are still unknown. Finally, the acetylation of 12 lysine residues on HSF1 have been discovered to be important for the activation and attenuation of the HSR (Westerheide et al. 2009; Raychaudhuri et al. 2014). For instance, acetylation of individual lysine residues, lysine 208 and 298, during normal conditions have been shown to stabilize HSF1 and protect it from being proteolytically degraded (Raychaudhuri et al. 2014). In contrast, elevated HSF1 acetylation of lysine 80 and lysine 118, which are located in the DBD, in response to heat shock have been shown to result in attenuation of the HSR (Westerheide et al. 2009; Raychaudhuri et al. 2014), which, as previously mentioned, is a consequence of HSF1-releasement from DNA.

The activity of HSF2 is mainly modulated by its level of expression. The expression pattern of HSF2 is distinct depending on the type of tissue, type of cell, experienced stress factors, and the phase of cell cycle (Sarge et al. 1994; Fiorenza et al. 1995; Mathew et al. 1998; Elsing et al. 2014). Elevated HSF2 expression has been shown to correlate with an induced DNA-binding activity, indicating that its activity is mainly regulated by the level of its expression (Sarge et al. 1994; Mathew et al 1998). However, HSF2 is also susceptible to PTMs, especially when predisposed to elevated temperatures as it has been demonstrated that HSF2 is ubiquitylated by the E3-ubiquityn ligase anaphase-promoting complex/cyclosome (APC/C), leading to proteosomal degradation of HSF2 (Ahlskog et al. 2010). Furthermore, the expression of HSF2 in testis is, in contrast, modulated at the mRNA level via microRNAs, predominantly by microRNA-18 (miR-18) (Björk et al. 2010). miR-18 is expressed cell type-specifically during spermatogenesis and functions to downregulate HSF2 expression by targeting the 3'UTR of HSF2 (Björk et al. 2010), demonstrating a mechanism how HSF2 is modulated during development. In addition, HSF2 has also been shown to be subjected to sumoylation. It was first suggested that the sumoylation of certain lysine residues, especially lysine 82, located in the DBD of HSF2 would be necessary in obtaining an efficient binding event between HSF2 and DNA upon HSR (Goodson et al. 2001). However the impact of this modification was later contradicted by multiple studies, reciprocating the perception that is currently acknowledged as an inhibitory modification (Anckar et al. 2006; Tateishi et al. 2009; Feng et al. 2016). Furthermore, mass-spectrometric analysis has recently identified 20 novel sumoylation sites in the DBD and HR-A/B of HSF2 (Hendriks & Vertegaal, 2016),

suggesting that the modulatory effect of PTMs might regulate HSF2 activity to a greater extent than was originally anticipated.

2.7.4 Physiological impacts of HSFs

The classical model of HSFs modulating a cellular protective mechanism in response to stress has been substantially expanded during the past decades. The importance of these transcription factors has been signified in a large cohort of additional processes, as they have been identified to function as important developmental factors, assist in differentiation processes, and display critical roles upon several pathologies. The physiological impact of HSFs in processes beyond the HSR was demonstrated over 30 years ago when the function of HSFs was shown to be vital for yeast cell survival (Sorger & Pelham, 1988). Since then, studies have revealed that HSFs are of key importance during e.g. developmental processes, as HSF1 was demonstrated to be critical for the early stage development of *Drosophila melanogaster* larvae (Jedlicka et al. 1997). Recently, HSF-1 was shown to be indispensable for *C. elegans* development, demonstrating its function as an important developmental factor and revealing that a set of key target genes important for nematode development are different from the gene targets that HSF-1 displays under heat shock (Li et al. 2016).

Studies utilizing HSF knockout mice, HSF-null mice, have further demonstrated the importance of HSFs during developmental processes. HSF-null mice are viable but display certain phenotypic aberrations in sensory organs, the brain and in fertility (Xiao et al. 1999; Inouye et al. 2004; Takaki et al. 2006; Uchida et al. 2011; Jin et al. 2011). For instance, HSF1-null mice display aberrations in the olfactory epithelium due to an HSF1-dependent suppression of a cytokine important for olfactory epithelium development called leukemia inhibitory factor (LIF) (Metcalf, 2003; Takaki et al. 2006). HSF1-null female mice have also been shown to suffer from abnormal oocyte development (Christians et al. 2000) and prenatal lethality (Xiao et al. 1999). In addition, HSF2-null mice display an impaired gametogenesis as female mice fail to produce normal egg cells and male mice suffer from an elevated disruption of spermatocytes (Kallio et al. 2002). In the brain, HSF2-null mice show aberrations in the small hippocampus and they also display enlarged ventricles and miss-positioned neurons (Kallio et al. 2002; Chang et al. 2006). The lack of both HSF1 and HSF2 has been reported to cause male sterility in HSF1/2-null mice, suggesting an

additive function in spermatogenesis when both HSFs are lost (Wang et al. 2004). Also, the importance of HSF2 has been highlighted in neuronal migration as HSF1 and HSF2 were shown to form heterotrimers when exposed to alcohol, resulting in a specific pattern of stress-inducible gene expression enhancing survival but impairing the activity of genes involved in neuronal migration (El Fatimy et al. 2014).

The function of HSF4, on the other hand, has thus far only been identified in the development of the lens (Fujimoto et al. 2004; Jin et al. 2011), where it displays a critical function in promoting the transcription of genes encoding structural lens proteins called crystallins (Somasundaram & Bhat, 2004; Shi et al. 2009; Roskamp et al. 2019). HSF4-null mice characteristically display early lens deterioration followed by cataract and blindness as a consequence of impaired lens epithelial cell differentiation and proliferation (Fujimoto et al. 2004). Furthermore, HSF4 has also been shown to be involved in olfactory neurogenesis. In this process, the expression of LIF is modulated by HSF4 but unlike the function of HSF1, which suppresses LIF, the modulatory role of HSF4 is reciprocal (Takaki et al. 2006). The mechanistical functions and importance of the other identified human HSFs, HSF5, HSFX, and HSFY, have not yet been elucidated humans. However, HSFX and HSFY have been identified to be localized in X and Y sex chromosomes, respectively (Tessari et al. 2004; Fujimoto & Nakai, 2010). Whereas the human HSF5 has thus far been validated only at the transcriptional level (Gomez-Pastor et al. 2018).

The diverse roles of HSFs have been identified in a large cohort of different biological processes and the function of these transcription factors has also been linked to multiple pathologies. HSFs are of high importance in brain development and brain function via engagement in neuronal migration programs as well as neural synapse maintenance (Homma et al. 2007; El Fatimy et al. 2014; Hooper et al. 2016; Gomez-Pastor et al. 2018). The importance is supported by studies showing that impaired HSF1-activity contributes to aging and neurodegeneration. Many neurodegenerative diseases are associated with aggregation of misfolded proteins as a result of a malfunctional protein quality-control machinery (Gomez-Pastor et al. 2018). The advancement of the disease is lubricated by an impaired functionality of HSF1, which itself does not cause the disease but contributes to the progression by contributing to the decreased functionality of the protein quality-control machinery via reducing chaperone expression. Whereas studies utilizing cell, fruit fly, and mice as

neurodegenerative disease models have shown that the protein-folding capacity can be rescued to some extent by inducing HSF1 expression, illustrating that HSF1 possesses therapeutic potential in diseases involved in neuronal degeneration (Neef et al. 2011). Moreover, mounting evidence showing that HSFs might display critical roles in several different forms of cancer have led to an increased interest towards this research area. The association between HSFs and malignant transformation was also of high importance in this thesis study, which is why I will proceed with discussing this topic in more detail in the following section.

2.8 Heat shock factors in cancer

The development of cancer is modulated by major alterations in key processes that are fundamental for cell survival such as signaling pathways modulating cellular metabolism, development, motility, and stress responsiveness. Studies utilizing high-resolution genome-wide sequencing have revealed the importance of HSFs in regulating important transcriptional programs during various biological as well as pathological conditions (Mendillo et al. 2012; Li et al. 2016). Some of these transcriptional programs have been identified to operate in malignant transformation, and linked to an altered HSP expression contributing to cancer progression.

The importance of HSF1 in cancer was demonstrated by two pioneering studies in 2007 (Dai et al. 2007; Min et al. 2007). Dai and co-workers were able to show that HSF1-null mice experienced resistance towards induction of skin carcinogenesis and tumorigenesis induced by mutant p53 (Dai et al. 2007). These findings were confirmed by further studies demonstrating that a similar resistance of HSF1-null mice was displayed also in response to the induction of liver and breast cancer (Jin et al. 2011; Xi et al. 2012). The second pioneering study illustrated that the lack of HSF1 in p53-null mice resulted in a decreased development of lymphomas, however the development of carcinomas and sarcomas were instead increased (Min et al. 2007), illustrating that the ablation of HSF1 results in a shift in the tumor development. This observation was confirmed later by a study utilizing HSF4 and p53 double-knockout mice, where the shift in tumor development was shown to be similar (Jin et al. 2012).

Considering that HSF1 is known to modulate chaperone expression, it is no surprise that in cancer, where cells are predisposed to an increased amount of stress caused by proteomic imbalance as a result of genomic instability, an increase in HSPs help to

counteract the elevated metabolic burden (Liao et al. 2015; Kourtis et al. 2018). Specific transcriptional networks modulated by HSF1 that contribute to malignant transformation, have been demonstrated by two separate studies (Mendillo et al. 2012; Scherz-Shouval et al. 2014). The first study reported of a specific transcriptional program identified as the HSF1 cancer signature (HSF1-CaSig), providing a tool for predicting cancer severity, as the HSF1-CaSig was demonstrated to correlate with the disease outcome in breast cancer patients (Mendillo et al. 2012). The second study illustrated the importance of HSF1 in reprogramming the tumor stroma of cancer-associated fibroblasts (CAFs) (Scherz-Shouval et al. 2014). CAFs consist of reprogrammed normal tissue-derived fibroblast variants and myofibroblasts, and are the most frequently existing cells in the tumor microenvironment. The high HSF1 expression observed in CAFs allows them to create a tumor-supporting microenvironment by inducing the secretion of factors promoting cancer cell proliferation and survival (Scherz-Shouval et al. 2014). HSF1 has been reported to drive a non-cell-autonomous transcriptional program in CAFs, which is different from the HSF1-CaSig program driven by the neighboring cancer cells, supporting development of malignant transformation (Sahai et al. 2020). Similarly, HSF2 has been shown to modulate cancer-involved gene regulatory networks (Björk et al. 2016; Joutsen et al. 2020). Although no specific cancer signature has yet been discovered for HSF2, its function as an important survival factor has been highlighted in a recent study by Joutsen and co-workers, who reported that HSF2 preserves cell-cell adhesions via cadherin expression upon proteasome inhibition (Joutsen et al. 2020). Furthermore, the transcriptional program of HSF2 is also altered during prostate cancer progression, where its expression has been reported to be decreased in response to the development of the disease (Björk et al. 2016). Although HSF1 is the foremost studied HSF also in the context of cancer, there is a number of studies indicating that the expression of HSF2 and HSF4 can likewise be of key importance in malignant transformation (Björk et al. 2016; Yang et al. 2019; Ma et al. 2020). To this date, a plethora of studies have reported the involvement of HSFs in different forms of cancers, and some of them are summarized in Table 1.

Table 1. Identified functions of HSFs in different types of cancers. The expression of HSF1, HSF2, and HSF4 have been found to display various functions in different types of cancers. This table summarizes some of the identified effects of these transcription factors in cancer reported by research thus far. HCC = hepatocellular carcinoma, CRC = colorectal cancer, ESCC = esophageal squamous cell carcinoma, MM = multiple myeloma.

HSF	Type of cancer	Level of HSF expression	Effect	Reference
HSF1	Breast cancer	Increased	Augments anchorage-independent cell growth, induces EMT, and enhances tumor survival and progression.	Citri et al. 2004; Xi et al. 2012; Yarden & Pines, 2012; Schulz et al. 2014; Carpenter et al. 2015; Asano et al. 2016; Yasuda et al. 2017; Vydra et al. 2019; Guo et al. 2020
HSF2	Breast cancer	Increased	Enhances tumorigenesis, induces cell proliferation, migration, angiogenesis and tumor survival.	Chen et al. 2011; Li et al. 2014; Yang et al. 2018
HSF4	Breast cancer	Increased	Stimulates angiogenesis and tumor survival.	Chen et al. 2011
HSF1	Prostate cancer	Increased	Enhances tumor progression.	Davoli & de Lange, 2011; Björk et al. 2018
HSF2	Prostate cancer	Decreased	Induces tumorigenesis and invasion capacity.	Björk et al. 2016
HSF1	Lung cancer	Increased	Induces angiogenesis, stimulates tumor progression and metastasis.	Scherz-Shouval et al. 2014; Cui et al. 2015
HSF2	Lung cancer	Increased	Stimulates cell proliferation and migration.	Ocejo-Garcia et al. 2005; Zhong et al. 2016
HSF1	HCC	Increased	Stimulates cell proliferation and migration.	Clark et al. 2007; Li et al. 2014; Li et al. 2015
HSF2	HCC	Increased	Induces aerobic glycolysis, which enhances cell proliferation.	Chen et al. 2011; Jiang, 2017; Yang et al. 2019;
HSF1	CRC	Increased	Enhances glutaminolysis, promotes cell survival by inhibiting apoptosis.	Jacobs & Marnett, 2009; Li et al. 2017
HSF4	CRC	Increased	Advances cancer progression.	Yang et al. 2017
HSF1	ESCC	Increased	Advances cancer progression.	Liao et al. 2015; Meng et al. 2017; Tsukao et al. 2017
HSF2	ESCC	Increased	Inhibits apoptosis and promotes cell survival.	Liao et al. 2015; Meng et al. 2017; Tsukao et al. 2017
HSF1	MM	Increased	Promotes metastasis, enhances drug efflux and drug resistance.	Heimberger et al. 2013; Kourtis et al. 2015

2.8.1 HSF1 in cancer

Several studies have characterized that an elevated HSF1 expression can contribute in the progression of numerous types of cancers, as summarized in Table 1 and illustrated in Figure 6 (Santagata et al. 2011). For instance in breast cancer, where HSF1 has been shown to be frequently overexpressed, an oncogenic role of HSF1 has been characterized in multiple studies (Citri et al. 2004; Xi et al. 2012; Yarden & Pines, 2012; Schulz et al. 2014; Carpenter et al. 2015; Asano et al. 2016; Yasuda et al. 2017; Vydra et al. 2019; Guo et al. 2020). Breast cancer cells can roughly be divided into three categories based on breast cancer marker expression: 1) luminal breast cancer cell lines, which are characterized by the expression of progesterone receptors (PRs) and estrogen receptors (ERs), 2) human epidermal growth factor receptor 2-positive (HER2-positive) breast cancer cell lines, which are characterized by HER2-positivity and ER-negativity, and 3) triple-negative breast cancer cell lines, where none of the three markers are expressed. Studies have demonstrated, that in ERα-positive breast cancer cells, ERα stimulates the MAPK/ERK signaling pathway, which in turn induces the activation of HSF1. In this case, the activated MEK and ERK kinases phosphorylate HSF1 on serine 326 (Vydra et al. 2019), which is one of the major so-called activating phosphorylation sites on HSF1 (Yasuda et al. 2017). This HSF1-activating phosphorylation leads to overexpression of an HSP called HSP90/*HSPC*, which is a chaperone promoting ERα maturation and the function of several kinases that together drive tumor progression (Whitesell & Lindquist 2005; Xi et al. 2012). Another important signaling axis in breast cancer is HER2, which expression is increased in approximately 25% of cases and it has been shown to induce HSF1 expression, which can partly contribute to the metastatic features observed in this type of cancer (Xi et al. 2012; Yarden & Pines, 2012). The activation of HSF1 in HER2-positive breast cancer cells is also dependent on the phosphorylation of serine 326, in this case by a kinase called alpha serine/threonine-protein kinase (AKT) (Schulz et al. 2014; Carpenter et al. 2015), which is one of the key components of the phosphoinositide 3-kinase (PI3K)/AKT signaling pathway, functioning to phosphorylate a plethora of target proteins including those involved in cell survival and growth. Activated HSF1 induces the expression of several HSPs, including HSP90/*HSPC,* and, importantly, also modulates the expression of one of the key EMT-TFs, SNAI2, which in turn facilitates EMT and thus an enhanced cellular

invasion capacity (Carpenter et al. 2015). A high HSP90/*HSPC* expression is maintained by the HER-AKT-HSF1 signaling axis, which contributes to sustain the functionality of mutated and overexpressed components, such as transcription factors and kinases, supporting cancer cell survival. The cancer-supporting function of HSF1 has additionally been reported in other types of breast cancers and in several other types of cancer, such as in lung (Scherz-Shouval et al. 2014; Cui et al. 2015), prostate (Wang et al. 2004; Björk et al. 2018), and colorectal cancer among others (Jacobs & Marnett, 2009; Li et al. 2017).

In prostate cancer, HSF1 overexpression has been demonstrated to contribute to prostate carcinoma progression by causing polyploidy, which is a characteristic shown to facilitate tumor progression (Wang et al. 2004; Davoli & de Lange, 2011). The reduction of HSF1 expression has been reported to partially enable the regain of diploidy in a prostate cancer cell line (PC-3) (van Bokhoven et al. 2003). Furthermore, Björk and co-workers recently suggested HSF1 as a predictive biomarker for prostate cancer (Björk et al. 2018), as a high HSF1 mRNA expression was observed in clinical prostate cancer samples in addition to a highly increased nuclear localization of HSF1 observed in patients with an advanced form of prostate cancer. Nuclear HSF1 localization also correlated with a high Gleason score, which is a system utilized to characteristically grade prostate biopsies, and predisposed to a poor disease outcome (Björk et al. 2018).

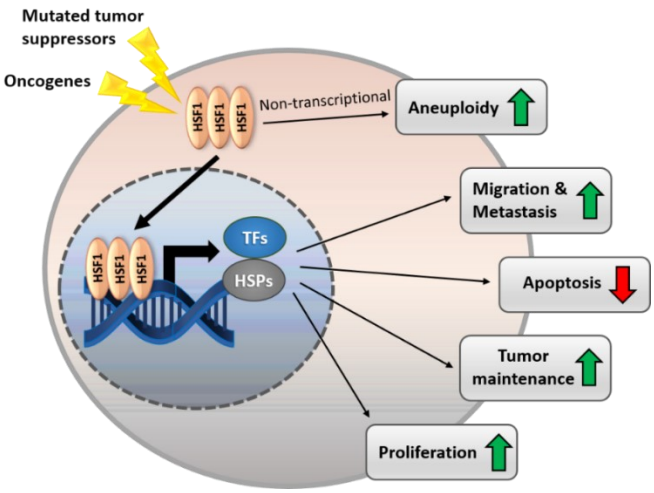

Figure 6. The tumor-supporting functions of HSF1. Mutated tumor suppressors and oncogenes induce the expression of HSF1, which results in an increased transcription of multiple transcription factors (TFs) and heat shock proteins (HSPs). Overexpression of these TFs and HSPs promote several cancer-supporting features such as migration and metastasis, anti-apoptotic features, enhanced tumor maintenance as well as improved proliferation. An increased HSF1 expression also promotes cancer progression non-transcriptionally by inducing aneuploidy.

2.8.2 HSF2 in cancer

An accumulating amount of evidence have illustrated that HSF2 play an important function in the development of several different types of malignancies. However in contrast to HSF1, the expression of HSF2 has been shown to be downregulated in some carcinomas, such as prostate cancer, while an increased HSF2 expression has been observed in esophageal squamous cell carcinoma (ESCC), low-grade gliomas, and lung cancer (Mustafa et al. 2010; Björk et al. 2016; Zhong et al. 2016; Meng et al. 2017). To this date, HSF2 has been reported to display a dual role in cancer progression, functioning as a tumor suppressor in some cancers and as an inducer in others (Figure 7).

The role of HSF2 in breast cancer progression has recently been identified. HSF2 has been shown to interact with one of the important EMT-TFs, ZEB1, and together promote the expression of a microRNA cluster called miR-183/-96/-182 (Li et al. 2014). Each of these miRNAs have been shown to individually facilitate migration in breast cancer cell lines T47D and MCF-7 (Li et al. 2014). Moreover, it has been demonstrated that miR-183 downregulates RAB21, a member of the small GTPase family, resulting in aneuploidy which in turn has been linked to tumor evolution (Sansregret & Swanton, 2017). HSF2 has also been reported to impact the expression of an enzyme called ALG3, whose high expression has been demonstrated to induce the proliferation rate and motility of MCF-7 cells (Yang et al. 2018). Additionally, a positive feedback mechanism between HSF2 and ALG3 has been proposed, since the ablation of ALG3 was shown to both halt the tumor progression and decrease the expression of HSF2 when injected into nude mice (Yang et al. 2018).

A contradictory role of HSF2 has been proposed in prostate cancer, as the transcription factor seems to operate as a tumor suppressor in this specific type of cancer (Björk et al. 2016). A heterozygous loss of HSF2 as well as decreased HSF2 expression has been correlated with a high Gleason score and hence with a poor patient survival, and the expression of HSF2 in most prostate cancer tissues has been observed to be low. The tumor-suppressing role of HSF2 in prostate cancer has been further supported by a study where knockout of HSF2 in PC-3 cells was shown to enhance invasive growth in 3D organotypic cultures and *in vivo* in a chorioallantoic membrane model (Björk et al. 2016). Although mechanistical details driving the tumor-suppressive feature of HSF2 in prostate cancer are still unclear, gene expression profiling has implied that

the activity of GTPases, dynamics of cytoskeletal components, and cell-cell adhesions are affected by HSF2, and these are all factors that are also altered in cancer cells (Björk et al. 2016). The same study also demonstrated that downregulation of HSF2 in PC-3 cells displayed a stimulating effect on key EMT regulators, implying that there is a connection between HSF2 and EMT. Furthermore, a meta-analysis indicated that the mRNA expression of HSF2 was downregulated in several other cancer tissues in addition to prostate cancer (Björk et al. 2016), signifying that a decreased expression of HSF2 might be a key contributor in the progression of some cancers. This emphasizes the need for further research in order to reveal the mechanistical details driving the tumor-suppressive role of HSF2 in distinct types of cancers. HSF2 has however been identified to display a function in several types of cancers, which are summarized in Table 1.

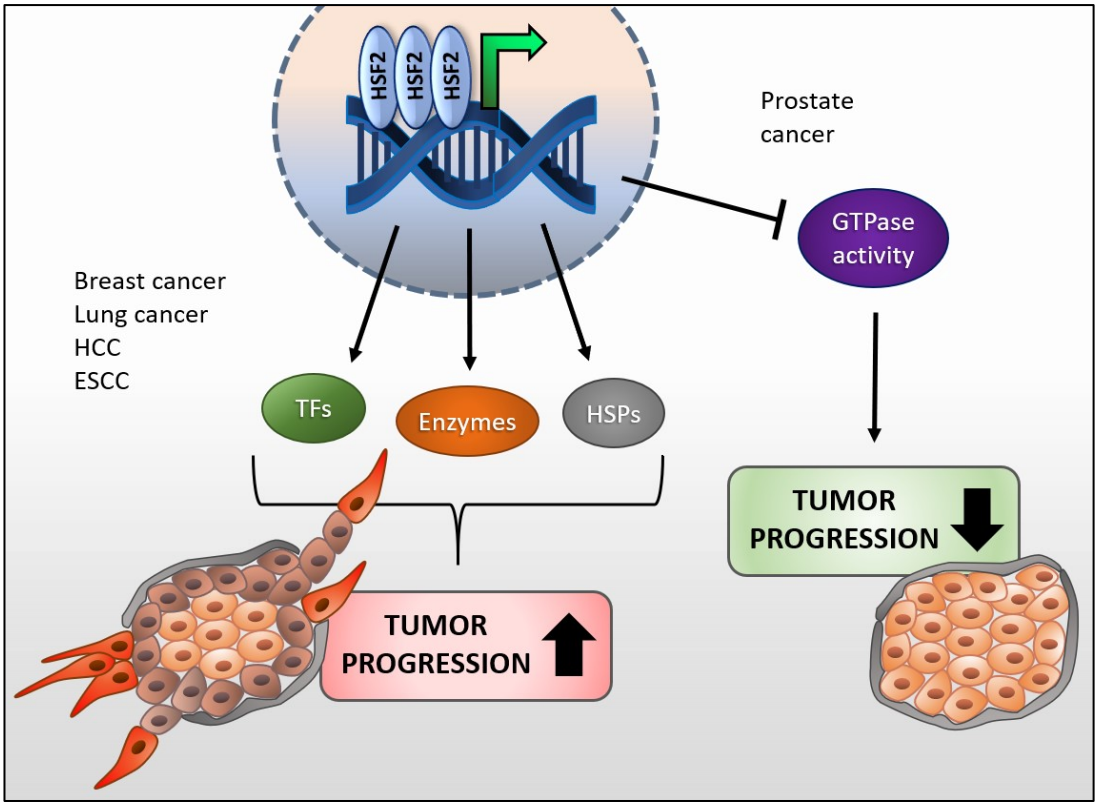

Figure 7. The function of HSF2 in different types of cancers. Increased expression of HSF2 induces the transcription (indicated by the green arrow) of several transcription factors (TFs), enzymes, and heat shock proteins (HSPs), that via various mechanisms promote the acquisition of cancer-supporting features and facilitate tumor progression in breast cancer, lung cancer, hepatocellular carcinoma (HCC), and esophageal squamous cell carcinoma (ESCC). In prostate cancer, HSF2 expression affects the activity of GTPases, reducing invasiveness and suppressing tumor progression.

2.8.3 HSF4 in cancer

The correlation between HSF4 and cancer have recently been discovered. Research regarding HSF4 is still significantly lagging behind that of HSF2 and especially HSF1, but there is a growing interest towards elucidating the role of this transcription factor in the context of cancer. In MCF-7 breast cancer cells, HSF4 has, in addition to HSF2, been suggested to modulate the level of hypoxia-inducible factor-1-aplha (HIF-1α) expression (Chen et al. 2011). HIF-1α is a transcriptional regulator of hypoxia, stimulating the production of vascular endothelial growth factor (VEGF) in response to low oxygen levels, which in turn facilitates angiogenesis (Forsythe et al. 1996). Cancer cells require an induced amount of oxygen, provided by blood vessels, to keep up with their rapid growth, and blood vessel formation is also required in order to enable metastasis (Nishida et al. 2006). In these cells, both overexpression and knockout of HSF4 and HSF2 induced the expression of HIF-1α and therefore also the expression of VEGF, suggesting that the maintenance of HIF-1α expression is modulated by these HSFs. The possible modulatory effect of HSF4 on HIF-1α indicates that HSF4 might display an important role in breast cancer progression by promoting tumor survival and growth as well as by supporting cancer metastasis, if not individually at least in cooperation with HSF2. However, whether HSF4 displays a direct role in the progression of breast cancer remains to be elucidated. Furthermore, HSF4 has also been shown to be overexpressed in primary hepatocellular carcinoma (HCC) tissues (Ma et al. 2020). The abnormally elevated expression of HSF4 was correlated with a poor HCC patient survival. Also similarly to its proposed modulatory effect in breast cancer (Chen et al. 2011), it was shown that HSF4 could stimulate cancer progression by promoting EMT via HIF-1α-based induction of AKT in Huh-7 and SMMC-7721 cells (Ma et al. 2020), indicating that HCC cells might be able to exploit the HIF-1α-stimulating function of HSF4 to enable cancer progression.

Evidence supporting that HSF4 might exhibit a key role in colorectal cancer has been recently reported in a study where frequent HSF4 expression was observed in colorectal cancer (CRC) cells (Yang et al. 2017). This finding demonstrated the potential clinical relevance of HSF4 in cancer for the first time, showing that HSF4 expression correlated with cancer progression and poor patient survival (Yang et al. 2017). In addition, analysis utilizing bioinformatics tools have indicated that HSF4 might interact with a phosphatase called DUSP26, which has in previous studies been

shown to decrease the activity of HSF4 by regulating its phosphorylation status (Hu & Mivechi, 2006). Although a correlation between HSF4 and colorectal cancer has now been demonstrated, the mechanistical function of HSF4 in CRC remains to be elucidated.

3 Research Aims

Several cellular processes contribute to cancer progression, one of which is epithelial-mesenchymal transition (EMT), a program responsible for regulating cellular motility. EMT plays a major role in the evolution of cancer as it enables the development of invasive traits that facilitate metastasis. The transforming growth factor beta (TGFβ) signaling pathway is among the most prominent pathways inducing EMT. The crosstalk between distinct pathways is of high importance in both normal and transformed cells. Another pathway which has recently been linked to cancer is the heat shock response (HSR), which is regulated by heat shock factors (HSFs), and an abnormal expression of these transcription factors have frequently been associated with malignant transformation. Previous research has indicated that HSF2 is involved in regulating EMT in prostate cancer cells (Björk et al. 2016), and unpublished results from the Sistonen laboratory have suggested that the TGFβ signaling pathway modulates HSF2 expression. However, it remains unknown how this downregulation is achieved and whether it has any physiological impact on cancer cells in EMT. Based on these findings, my main research aims were to first determine which part of the HSF2 promoter modulates the expression of HSF2 during EMT, second elucidate whether HSF2 affects the cellular invasion capacity during EMT, and third determine if HSF1 impacts HSF2 expression during EMT. For the first aim, I generated plasmids where luciferase gene expression was driven by different sizes and regions of the HSF2 promoter, enabling quantification of the transcriptional activity utilizing luciferase reporter assay. For the second aim, I overexpressed exogenous HSF2 in breast cancer cells and assessed the invasion capacity of cells under control conditions and upon EMT stimuli using wound healing assays. For the final aim, I generated cells where the expression of endogenous HSF1 was downregulated, and western blot was subsequently used to assess the level of HSF2 protein expression in these cells under control conditions and upon EMT stimuli.

The main research aims in this thesis study were to:

1. Determine which part of the HSF2 promoter regulates HSF2 gene expression during EMT
2. Determine whether HSF2 impacts the cellular invasion capacity during EMT
3. Determine if HSF1 modulates the expression of HSF2 during EMT

4 Materials & Methods

4.1 Cell lines

A transformed breast epithelial cell line, MDA-MB-231, was used as a model system in this experiment. MDA-MB-231 cells are isolated from a metastatic site in pleural effusion and are extensively used in research associated with studying the underlying mechanisms of EMT, hence the choice of these specific cell line. For culturing MDA-MB-231 cells Dulbecco's Modified Eagle Medium (DMEM) (Biowest) was supplemented with 5% fetal bovine serum (FBS) (Biowest), 2.5 mM glutamine (Biowest), 50 U/ml penicillin, and 50 µg/µl streptomycin. The cells were cultured at 37 °C and 5% CO_2.

4.2 Treatments

With the purpose of inducing EMT, the culture medium for each cell line was switched to an assay medium. The assay media differed from the culture media in that no penicillin or streptomycin was added, and they were supplemented with 2% serum instead of 5%. In order to activate EMT, cells were treated with TGFβ-1 or StemXvivo (XV), which have previously been established in numerous studies to induce EMT in these cell lines. Thus, cells were treated with assay medium supplemented with either 10 ng/ml of TGFβ-1 or 10 µl/ml of XV, and control cells were treated with assay medium lacking the EMT-inducing supplement. The TGFβ-1 or XV treatment lasted either 4 or 24 h, after which the cells were harvested.

4.3 Harvest and lysis of cells

Following treatments, cells were harvested and lysed. The cells that were used for luciferase assay were first washed with cold phosphate-buffered saline (PBS, Biowest) and then harvested by scraping using PBS. The cell suspensions were centrifuged and the resulting supernatant was aspirated. The cell pellets were then lysed using a commercial reagent, Passive lysis buffer (Promega). A dilution of the buffer was prepared from 5x Passive lysis buffer by adding MQ-H_2O to obtain a 1x final concentration. The pellets were resuspended in 40 µl of 1x Passive lysis buffer and incubated on ice for 10 min. Finally, the cell lysates were centrifuged at 15,000 rcf for 2 min at 4 °C, and the resulting supernatants were transferred into new tubes.

Cells that were used for western blot analysis were washed with PBS and then harvested by scraping using 3x Laemmlie lysis buffer (see recipe attachment). Laemmlie lysis buffer contains e.g. β-mercaptoethanol and sodium dodecyl sulfate (SDS), which denatures proteins by breaking disulfide bonds, and disrupts the tertiary folding pattern reverting the proteins to a linearized form, respectively. The cell lysates were then boiled for 10 min, to further support the denaturing process of proteins, and stored at 4 °C until further usage.

4.4 Transfection

Transfection is a method that can be used to achieve expression of a desired protein by introducing exogenous DNA into a cell. The transfection technique utilized in my study was electroporation, where short pulses of an electric field is used to obtain a transient permeability of the cell membrane, thus enabling the transfer of plasmids into the cell (Neumann et al. 1982).

For transfecting cells with specific plasmids, Neon^{TM} Transfection System (Thermo Fisher Scientific) and the associated 100 µl transfection kit was utilized. For each round of transfection, 2.2 million cells were resuspended in R buffer and 15 µg plasmid was added to the cell suspension. Next, transfection was performed using the 100 µl pipet provided by the kit, which was placed in the transfection cuvette containing 3 ml E2 buffer. MDA-MB-231 cells were transfected according to the setups indicated in Table 2. Transfected cells were plated on new cell culture plates and let to recover for 48 h after which they were treated with TGFβ-1 or StemXvivo to induce EMT.

Table 2. Electroporation parameters used for the transfection of MDA-MB-231 cells.

Cell line	Pulse voltage (V)	Pulse width (ms)	Pulse number	Cell density (cells/ml)	Tip type
MDA-MB-231	1350	10	4	2.2 x 10^7	100 µl

4.4.1 Transfection of cells for luciferase reporter assay

In order to elucidate which part of the HSF2 promoter is responsible for regulating HSF2 gene expression during EMT, luciferase reporter assay was used. For this purpose, MDA-MB-231 cells were transfected with plasmids where different regions of the HSF2 promoter was driving the expression of a luciferase gene (Figure 12A). In addition, two positive controls were generated for these experiments by transfecting cells with plasmids where a SNAI2 or an MMP9 promoter was driving the expression of the luciferase gene (Figure 12A). These promoters were selected since the expression of their corresponding genes are known to be induced upon EMT. An additional control was obtained by transfecting cells with an empty pSTARR plasmid containing the luciferase gene. Furthermore, each transfection was accompanied by a co-transfection of 5 µg β-galactosidase plasmid to enable β-galactosidase activity measurement and allow normalization of transfection efficiency for the luciferase reporter assay. In β-galactosidase plasmids, a ubiquitously active viral promoter is driving the expression of an *E. coli* lacZ gene, which allows quantification of β-galactosidase in transfected cells and the use of it as an internal control for normalization.

4.4.2 Transfection of cells for wound healing assays

In order to determine whether HSF2 impacts the cellular invasion capacity during EMT, the wound healing assay method was used. For this assay, I needed to generate cells that continuously overexpress exogenous HSF2, even upon active EMT. Hence, MDA-MB-231 cells were transfected with plasmids where the gene expression of HSF2 and GFP was driven by a cytomegalovirus (CMV) promoter. This construct also contained a *Thosea asigna* virus 2A self-cleaving peptide (T2A) sequence between the two genes to allow ribosomal skipping and, thus, the production of two distinct proteins instead of one fusion protein. The CMV-HSF2-T2A-GFP plasmid had been generated prior to this experiment. In order to generate a control for the wound healing assay, cells were transfected with a plasmid encoding GFP (pEGFP-N2). Cells expressing GFP plasmids maintain a basal level of endogenous HSF2 expression, which can be affected by stimulating EMT, thus functioning as control in the assay.

4.4.3 Transfection of cells for western blot analysis

To study whether HSF1 modulates the downregulation of HSF2 gene expression during EMT, western blot analysis was utilized. For this purpose, I needed to generate cells where the gene expression of endogenous HSF1 was downregulated. In order to achieve this, MDA-MB-231 cells were transfected with a plasmid encoding an shRNA molecule targeting HSF1 (shHSF1).

Short hairpin RNAs (shRNAs) are a commonly used technique of RNA interference (RNAi) to knock-down the production of a specific endogenous protein. In the cytosol, the shRNA is first processed into small interfering RNA (siRNA) by an enzyme called Dicer, enabling its binding to the target mRNA through complementary base pairing. The degradation of target mRNA is achieved via an enzymatic pathway involving the endogenous RNA-induced silencing complex (RISC), which exploits the siRNA to recognize and bind to the target mRNA, and the protein Argonaute (Ago), which is responsible for the cleavage event initiating the degradation process (Elbashir et al. 2001).

Additionally, a control for the western blot analysis was generated by transfecting cells with plasmids encoding a so called scrambled control (Scr) shRNA molecule. A scrambled control contains randomly rearranged siRNA or shRNA sequences, and will induce the RNAi pathway, however the sequence is designed in such manner that it should not target any specific mRNA sequence.

4.5 In-fusion cloning

In-fusion cloning is a method to introduce a desired DNA sequence into a vector. The method relies on the use of a plasmid vector, which is linearized at a specific target site and utilizes a commercial kit containing In-Fusion Enzyme to incorporate a desired DNA fragment at this target site. The vector is linearized and amplified in a polymerase chain reaction (PCR) using forward and reverse primers (Figure 8: A). PCR is a method to exponentially amplify a desired DNA sequence and it relies on thermal cycling which involves repeated rounds of heating and cooling. The DNA helix is denatured during the heating step, which enables primer-binding to the complementary sequences when the temperature is lowered. These primers function as starting points for DNA polymerase to begin complementary strand synthesis, thus generating a copy of the original DNA strand. A linearized plasmid vector is obtained

during PCR amplification as the DNA polymerase uses the specific forward and reverse primers as starting points for strand elongation, leaving a nick between the back ends of the primers, thus resulting the production of a linear DNA strand (Figure 8A). The insert fragment is also amplified with PCR using forward and reverse primers, but the primers used for this PCR reaction have 15-base pair (bp) overhangs that are complementary to the ends of the linearized vector (Figure 8B). Thus, when the linearized vector, amplified fragment of interest, and 5x In-Fusion HD Enzyme Premix (Takara Bio) are mixed together in an in-fusion cloning reaction, the fragment will be incorporated into the vector via homologous recombination events that occur between the complementary sequences (Figure 8C).

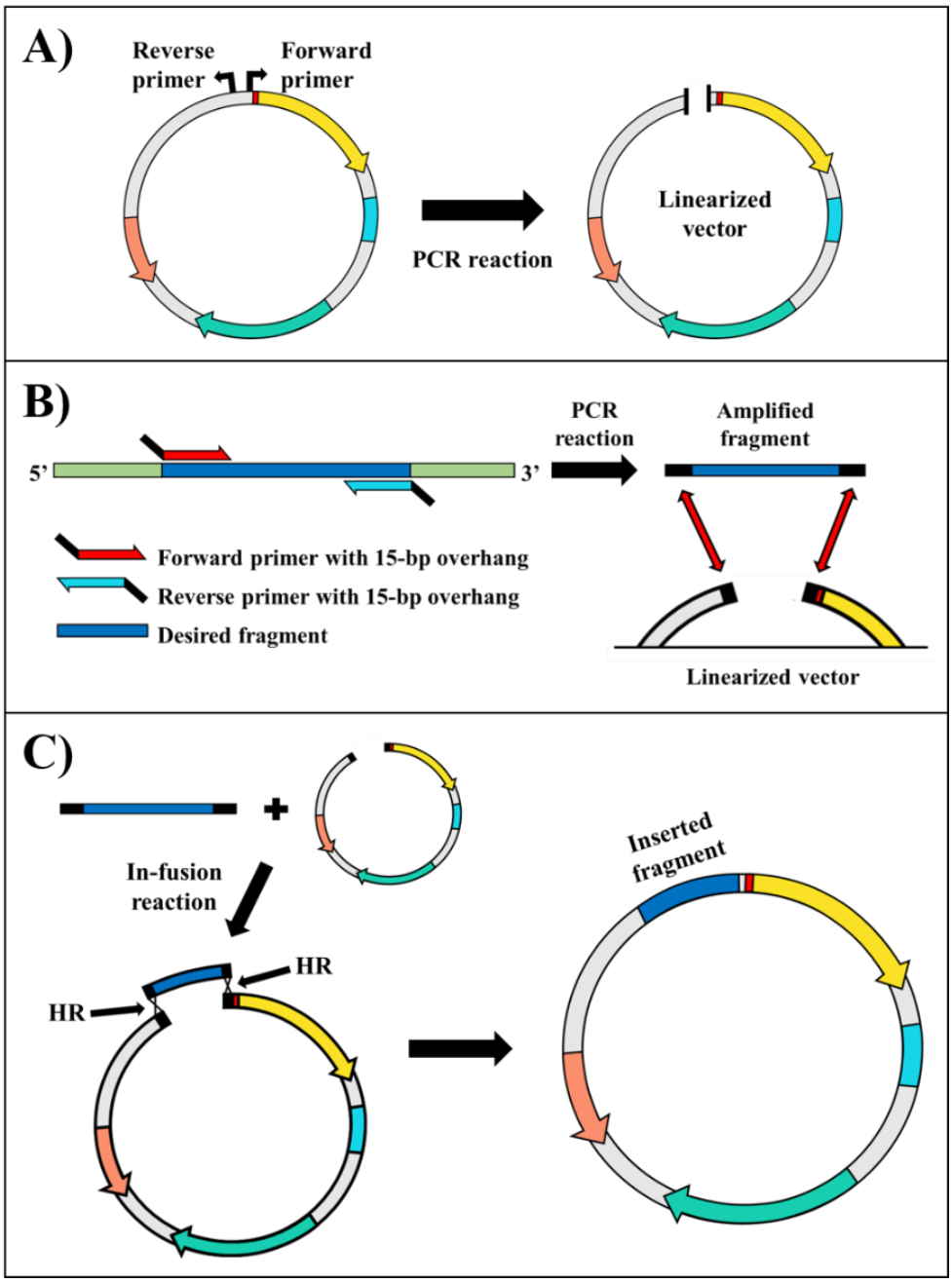

Figure 8. Schematic of the basic steps in in-fusion cloning. A) The in-fusion cloning technique is based on the use of a linearized vector, which is obtained via a PCR reaction. In this reaction, forward and reverse primers (black arrows) are used that amplify the vector and linearize it at the desired insertion site. The site where the vector is linearized (indicated as black lines in the linearized vector) is used in the following steps and will ultimately function as the site of fragment insertion. **B)** The fragment of interest is amplified from DNA in a PCR reaction also by using forward and reverse primers. However, these primers are unique in the sense that they contain specifically designed 15-base pair (bp) overhangs (indicated as red arrows), that are fundamental for the subsequent in-fusion reaction step. **C)** The final step in the in-fusion cloning technique is the in-fusion cloning reaction, where the amplified fragment, containing the 15-bp overhangs, and the linearized vector are mixed in an in-fusion cloning reaction together with 5x In-Fusion HD Enzyme Premix (Takara Bio). In this reaction, the fragment is incorporated into the vector through homologous recombination (HR) events that take place between the complementary sequences displayed by the fragment overhangs and the ends of the linearized vector.

In-fusion cloning was used to generate reporter constructs that enabled me to determine which part of the HSF2 promoter is accountable for suppressing HSF2 gene expression during EMT. For this purpose, two plasmids were generated where the gene expression of luciferase was driven either by a 2.5 kb HSF2 promoter region containing the 5'UTR of HSF2 (pHSF2-2.5kb), or a 1 kb HSF2 promoter region lacking the 5'UTR of HSF2 (pHSF2-1kb-(Δ5'UTR)). Additionally, in-fusion cloning was also used to generate two control plasmids, where the gene expression of luciferase was driven either by a SNAI2 promoter (pSNAI2) or an MMP9 promoter (pMMP9). These promoters were selected based on the known EMT-induced function of their corresponding genes, therefore they function as positive controls when assessing induction of EMT.

4.5.1 In-fusion cloning reaction

The first step in the in-fusion cloning technique was to linearize the vector at the desired fragment insertion site. For this purpose, a plasmid containing a luciferase gene, STARR-seq luciferase validation vector_ORI_empty (#99297, AddGene), was used in a PCR reaction with primers indicated in Table 3. These forward and reverse primers were designed using SnapGene software to linearize the vector at the desired site upstream of the luciferase gene.

Table 3. Primers used for pSTARR-luciferase vector linearization.

Target DNA		**Primer sequence**
pSTARR-luciferase vector	Forward primer	5'-GCCACCATGGAAGATGCCAAAA-3'
	Reverse primer	5'-AGCTTCAAAATCCCTTAACGTGAG-3'

In order to amplify and linearize the vector in a PCR reaction, 1x Q5 Reaction Buffer (New England BioLabs), 0.16 mM dNTP, 0.5 µM forward primer, 0.5 µM reverse primer, 15 ng vector DNA, 1 mM MgCl, and 0.02 U/µl Q5 High-Fidelity DNA Polymerase (New England BioLabs) were mixed together. RNase-free H_2O was used to adjust the reaction volume to 25 µl. The reaction mixture was then placed in a PCR machine and a PCR reaction was performed according to the settings indicated in Table 4.

Table 4. Thermocycling conditions used for PCR.

Step	Temperature (°C)	Time
Initial Denaturation	98	2 min
29 cycles	98 Gradient: 59 and 63 72	10 s 30 s 30 s/kb
Final Extension	72	2 min
Hold	4	∞

Following the PCR reaction, the linearized vector was separated on a 1 % agarose gel (see recipe attachment), which was prepared by mixing 0.4 g agarose with 40 ml 1x Tris-Borate-EDTA (TBE) buffer (see recipe attachment), and 2 µl Midori^{Green} (NIPPON Genetics). The prepared agarose gel was placed in an electrophoresis machine and 1x TBE was applied to the machine chamber. The TBE buffer contains EDTA, which is a chelator of divalent cations, hence inactivating many nucleases that rely on the use of divalent cations for their function, thereby protecting DNA from being enzymatically degraded. Borate induces the buffering capacity of TBE, and since Tris is a base, the combination of borate and Tris maintains a nearly neutral pH in the buffer keeping DNA deprotonated and soluble in water. Additionally, Midori^{Green} is a non-carcinogenic alternative to the traditionally used ethidium bromide, and it is added to the gel solution in order to visualize the DNA with UV light. Next, 5 µl 6x DNA Gel Loading Dye (ThermoFisher Scientific) and 0.4 µl glycerol were added to the PCR reaction product. The DNA Gel Loading Dye contains two dyes that enable visual tracking of DNA migration, and EDTA, which protect DNA against enzymatic degradation. The addition of glycerol makes the sample heavier and ensures that the sample DNA forms a layer at the bottom of the well. A GeneRuler 1 kb DNA Ladder (ThermoFisher Scientific), also supplemented with 6x DNA Gel Loading Dye and glycerol, was added in the first well of the agarose gel to allow size estimation of the amplified DNA product, and the linearized vector sample was pipetted into the following well. An electric field of 70 V was applied on the gel for 40 min to enable separation of DNA. The phosphate backbone of DNA is negatively charged and will therefore result in the migration of DNA fragments towards the positively charged anode when an electric field is applied. Since DNA has a uniform mass-to-charge ratio the separation is based on size, however several factors affect the rate of migration including e.g. agarose concentration, conformation of

DNA, applied voltage, and used electrophoresis buffer. The agarose polymer contains negatively charged sulphate and pyruvate groups. These functional groups enable a process called electroendosmosis in which a flow of water in the opposite direction of DNA movement is generated, dampening the movement of DNA fragments and resulting in the blurring of bands. Next, bands of correct sizes were excised from the gel and the DNA was purified by a commercial kit, PureLink Quick Gel Extraction and PCR Purification Combo Kit (Invitrogen).

To purify DNA from the gel, 900 µl of Gel Solubilization Buffer (L3) was first added to the tube containing the excised gel and incubated at 50 °C at least 10 min until the gel slice had dissolved. The tube was inverted a few times during the incubation to accelerate the dissolving process. Next, 300 µl of isopropanol was added to the dissolved gel and the solution was mixed thoroughly. The solution was then pipetted onto a column inside a wash tube and centrifuged at 12,000 x g for 1 min. The flow-through was discarded and the column was next washed by adding 500 µl Wash Buffer (W1) and centrifuging at 12,000 x g for 1 min. The wash buffer contains ethanol, which washes salts and impurities away while the DNA remains in the column. The flow-through was again discarded and the columns were then moved to new tubes and dried by an additional centrifugation at maximum speed for 3 min. Subsequently, the column was placed in a new eppendorf tube and 30 µl RNase-free H_2O was added to the column followed by a 5-minute incubation at RT and a centrifugation at 12,000 x g for 1 min to elute the DNA. Finally, the DNA concentration was measured using the NanoDrop machine and the purified DNA was stored at 4 °C.

The next step in the in-fusion cloning technique was to amplify the desired promoter DNA fragment (Figure 12A: pHSF2-2.5kb, pHSF2-1kb-(Δ5'UTR), pSNAI2, and pMMP9) and generate 15-bp overhangs that were complementary to the linearized pSTARR-luciferase vector. In order to achieve this, a larger DNA region, approximately 3-5 kb, containing the desired promoter and the surrounding sequence area, was first amplified from genomic DNA isolated from human embryonic kidney 293 (HEK 293) cells in a PCR reaction (Figure 9). It was necessary to first amplify and purify a larger promoter region as the 15-bp overhang primers would result in several amplification products, if used directly in a PCR reaction with genomic DNA. One PCR reaction was made for HSF2, another for SNAI2, and a third for MMP9. The PCR reaction mixtures were prepared similarly as described for the reaction where

the vector was linearized, however HEK 293 genomic DNA was used as template DNA in these reactions, and distinct forward and reverse primers were used for respective reaction (Table 5). The PCR reactions were performed according to the thermocycling conditions indicated in Table 4. The PCR products from these reactions were separated on an agarose gel, excised, and the DNA fragments were purified as described earlier.

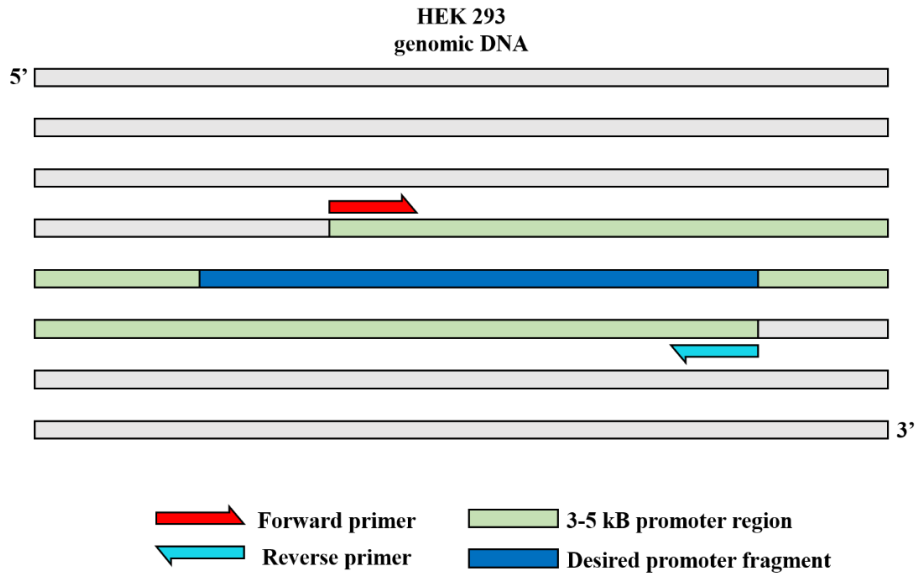

Figure 9. Amplification of 3-5 kb promoter region from HEK 293 genomic DNA. Promoter regions (light green), containing the desired promoter fragment (blue) and the surrounding sequence areas, were first amplified from genomic DNA isolated from HEK 293 cells (grey). This was achieved by a PCR reaction using forward (red) and reverse (turquoise) primers, that were designed to amplify the sequence between them, resulting in a PCR product of the promoter region approximately 3 to 5 kb in size.

Table 5. Primers used for amplifying 3-5 kb promoter regions, containing the specific promoter fragment and surrounding sequence areas, from HEK 293 genomic DNA.

Target DNA		Primer sequence
MMP9	Forward primer	5'-TGGCTTCCTTACTGACGGTG-3'
	Reverse primer	5'-TCAAAGCCTCCACAAGACCC-3'
SNAI2	Forward primer	5'-CGGCTTGCGTTTTTACCACA-3'
	Reverse primer	5'-CTTCTCCCCCGTGTGAGTTC-3'
HSF2	Forward primer	5'-CCAAGGTGGCAGATCACTTGA-3'
	Reverse primer	5'-GGTTCATTCTGCTCTCCACTC-3'

The obtained purified DNA containing a 3-5 kb promoter region of HSF2, SNAI2, and MMP9 were next used for another PCR reaction. The purpose of this reaction was to amplify the specific promoter fragment and generate the 15-bp overhangs (Figure 10), which were required for the homologous recombination to succeed. For this purpose, forward and reverse primers, containing overhangs complementary to the ends of the linearized pSTARR-luciferase vector, were designed using SnapGene software (Table 6). Next, separate PCR reactions were performed to obtain the specific fragments for 2.5 kb of the HSF2 promoter (HSF2-2.5kb), 1 kb of the HSF2 promoter (HSF-1kb-(Δ5'UTR)), the SNAI2 promoter, and the MMP9 promoter. These reactions were done similarly as the reaction that linearized the vector, using the respective purified 3-5 kb promoter region DNA as a template. The PCR products from each of the four reactions were separated on an agarose gel, excised, and the DNA purified as described previously. Each purified promoter fragment with overhangs and the linearized pSTARR-luciferase vector were next used in an in-fusion cloning reaction.

Table 6. Primers used for amplifying the specific promoter fragment and generating 15-bp overhangs.

Promoter		**Primer sequence**
MMP9	Forward primer	5'-CTGACGCTCAGTGGAACGAATGAGCCGAGATCACGCCAC-3'
	Reverse primer	5'-TTGGCATCTTCCATGGTGGCGACTGCAGCTGCTGTTGTGGGGG-3'
SNAI2	Forward primer	5'-CTGACGCTCAGTGGAACGAACTGCAATGGACAGAGATGCT-3'
	Reverse primer	5'-TTGGCATCTTCCATGGTGGCCTTGCCAGCGGGTCTGG-3'
HSF2-2.5 kb	Forward primer	5'-AGGGATTTTGAAGCTTCTCAAAATGCGGTCCCAGGG-3'
	Reverse primer	5'-ATCTTCCATGGTGGCTGTTAACGCGGCGCAGG-3'
HSF2-1kb-(Δ5'UTR)	Forward primer	5'-CGTTAAGGGATTTTGAAGCTGTTTTTGCCTTCACATGCTG-3'
	Reverse primer	5'-TTGGCATCTTCCATGGTGGCAATCCCAGGAGCCGACTG-3'

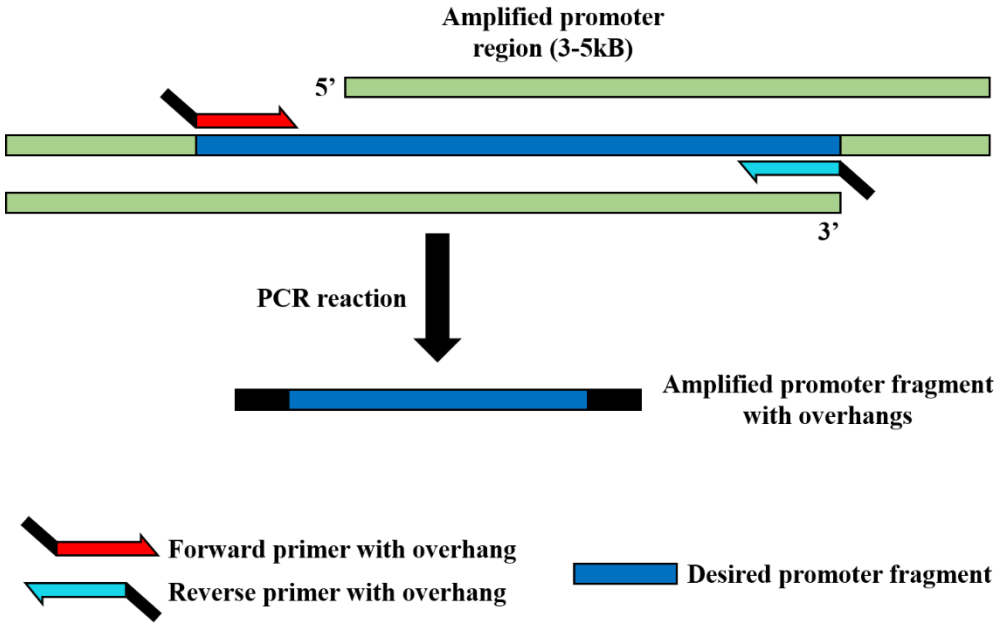

Figure 10. Amplification of promoter fragment and generation of overhangs. In order to obtain the specific promoter fragment from the previously amplified 3-5 kb promoter region, forward and reverse primers were designed to specifically amplify the promoter fragment of interest (blue). Additionally, these primers displayed a unique feature as they also contained 15-bp overhangs, which were designed to be complementary to the ends of the linearized vector. Thus, the resulting PCR product contained the amplified promoter fragment of interest with overhangs at its 5' and 3' ends.

The final step in the in-fusion cloning technique was to perform the in-fusion cloning reaction with the amplified and purified linear pSTARR-luciferase vector and each of the generated promoter fragments with overhangs (HSF2-2.5kb, HSF-1kb-(Δ5'UTR), SNAI2, and MMP9). During this reaction, the promoter fragment will be incorporated into the linearized vector via homologous recombination that occur between the complementary sequences of the fragment overhangs and the ends of the linearized vector, as depicted in Figure 8: C. In each reaction 5 ng of the linearized pSTARR-luciferase vector, 1 ng of the promoter fragment, and 0.5 µl of 5x In-Fusion HD Enzyme Premix (Takara Bio) were mixed. RNase-free H_2O was added to the mixture to adjust the reaction volume to 2.5 µl. Next, the mixture was incubated at 50 °C for 15 min, whereafter each construct was separated on a 1% agarose gel to verify construct size, and then transformed into bacteria.

4.5.2 Bacterial Transformation

Plasmids generated through the in-fusion cloning reaction were next transformed into *Escherichia coli* (*E. coli*) Stellar Competent cells (Takara Bio) with the purpose of

creating bacterial colonies expressing each plasmid. This *E. coli* strain lacks the gene cluster that cuts methylated DNA and, additionally, possesses a highly efficient transformation capacity, making it specifically useful for cloning purposes. Stellar competent cells were first thawed on ice. Next, 1-2 µl of in-fusion cloning product was pipetted into 30 µl of bacteria and the mixture was incubated on ice for 30 min. The incubation was followed by a 45-second heat shock at 42 °C, to increase cell membrane permeability and allow entry of DNA into the cells. Next, cells were incubated on ice for 2 min to allow the membrane to restore, before the addition of 400 µl of Super Optimal Broth with Catabolite repression (SOC) medium, which is a nutritional medium used to further support the recovery of the cells. The mixture was then incubated on a shaker at 37 °C for 60 min. Subsequently, 200 µl of LB medium was added, and 300 µl of the mixture was spread out on a prewarmed agar plate containing ampicillin. The agar plate was then incubated at 37 °C overnight. Finally, grown bacterial colonies were selected for subculturing and plasmids were isolated for sequencing, which was required to confirm that each fragment had been incorporated appropriately into the vector.

4.5.3 Site-directed mutagenesis

Following sequencing of the generated plasmids, three point mutations were observed in the promoter region of the pHSF2-2.5kb plasmid. These mutations were corrected using site-directed mutagenesis in which specific primers for each mutated site were made. These primers were complementary to the HSF2 promoter sequence except for the correcting one-nucleotide-change at the site of mutation (Figure 11A). The primers hybridize to the complementary sequence of HSF2-2.5kb during PCR, where a special type of DNA polymerase, PfuTurbo, is used. PfuTurbo DNA polymerase replicates the plasmid strands without displacing the primers, hence the primers containing the correcting mutations will remain intact in the newly synthesized vector (Figure 11B). The PCR reaction linearizes the plasmids by leaving gaps on the back-side of the primers, resulting in so-called nicked circular strands (Figure 11B). The non-mutated parental DNA is digested with a restriction enzyme that specifically targets methylated DNA, and since the newly synthesized nicked circular strands are unmethylated, they are resistant against this degradation. In the final step of site-directed mutagenesis, the nicked circular strands are transformed into competent bacterial cells, which are able to repair the nicks during replication and re-establish circular plasmids (Figure 11B).

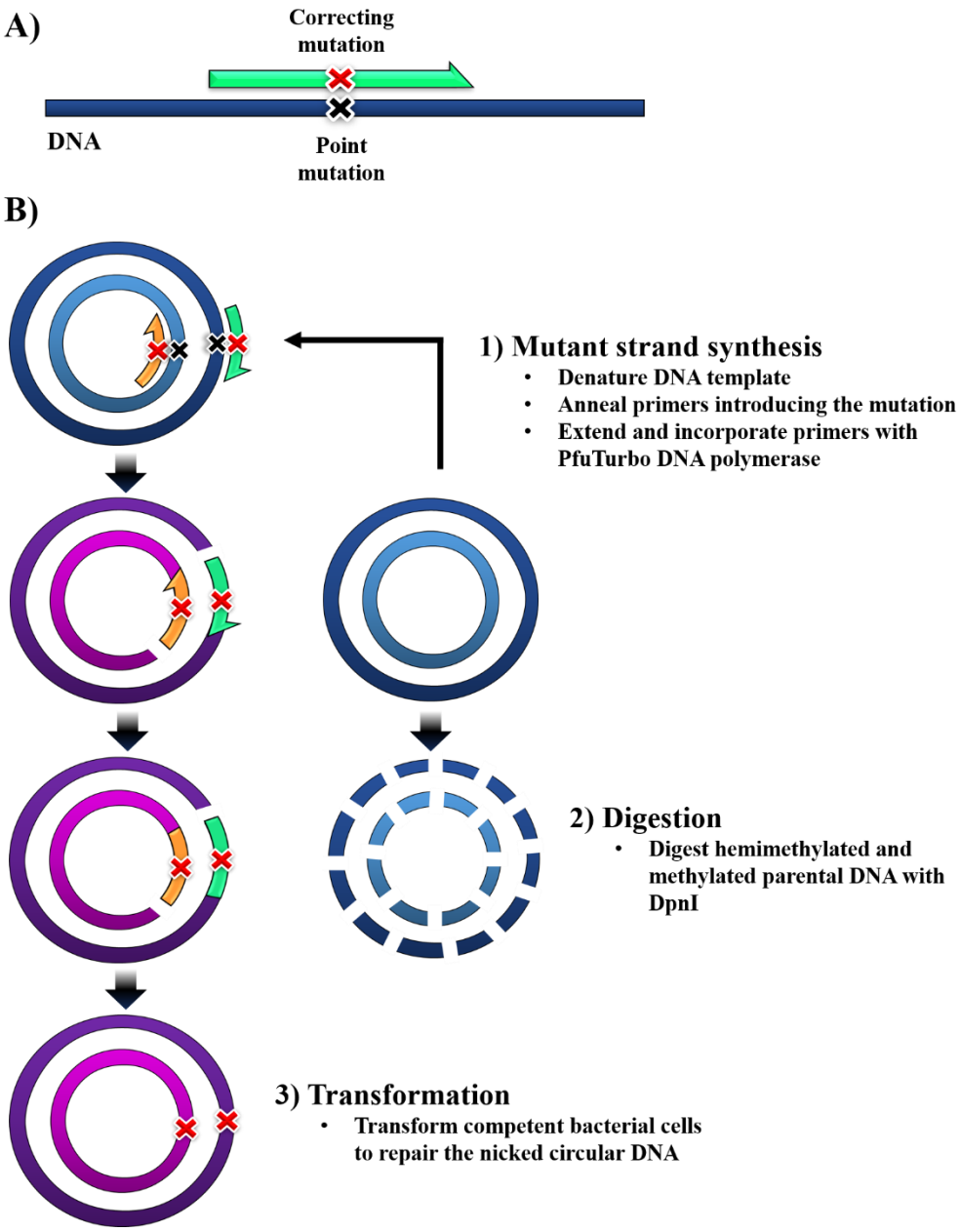

Figure 11. The principle of site-directed mutagenesis. A) The plasmid DNA (blue) contains a mutated nucleotide (black cross) in its sequence. The forward primer used in a site-directed mutagenesis reaction binds to the plasmid DNA as it displays otherwise a fully complementary sequence to the plasmid DNA, expect for the one nucleotide that is the correcting mutation (red cross). For simplicity, only the forward primer is indicated in this figure. **B) 1)** A PCR reaction is performed with parental DNA template (blue) containing the site of mutation (indicated as black crosses), oligonucleotide primers (orange and green) introducing the correcting mutation (indicated as red crosses), and high-fidelity PfuTurbo DNA polymerase. During the temperature cycling in PCR, the DNA template is denatured and oligonucleotide primers are allowed to anneal to the template. PfuTurbo DNA polymerase extends and incorporates the oligonucleotide primers, without displacing the primers, resulting in nicked circular DNA containing the correcting mutation. **2)** The hemimethylated and methylated parental DNA is digested with DpnI restriction enzyme, which specifically targets methylated DNA, thus the newly synthesized nicked circular DNA is protected against its enzymatic degradation. **3)** In the final step of site-directed mutagenesis, the nicked circular DNA is transformed into competent bacterial cells that are able to repair the nicks, resulting in an intact, fully functional plasmid.

The mutagenesis primers were designed, using SnapGene and Primer-BLAST software, so that both the forward and reverse primers for each of the three mutations contained the desired mutation site in the middle region of the approximately 30 nucleotides long primer. The T_m value for mutagenesis primers was approximately 70 °C. The mutagenesis reaction was done by employing the QuickChange XL Site-Directed Mutagenesis Kit (Agilent Technologies). In the sample reaction, 15 ng of double-stranded DNA (dsDNA) template was mixed with 2.5 µl of 10x reaction buffer, 0.75 µl (10 µM) of each forward and reverse mutagenesis primer (Table 8), 0.5 µl of dNTP mix, 1.5 µl of QuickSolution, and RNase-free H_2O to achieve a total reaction volume of 25 µl. Finally, 0.5 µl (2.5 U/µl) of PfuTurbo DNA polymerase was added prior to initiation of thermal cycling. PfuTurbo DNA polymerase is a combination of Pfu DNA polymerase and thermostable ArchaeMaxx polymerase-enhancing factor, and it enables amplification of complex target DNA in a high yield, without displacing the mutant oligonucleotide primers, and with a low error rate. A PCR reaction was then performed as indicated in Table 7.

Table 7. Thermocycling conditions used for site-directed mutagenesis.

Cycles	Temperature (°C)	Time
1	95	1 min
17	95 60 68	50 s 50 s 1 min/kb
1	68	7 min
Hold	4	∞

Following PCR reaction, 0.5 µl (10 U/ µl) of DpnI restriction enzyme (Agilent) was added to the reaction product in order to cleave methylated DNA lacking the corrected mutations, and incubated at 37 °C for 60 min. DpnI is a type IIM restriction enzyme that specifically cleaves methylated or hemimethylated adenine at its GATC recognition sequence in DNA. Since the newly synthesized PCR-amplified DNA, containing the corrected mutation, is unmethylated, it is resistant against DpnI, whereas the parental DNA lacking the correction is methylated and is thereby prone to digestion by the enzyme. Subsequently, the site-directed mutagenesis reaction product was sequenced to verify whether the mutation had been successfully corrected. A similar procedure was carried out to revise each observed mutation in the

HSF2-2.5kb promoter region. Finally, the vector containing the corrected mutations in the HSF2-2.5kb promoter fragment, was then transformed into bacteria as previously described.

Table 8. Primers used for site-directed mutagenesis.

Mutation		Primer sequence
1.	Forward primer	5'-GAATGTCCAAAGACAAGTTTCTGCTTCTATCTAATCACACCTTCT-3'
	Reverse primer	5'-AGAAGGTGTGATTAGATAGAAGCAGAAACTTGTCTTTGGACATTC-3'
2.	Forward primer	5'-AAGAGATATACATATATCTTCCATTAAATGATAGATATATATTTAATGTACTATTTTACATTCACCC-3'
	Reverse primer	5'-GGGTGAATGTAAAATAGTACATTAAATATATATCTATCATTTAATGGAAGATATATGTATATCTCTT-3'
3.	Forward primer	5'-GGCGTTCTCGGGGAGCTGCTGCCGT-3'
	Reverse primer	5'-ACGGCAGCAGCTCCCCGAGAACGCC-3'

4.5.4 Plasmid shortening

In order to generate additional plasmids containing either a 2 kb, 1 kb, or 0.5 kb region or just the 5'UTR of the HSF2 promoter (Figure 12A: pHSF2-2kb, pHSF2-1kb, pHSF2-0.5kb, and pHSF2-5'UTR), the previously generated pHSF2-2.5kb plasmid was shortened using a three-step process that involved linearization of the circular plasmid, phosphorylation of the 5' DNA ends, and ligation in order to re-establish a circular plasmid. In the first step, the pHSF2-2.5kb plasmid was linearized in four separate PCR reactions, which were performed similarly as previously described for the vector linearization reaction, using distinct forward and reverse primers to generate a shortened version of the pHSF2-2.5kb plasmid (Table 9). Each of these primers were designed to linearize the pHSF2-2.5kb plasmid at a specific site so that when the DNA polymerase elongated the plasmid DNA during PCR, a desired region of the HSF2 promoter was excluded (Figure 12B). The PCR products from each of the four reactions were then separated on an agarose gel, excised, and the DNA was purified as described previously.

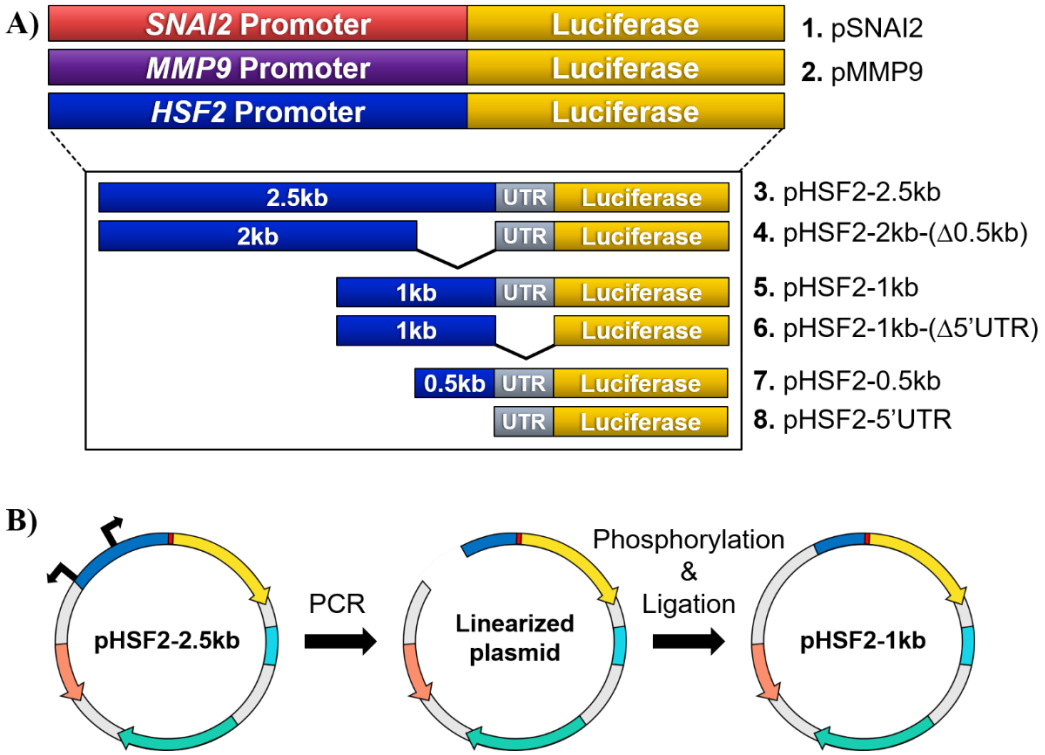

Figure 12. The constructs generated for luciferase reporter assay and the mechanism of plasmid shortening. A) Each promoter, SNAI2, MMP9, and HSF2, were cloned into the vector upstream of a luciferase gene. The designated nomenclature of constructs is indicated on the right (Δ indicates the removed fragment). Six different constructs containing a region of the HSF2 promoter were generated. The black line between the promoter region and the UTR or the luciferase gene, respectively, indicates that a fragment was deleted from this position. **B)** In the plasmid shortening approach, the pHSF2-2.5kb plasmid was first linearized in a PCR reaction using forward and reverse primers (black arrows), which were designed to exclude a specific region from the promoter. After a PCR reaction, a linearized plasmid is obtained that lacks a specific region of the HSF2 promoter. Subsequent phosphorylation of the ends of the linearized plasmid followed by a ligation reaction reseals the plasmid generating a construct that contains a shorter region of the HSF2 promoter. This figure illustrates the generation of pHSF2-1kb from the pHSF2-2.5kb plasmid via plasmid shortening.

In the second step, the 5' end of the linearized plasmid DNA is phosphorylated to obtain a 5' phosphate, which is required for the subsequent ligation to be successful. The DNA 5' end phosphorylation is achieved by T4 Polynucleotide Kinase (T4 PNK, New England BioLabs), which is an enzyme that catalyzes both the transfer and exchange of inorganic phosphate (P_i) from ATP to the 5' end of DNA (Figure 13), and removes phosphoryl groups from the 3' end of DNA. The DNA 5' end phosphorylation enables ligation and resealing of the plasmid in the third step, which relies on the use of T4 DNA Ligase (New England BioLabs). T4 DNA Ligase is an enzyme that catalyzes phosphodiester bond formation between juxtaposed 5' phosphate and 3' hydroxyl ends in double-stranded DNA (Figure 13), that is, between the phosphorylated ends of the linearized vector.

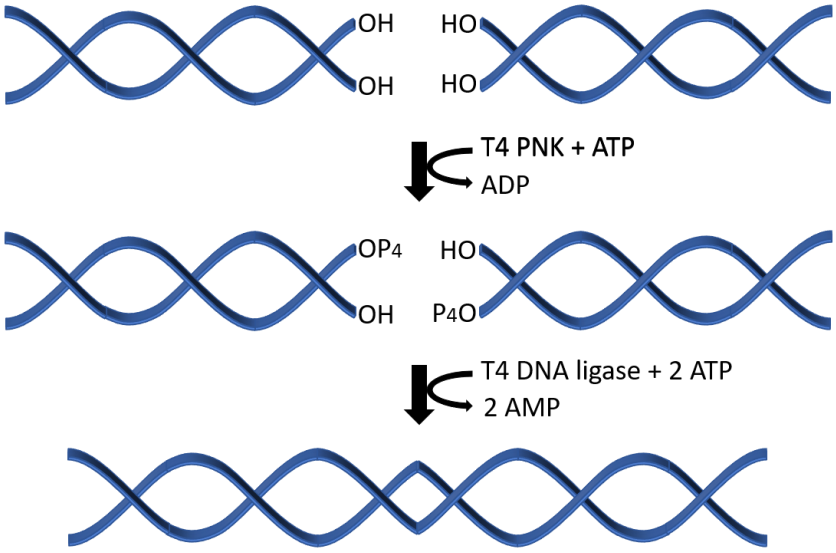

Figure 13. DNA 5' end phosphorylation and phosphodiester bond formation during ligation. In the first reaction, T4 polynucleotide kinase (T4 PNK) catalyzes the transfer and exchange of inorganic phosphate from ATP to the free 5' hydroxyl end of DNA, resulting in phosphorylation of the 5'end of DNA and the generation of ATP. In the second reaction, T4 DNA ligase catalyzes phosphodiester bond formation between the two DNA molecules. The enzymes requires ATP as a cofactor in the reaction where two ATP molecules are consumed to form two AMP molecules and a single phosphodiester bond. The phosphodiester bond is formed between the 3' hydroxyl group of the acceptor and the 5' phosphate group of the donor.

Table 9. Primers used for amplifying HSF2-2kb, HSF2-1kb, HSF2-0.5kb, and HSF2-5'UTR fragments.

Promoter region		**Primer sequence**
HSF2-2kb	Forward primer	5'-CGGAGACTTGTCCGTCACGT-3'
	Reverse primer	5'-CAGTCATCAAGTGCCTACTC-3'
HSF2-1kb	Forward primer	5'-GTTTTTGCCTTCACATGCTG-3'
	Reverse primer	5'-AGCTTCAAAATCCCTTAACGTGAG-3'
HSF2-0.5kb	Forward primer	5'-GGCACTTGATGACTGGAT-3'
	Reverse primer	5'-AGCTTCAAAATCCCTTAACGTGAG-3'
HSF2-5'UTR	Forward primer	5'-CGGAGACTTGTCCGTCACGT-3'
	Reverse primer	5'-AGCTTCAAAATCCCTTAACGTGAG-3'

To establish the 5' end phosphorylation of the four newly linearized plasmids, 15 ng of each purified fragment DNA was mixed in a separate reaction with a commercial kit of 10x T4 PNK Buffer (New England BioLabs), 1 mM ATP, 10 U (units) T4 PNK enzyme (New England BioLabs), and RNase-free H_2O to adjust reaction volume to 25 µl. The mixture was then incubated at 37 °C for 2 h followed by a 10-minute heat-inactivation at 75 °C to inactivate the enzyme. Next, the linearized vectors containing the phosphorylated ends were used in four different ligation reactions. In these reactions, 15 ng of linearized vector was mixed with Quick Ligase Reaction Buffer (2x), 0.5 µl of Quick T4 DNA Ligase (New England BioLabs), and RNase-free H_2O to adjust reaction volume to 25 µl. Finally, the reaction mixtures were incubated at RT overnight and the reaction products were separated on a 1% agarose gel to verify that each shortened plasmid was of correct size. Each plasmid was subsequently used to transform bacteria as previously described.

4.6 Luciferase reporter assay

Luciferase assay is a method applied to indirectly measure gene transcription. It is a widely used technique due to its relatively low cost, high sensitivity, as well as a simple and fast mode of action. The assay is based on the use of a plasmid, which contains a promoter sequence that drives the expression of a luciferase gene. The luciferase gene is originated from *Phoinus phyralis*, more commonly known as the firefly. This gene encodes for a 61 kDa enzyme that functions to oxidize its substrate, D-luciferin, when Mg^{2+}, O_2, and adenosine triphosphate (ATP) are accessible (Figure 14). In principle, the luciferase enzyme catalyzes D-luciferin oxidation through a chemical energy conversion powered by electron transition, leading to the production of oxyluciferin and quantitatively measurable fluorescent light (Brasier & Ron, 1992; Fan & Wood, 2007). Hence, by quantifying the amount of produced luciferase, the level of target gene transcription can indirectly be measured. In addition, another reporter assay, β-galactosidase, is traditionally used to normalize the transfection efficiency in the luciferase reporter assay system.

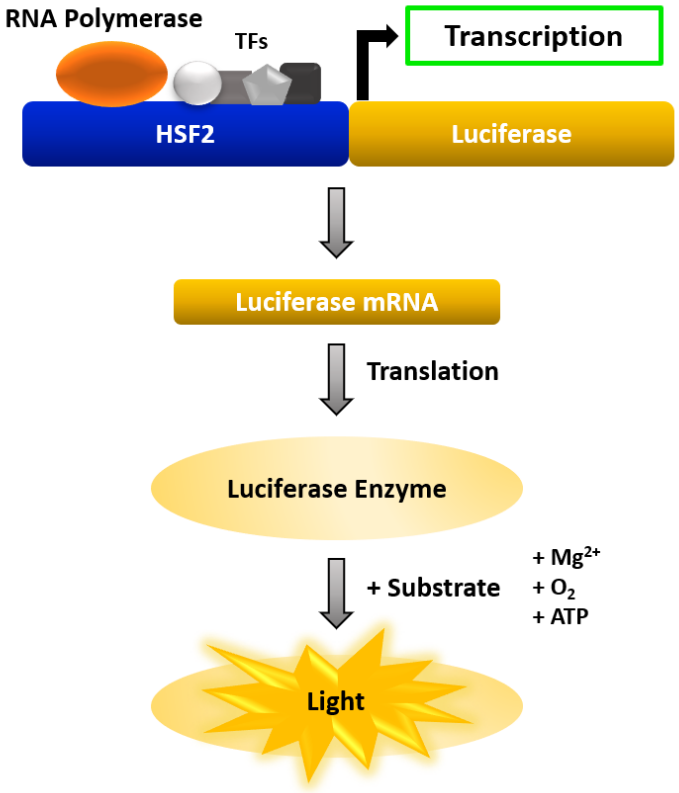

Figure 14. Schematic illustration of the luciferase reporter assay.
A genetic regulatory element, called a promoter, (blue) is placed upstream of a luciferase gene in a plasmid and the construct is transfected into cells. The promoter will determine to what extent the luciferase gene is expressed. Transcription of the luciferase gene results in the production of luciferase mRNA, which is subsequently translated into luciferase enzyme. The produced luciferase enzyme oxidizes its substrate, D-luciferin, in an in vitro reaction when Mg^{2+}, O_2, and ATP are present. This oxidation reaction results in the production of fluorescent light, which can be detected using a luminometer. The measured fluorescence is then analyzed and used to quantify the amount of luciferase, which is in a direct proportion to the promoter activity, thus enabling indirect assessment of target gene transcription. TFs = Transcription factors. (Figure modified from ThermoFisher Scientific User Manual).

Previous results from Professor Lea Sistonen's laboratory have indicated that HSF2 is downregulated on the transcriptional level. Owing to this discovery, one of the main goals of this thesis was to determine which part of the HSF2 promoter is responsible for regulating HSF2 gene expression during EMT. Thus, it was necessary for me to utilize the luciferase reporter assay in order to indirectly assess the level of HSF2 transcription. Hence, with the aim of identifying the specific HSF2 promoter region accountable for controlling HSF2 gene expression upon active EMT, multiple constructs were generated, each containing a variously sized portion of the HSF2 promoter sequence placed upstream of the luciferase gene. In addition, two positive controls were generated for this experiment, where either an SNAI2 promoter or an

MMP9 promoter was driving the expression of the luciferase gene. These promoters were selected since their corresponding genes are known to be upregulated during EMT. Furthermore, an additional control, an empty pSTARR vector containing the luciferase gene, was also used in this experiment.

Thus, MDA-MB-231 cells were transfected with plasmids expressing pSTARR-luciferase, pSNAI2, pMMP9, or one of the pHSF2-luciferase gene constructs. The 48-hour recovery was followed by a 4-hour or a 24-hour TGFβ-1 treatment, and the luciferase signal was measured for each sample under control conditions and upon EMT stimuli.

4.6.1 Measurement of luciferase activity

Passive lysis buffer (1x) was used as a blank solution and 3 µl was pipetted in the first three wells of a 96-well Packard plate. Next, 3 µl of each sample was pipetted as triplicates in the following wells, and 18 µl of 1x Passive lysis buffer was then added to each well. Finally, 90 µl of luciferase assay substrate solution, BriteLite Plus (Perkin Elmer), was applied to each well directly before initiating the analysis. The luciferase activity was then measured using Hidex Sense Microplate Reader (Hidex) with the following setup: luminescence IR cutoff 1 s. Measured values were normalized by utilizing β-galactosidase assay and the obtained data was processed by using Microsoft Excel.

4.7 β-galactosidase assay

β-galactosidase is a commonly used reporter gene to control the transfection efficiency in a reporter assay such as the luciferase method. In this assay, cells are co-transfected with a control plasmid, where a ubiquitously active viral promoter is driving the expression of an *E. coli* lacZ gene, in addition to the experimental plasmid encoding the promoter of interest and the luciferase gene. In this way, the amount of β-galactosidase in cells can be measured and, thus, used as an internal control in the transient transfection experiment. Special characteristics making β-galactosidase a highly suitable reporter gene, includes its especially stable nature and capacity to resist cellular proteolytic degradation. β-galactosidase is an enzyme that functions to hydrolyze lactose as well as the analog of galactosidase called o-nitrophenyl-β-D-galactopyranoside (ONPG) (Nielsen et al. 1983; Kang et al. 2002). During the

hydrolysis, ONPG substrate is converted into galactose and o-nitrophenol, which is a chromophore responsible for the observed change in coloration, resulting in a yellow-colored solution. The produced chromophore is directly proportional to the β-galactosidase expression, thus enabling quantitative measurement of β-galactosidase activity in the solution by using a microplate reader or a spectrophotometer.

In this experiment, the β-galactosidase activity was measured in order to normalize the transfection efficiency of cells used in the luciferase assay. The transfection of cells with pSTARR-luciferase, pSNAI2, pMMP9, and each HSF2 gene construct was therefore accompanied by a co-transfection of plasmids encoding β-galactosidase.

4.7.1 Measurement of β-galactosidase activity

In order to verify transfection efficiency and normalize the measured luciferase signals, β-galactosidase activity for respective sample was determined. This was done by employing the β-galactosidase assay. First, ONPG buffer was prepared shortly before use (see recipe attachment). Second, 1x Passive lysis buffer was once again used as a blank solution and 3 µl was pipetted in the first three wells of a 96-well plate. Concomitantly, 3 µl of each sample lysate was added in the following wells as triplicates. Third, 200 µl of ONPG buffer was applied to each well. The plate was then covered with transparent tape, to prevent evaporation, and incubated for at least 30 min at 37 °C until the color had turned yellowish. Finally, the β-galactosidase activity was assessed by measuring the absorbance at 420 nm using the Hidex Sense Microplate Reader (Hidex).

4.8 Wound healing assay

The directional migration capacity of cells during wound healing can be studied *in vivo* by utilizing a simple and inexpensive technique called wound healing assay. This method is useful in estimating cancer cell migration, hence it is commonly applicable for quantifying the migratory capacity of cells. The basic steps in this assay involve culturing of cells to a confluent monolayer, followed by the creation of a scratch to the confluent cell sheet, mimicking a wound, and ultimately the monitoring of wound closure by real-time imaging (Figure 15) (Grada et al. 2017). Images are captured at the beginning and in regular intervals until the wound has closed. The wound area within each image is compared and analyzed, enabling quantification of cell migration

and the rate of wound closure. The wound healing assay was utilized in this experiment to clarify whether HSF2 affects the migration capacity of MDA-MB-231 cells during EMT.

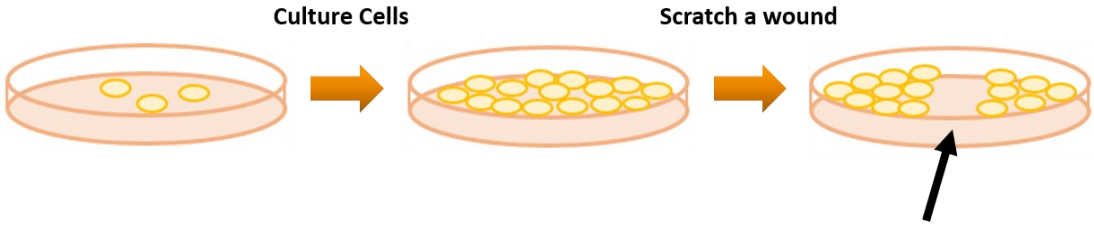

Figure 15. Schematic of the wound healing assay. In the wound healing assay cells are first plated and cultured until a suitable confluency is reached. A scratch is then made in the middle of the cell plate, indicated with the arrow, to mimic a wound. Finally, real-time imaging of wound closure is performed, and the rate of cell migration can subsequently be calculated based on the changes in area coverage over time.

4.8.1 The wound healing assay procedure

In order to determine if HSF2 affects cell migration during EMT, a setup of cells were made that overexpress exogenous HSF2 continuously, hence HSF2 is present in the cells both during control and EMT conditions. For this purpose, one set of MDA-MB-231 cells was transfected with a plasmid encoding HSF2 and another set of cells was transfected with a plasmid encoding GFP. Transfected cells were plated on a 12-well-plate so that six wells each contained 0.5 million cells of HSF2-overexpressing cells and each of the other six wells contained 0.5 million cells of GFP-expressing cells. In this way, three technical repeats were obtained for each biological replica. The cells were let to recover for 48 h before proceeding with the treatments.

Following recovery, culturing medium was aspirated and the transfected cells were washed with 1x PBS. Next, one set of cells was pre-treated for 3 h with assay medium (2% serum) supplemented with 10 ng/ml TGFβ, and a control set was treated only with assay medium. Thus, four different samples were generated for each biological replica, where cells overexpressing exogenous HSF2 and cells transfected with GFP were either treated with TGFβ-1, to induce EMT (HSF2 TGFβ and GFP TGFβ), or retained as untreated control cells (HSF2 C and GFP C).

Following the 3 h pre-treatment, a scratch was made in the confluent cell sheet of each well by using a 10 µl pipet tip. Next, the cell plate lid was replaced with a special lid that enables gas exchange, including CO_2, in the imaging machine. The cell culture plate was then placed in the Cell-IQ machine (Chip-Man Technologies), and the

wound closure process was imaged at three different positions in each well with a frame interval of 5 min for 24 h at 37 °C. Following the real-time imaging of cell migration, the acquired image data was analyzed with ImageJ and Prism for statistical analysis.

4.9 Western blot

Western blot is a commonly used method that combines several sub-techniques to allow for the detection of a specific protein. The method includes sodium dodecyl sulphate polyacrylamide gel electrophoresis (SDS-PAGE), transfer, and immunoblotting. In SDS-PAGE, proteins are separated in a polyacrylamide gel by utilizing gel electrophoresis. The proteins are subsequently moved from the gel to a nitrocellulose membrane, during transfer, with the help of an electric field. Finally, immunoblotting is used to identify a particular protein by using antibodies that specifically bind to the protein of interest.

Western blot was used in this experiment to determine whether HSF1 affects the downregulation of HSF2 during EMT. MDA-MB-231 cells expressing Scr and shHSF1 plasmids were treated with XV for 24 h, and specific antibodies were used to detect the level of HSF1, HSF2, and Hsc70 proteins in samples under control and EMT stimuli.

4.9.1 SDS-PAGE

Linearized proteins that display an overall negative charge due to SDS can be separated on a polyacrylamide gel by employing the SDS-PAGE method. For this purpose, cells were first lysed in 3x Laemmlie lysis buffer to denature and linearize the proteins, and boiled for 10 min to further support the denaturation process. Next, 8 µl of a protein marker, Dual-Color (Bio-Rad), was added into the first well of a polyacrylamide gel (see recipe attachment) to enable size evaluation of the separated proteins. An equal volume of protein lysates were subsequently applied into the following wells of the gel, and the proteins were separated by SDS-PAGE using an electric field of 120 V.

The polyacrylamide gel has multiple properties that contribute to the protein separation during gel electrophoresis. Firstly, the gel is constituted of a pore structure network created by acrylamide polymerization, which establishes the basis of protein

separation by dampening protein band migration along the gel. Secondly, the gel comprises two layers with distinct characteristics, an upper gel with a pH 6.3, and a lower gel with a pH 8.8. pH is a function of the ratio between H_3O^+ and OH^- ions. The buffer used in SDS-PAGE, 1x Running buffer (see recipe attachment), contains negatively charged chloride ions and glycine ions, whose charge depends on the prevailing pH in the environment. In the upper gel, the glycine ions display a neutral charge, and together with the negatively charged chloride ions, assist condensation of proteins to a tightly packaged band. The neutrally charged glycine ions dampen the movement of the negatively charged protein band in the upper gel, also maintaining the proteins as a tightly packaged band. However, when reaching the lower gel, the prevalent higher pH and negatively charged environment results in a change in the charge of the glycine ions. Thus, glycine ions obtain a negative charge and rapidly migrate towards the positively charged pole. Since the glycine ions no longer dampen the protein band movement, proteins are allowed to begin the migration towards the positively charged pole. The migration speed of a protein is based on its isoelectric point (pI), which encompasses a mass-to-charge ratio within a certain environment. Therefore, the proteins that are negatively charged due to the surrounding SDS are separated in a negative ion environment prevalent in the lower gel. However, the overall environment can be considered as neutral, hence it is ultimately the internal negative charge of the protein that drives its migration, but as the pores in the gel will dampen the migration of large proteins, it enables the separation of proteins of different sizes. Thus, proteins are separated in SDS-PAGE according to their size, but the separation is facilitated owing to the proteins' pI and the negatively charged environment.

Following SDS-PAGE, proteins were transferred from the polyacrylamide gel to a nitrocellulose membrane by utilizing an electric field, where negatively charged proteins move towards a positively charged pole. Ions are able to pass through the nitrocellulose membrane but proteins attach to the membrane through strong hydrophobic interactions. For transferring proteins from the gel to a nitrocellulose membrane a transfer machine, Semi-Dry Transfer Trans-Blot SD (Bio-Rad), was used. The polyacrylamide gel was placed on top of a nitrocellulose membrane and three layers of Whatman paper (Whatman) were laid on each side. Whatman papers were soaked in 1x Transfer buffer (see recipe attachment) prior to placement. The transfer

was then performed by utilizing an electric field of 25 V for 45 min. After the transfer of proteins, the membrane was incubated in a milk solution in order to saturate the membrane with proteins, hence reducing unspecific binding of antibodies to the membrane during the immunoblotting process.

4.9.2 Immunoblotting and ECL

Immunoblotting is a method that utilizes primary and secondary antibodies to detect particular proteins on a nitrocellulose membrane. In immunoblotting, primary antibodies bind specifically to their antigens. The secondary antibodies, which bind specifically to the primary antibodies, are coupled to horseradish peroxidase (HRP), enabling specified protein detection in a process called enhanced chemiluminescence (ECL). Consequently, when the membrane is treated with a luminol solution to induce ECL, HRP functions as a catalyst in a reaction where luminol is oxidized, resulting in freeing of photons that can be registered on a light-sensitive film. Hence, this method specifically enables the detection of the protein of interest.

During immunoblotting, specific antibodies were used to detect HSF2, HSF1, and Hsc70 protein levels in XV-treated and untreated control cells. A milk solution, containing 5% milk in PBS supplemented with 0.3% Tween 20 (PBS-0.3% Tween), was used to saturate the membrane during a 60-minute incubation at room temperature (RT) to avoid unspecific binding of antibodies to the membrane. The membrane was then washed three times with PBS-0.3% Tween for a period of 10 min each time and subsequently incubated with a primary antibody overnight at 4 °C. Primary antibodies, with respective dilutions, that were used in this study are indicated in Table 10. The primary antibodies were diluted in PBS containing 0.5% bovine serum albumin (BSA), and 0.02% sodium azide (NaN_3). The membrane was thereafter washed again three times with PBS-0.3% Tween before a one-hour incubation at RT with the secondary antibody (Table 10). The secondary antibodies were diluted in PBS-0.3% Tween supplemented with 3% milk. Next, the membrane was washed three times as previously and then treated with an ECL solution for 1 min. Finally, light-sensitive X-ray films (Medical X-ray film Super RX, Fuji) were utilized to detect the light produced by luminol in the oxidation reaction.

Table 10. Primary and secondary antibodies used for immunoblotting.

Primary antibody	Source	Dilution	Secondary antibody	Source	Dilution
HSF2 Sigma, HPA031455	Rabbit	1:500	**anti-Rabbit** Promega, W401B	Goat	1:10,000
HSF1 Stressgen, SPA-901	Rabbit	1:1000	**anti-Rabbit** Promega, W401B	Goat	1:15,000
Hsc70 Stressgen, SPA-815	Rat	1:3000	**anti-Rat** GE Healthcare, NA935V	Goat	1:3000

4.10 Statistical analysis

The values obtained from the luciferase reporter assay were analyzed in Microsoft Excel. A paired t test with a two-sided distribution was used for the statistical analysis and all control samples were set to 1. The luciferase values were also normalized to the measured β-galactosidase values for each corresponding sample in order to normalize the overall protein expression. The statistical analysis provided p values and the significance was indicated as stars: one star indicating a p value less than 0.05,and two stars indicating a p values less than 0.01. Analyzed results that were not significant (ns) had a p value above 0.05.

In the wound healing assay, images of each wound were taken every 5 minutes for 24 h, and the area of wound was measured with the MRI Wound Healing Tool of ImageJ. The initial wound area was compared to the wound area of each time point to calculate the percentage of wound closure over time. Due to minor variations in the acquisition time of images within biological replicas, the percentage of wound closure at specific time points was interpolated from all the values within each biological replica. The interpolation was performed using a polynomial function, which in turn was determined by the distribution of values corresponding to wound closure percentage. The statistical significance was analyzed with two-way ANOVA and Holm-Sidak's post hoc test using GraphPad Prism software. The statistical analysis was done using the values from last points of each curve in the obtained graph.

5 Results

5.1 Size verification of plasmids generated for luciferase reporter assay

Plasmids are commonly used as vectors in order to obtain cells that express a desired protein. In this thesis, one of the main aims was to determine which part of the HSF2 promoter regulates HSF2 expression upon EMT and luciferase reporter assay was used for this purpose. In order to successfully perform this assay, cells expressing luciferase were required. Thus, I had to generate multiple plasmids containing varying regions of the HSF2 promoter upstream of the luciferase gene to indirectly asses the promoter activity upon EMT and during control conditions. Two positive controls for the luciferase reporter assay were also made, where the gene expression of luciferase was driven either by an SNAI2 promoter or an MMP9 promoter. The four initially generated plasmids were prepared utilizing the in-fusion cloning technique as described in detail in section 4.5.1, whereas four additional plasmids were generated using plasmid shortening as described in section 4.5.4.

Besides sequencing, an additional approach was used to clarify that each gene construct was of correct size and had been successfully created. Hence, each completed plasmid was separated on a 1% agarose gel to allow estimation of construct size with the help of a GeneRuler 1kb DNA Ladder (ThermoFisher Scientific). The results from the DNA separation of the linearized pSTARR-luciferase vector and each plasmid are illustrated in Figure 16. The linearized pSTARR-luciferase vector is approximately 4000 base pairs in size and this was verified by the agarose gel electrophoresis (Figure 16. Panel A: lane 2). The positive controls, pSNAI2 and pMMP9, had construct sizes of approximately 5300 and 5400 base pairs, respectively. The sizes of these constructs were also verified to be correct (Figure 16: Panel B: lane 2 and 3). Each generated gene construct contained the same vector, thus the constructs containing different sizes and regions of the HSF2 promoter varied in size depending on how large fragment of the HSF2 promoter had been incorporated into the vector. The sizes of these gene constructs were validated to be correct as shown in Figure 16, where the pHSF2-2.5kb construct was demonstrated to be larger than pHSF2-2kb-(Δ-0.5kb), pHSF2-1kb, and pHSF2-1kb-(Δ5'UTR) (Figure 16. Panel C: lane 2, 3, 4, and 5, respectively). Also, the construct sizes for the smallest gene constructs, pHSF2-0.5kb and pHSF2-5'UTR, were confirmed to be correct and only a minor shift in the size was observed, as was expected (Figure 16. Panel D: lane 2 and 3).

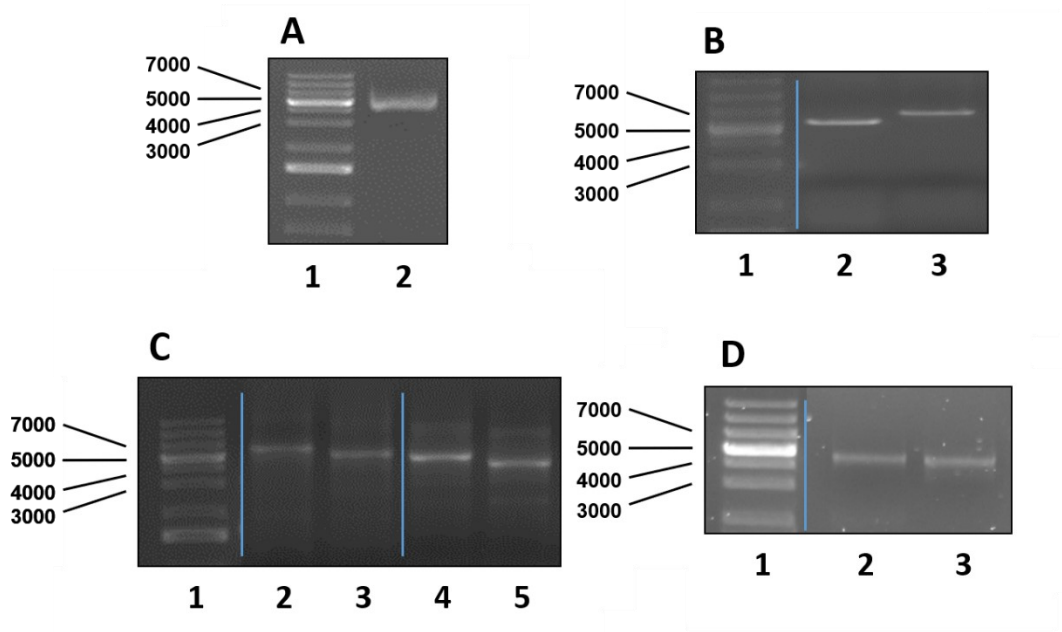

Figure 16. Agarose gel electrophoresis of plasmids generated for luciferase reporter assay. Lane 1 in each panel contained a GeneRuler 1kb DNA Ladder to allow size estimation of DNA bands, and the sizes indicated on the side of each panel are in bp. The lanes are numbered to clarify naming of samples. The blue lines between lanes indicate that a section had been excised from this area. **Panel A)** Lane 2: linearized pSTARR-luciferase vector. **Panel B)** Lane 2: pSNAI2 and lane 3: pMMP9 constructs. **Panel C)** Lane 2: pHSF2-2.5kb, lane 3: pHSF2-2kb-(Δ0.5kb), lane 4: pHSF2-1kb, and lane 5: pHSF2-1kb-(Δ5'UTR). **Panel D)** Lane 2: pHSF2-0.5kb and lane 3: pHSF2-5'UTR.

5.2 The 5' UTR of HSF2 is important for the downregulation of HSF2 during EMT

In order to determine which part of the HSF2 promoter is responsible for regulating HSF2 gene expression during EMT, several constructs containing different parts of the HSF2 promoter were analyzed by luciferase assay. Additionally, in the assays two positive controls were added, which contained promoters from SNAI2 and MMP9. These promoters were specifically selected since they are acknowledged EMT responsive genes. Furthermore, cells were transfected with an empty pSTARR plasmid with the purpose of generating an additional control, and each transfection was accompanied by a co-transfection of β-galactosidase to enable normalization of transfection efficiency. The plasmids were expressed in MDA-MB-231 cells, which were treated with TGFβ-1 for 4 or 24 h to induce EMT, or retained as untreated control cells (Ctrl).

The measured values from the assay were analyzed in Excel, and the results are presented in Figure 17. Each control was set to 1, followed by statistical analysis using a paired t test with a two-sided distribution. The analyzed results showed that cells expressing pHSF2-2.5kb, pHSF2-2.5kb-(Δ0.5kb), pHSF2-1kb, pHSF2-0.5kb, and pHSF2-5'UTR, display a significant reduction in the luciferase signal following TGFβ-1 treatment (Figure 17). Furthermore, pSTARR levels were not significantly changed (Figure 17. pSTARR), and the SNAI2 and MMP9 expressing cells displayed an increased luciferase expression in response to the treatment (Figure 17. pSNAI2 and pMMP9), which was expected. Surprisingly, the construct where the 5'UTR of HSF2 had been removed displayed no change in the luciferase signal following TGFβ-1 treatment (Figure 17. pHSF2-1kb-(Δ5'UTR): Ctrl vs. TGFβ-1). This indicates that the 5'UTR of HSF2 affects the regulation of HSF2 expression during EMT. In contrast to the other measurements, the observed luciferase signal for this sample was similar to the untreated control.

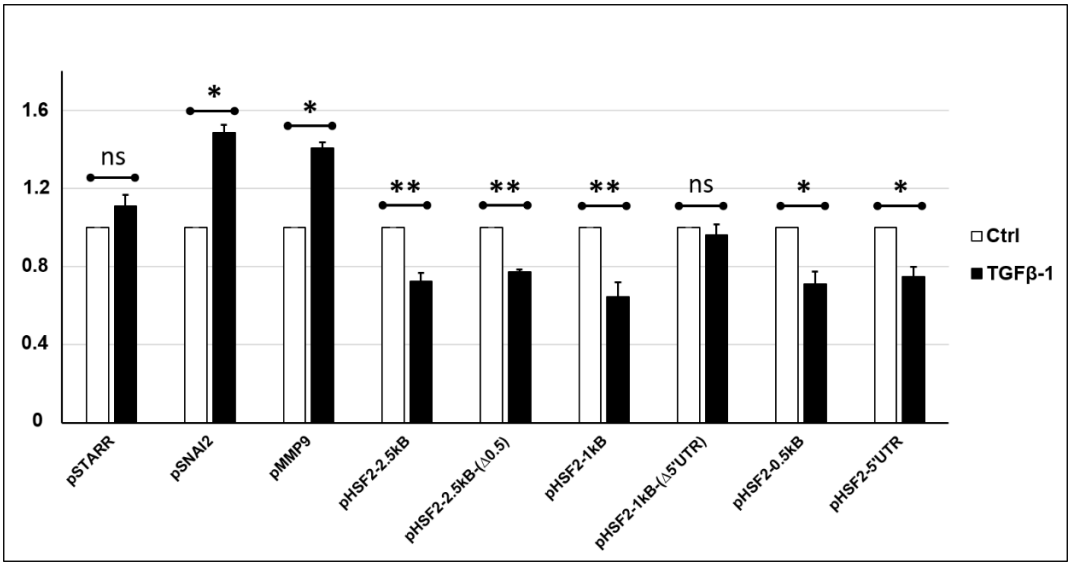

Figure 17. The effect of TGFβ-1-induced EMT on HSF2 promoter activity. The level of luciferase gene expression was assessed by luciferase assay in untreated control cells (Ctrl) and after a 24-hour TGFβ-1-treatment. Exceptionally, SNAI2 and MMP9 were instead treated for 4 h. MDA-MB-231 cells were transfected either with an empty pSTARR plasmid or with plasmids containing the promoters for SNAI2, MMP9, or one of the constructs comprehending a varying region and size of the HSF2 promoter. The prefix Δ indicates the region that had been deleted from the construct. β-galactosidase assay was used to normalize the transfection efficiency. Ctrl values were set to 1, and the statistical analysis of the measurement was performed using a paired t test with a two-sided distribution: n for pSTARR and pHSF2 constructs = 3, n for pSNAI2 and pMMP9 = 2; mean + SEM; * indicates p value ≤ 0.05; ** indicates p value ≤ 0.01; ns indicates p value > 0.05 = not significant.

5.3 HSF2 inhibits the cell invasion capacity of MDA-MB-231 cells

To elucidate whether HSF2 impacts the cellular invasion capacity of MDA-MB-231 cells during control conditions or upon EMT, wound healing assays were performed using cells expressing exogenous HSF2 or GFP. Since the level of endogenous HSF2 is known to be downregulated upon activated EMT, generation of cells expressing HSF2 even after an EMT-inducing TGFβ-1 treatment was required. This was established by transfecting MDA-MB-231 cells with plasmids encoding CMV-HSF2-T2A-GFP (HSF2). Concomitantly, a control was generated for this experiment by transfecting cells with pEGFP (GFP) plasmids. A TGFβ-1 treatment was added on the transfected cells (TGFβ) 3 h before assay initiation. Additionally, some of the cells were retained as untreated controls (Ctrl). The invasion capacity of cells was subsequently monitored in a wound healing assay by performing real-time imaging for 24 h. The obtained image data was analyzed in ImageJ and the statistical analysis was done using GraphPad Prism. The results are presented in Figure 18 and Table 11, and an illustrating figure further supporting the results is presented in Figure 19.

The results showed that the rate of wound closure was similar in cells overexpressing exogenous HSF2 despite the TGFβ-1 treatment (Figure 18: HSF2 Ctrl and HSF2 TGFβ), indicating that the presence of HSF2 can repress the enhanced invasion capacity obtained by TGFβ-1-induced EMT. In contrast, the wound closure rate for cells expressing GFP was shown to be induced in response to the TGFβ-1 treatment when compared to the untreated counterpart (Figure 18: GFP TGFβ vs. GFP Ctrl), which was expected and also verified the functionality of the treatment.

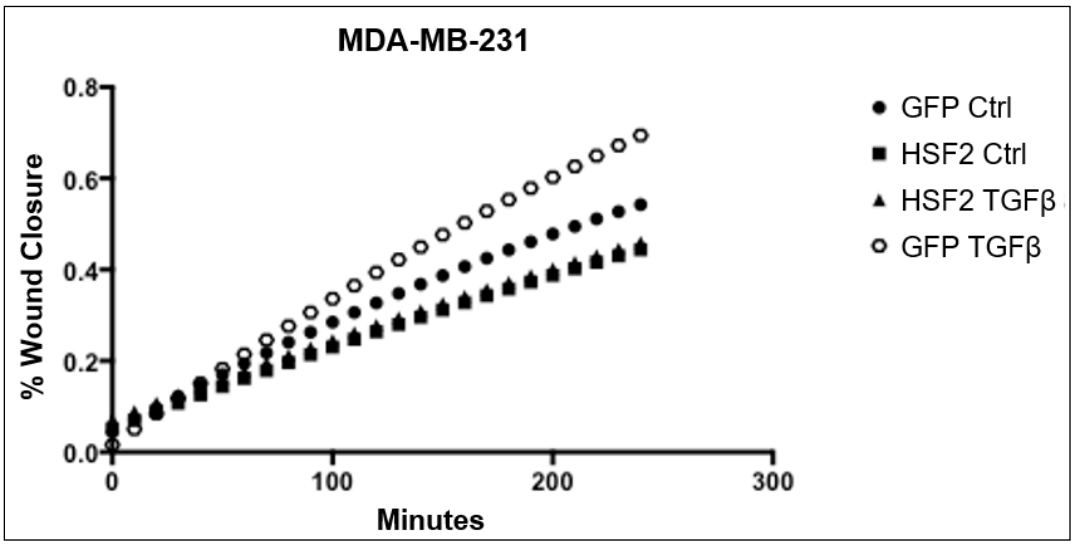

Figure 18. The measured wound closure rates of MDA-MB-231 cells expressing GFP or exogenous HSF2 under control conditions and EMT stimuli. The invasion capacity of cells expressing exogenous HSF2 or GFP was examined in a wound healing assay. Transfected cells were treated with 10 ng/ml TGFβ-1 (TGFβ) for 27 h or retained as untreated control (Ctrl) cells. Statistical analysis was performed using two-way ANOVA: n for GFP Ctrl = 3, n for HSF2 Ctrl = 3, n for GFP TGFβ = 3, n for HSF2 TGFβ = 3.

Furthermore, the statistical significance of wound closure rates were analyzed and compared using Holm-Sidak's post hoc test. These results confirmed the observations presented in Figure 18, showing that the difference between the wound closure rates of HSF2 Ctrl and HSF2 TGFβ samples was not significant (Table 11: HSF2 Ctrl vs. HSF2 TGFβ). This validated that the invasion capacity of cells overexpressing HSF2 was similar in both samples even after EMT was induced by TGFβ-1. This indicates that HSF2 can suppress EMT and the invasion capacity of MDA-MB-231 cells. In addition, the difference in the wound closure rates between GFP Ctrl and GFP TGFβ was shown to be statistically significant (Table 11: GFP Ctrl vs. GFP TGFβ), and thereby in accordance to the observation in Figure 18. Importantly, the statistical comparison of the wound closure rates between GFP TGFβ and HSF2 TGFβ were shown to be highly significant with a p value of <0.0001, also showing consistency to the results presented in Figure 18. The difference in wound closure rates between GFP Ctrl vs. HSF2 Ctrl was shown not to be significant, even though the curves were not similar in Figure 18. Hence, these results strongly suggest that HSF2 has an inhibiting effect on the cellular invasion capacity of MDA-MB-231 cells during EMT. The results presented in Figure 18 and Table 11 were also further verified by directly looking at images taken at different time points during the wound healing assay as presented in Figure 19.

Table 11. Analysis of statistical significance of measured wound closure rates in transfected MDA-MB-231 cells in the presence of EMT stimuli and under control conditions. The significance of compared pairs were analyzed statistically using Holm-Sidak's post hoc test: n for GFP Ctrl = 3, n for HSF2 Ctrl = 3, n for GFP TGFβ = 3, n for HSF2 TGFβ = 3; mean + SEM; * indicates p value ≤ 0.05; **** indicates p value ≤ 0.0001; ns indicates p value > 0.05 = not significant. The statistical analysis was done using the values from last points of each curve in Figure 18.

Compared pairs		p value
GFP Ctrl vs. HSF2 Ctrl	ns	0.2036
GFP Ctrl vs. GFP TGFβ	*	0.0138
HSF2 Ctrl vs. HSF2 TGFβ	ns	0.9895
HSF2 TGFβ vs. GFP TGFβ	****	<0.0001

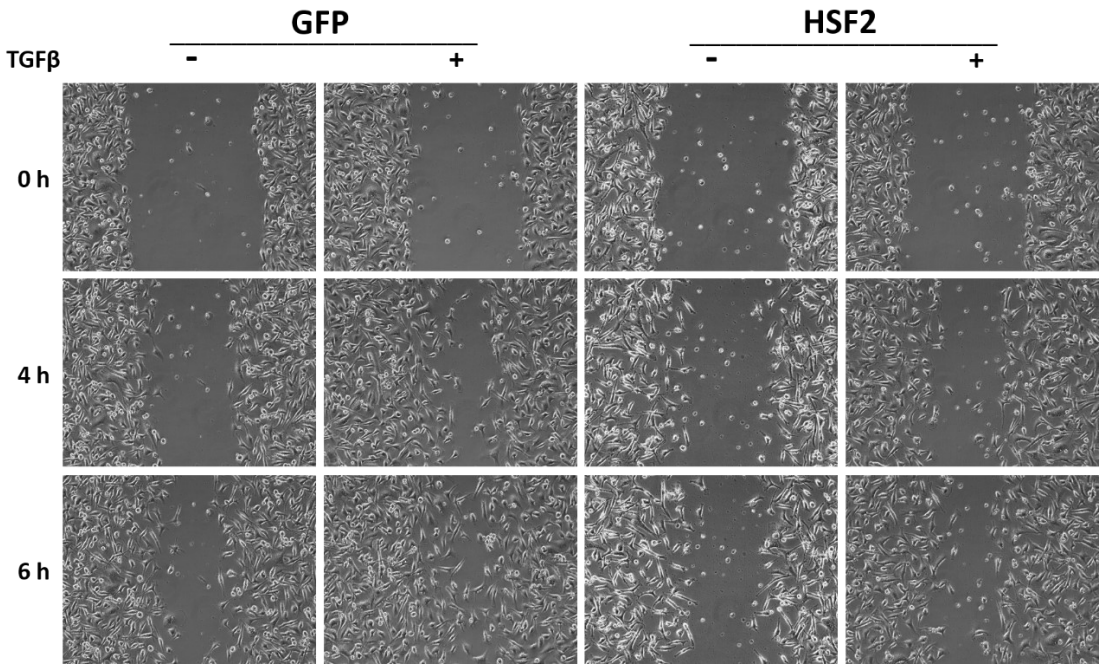

Figure 19. Representative figure of wound closure rates at different time points of cells expressing GFP or exogenous HSF2, during EMT stimuli or under control conditions. MDA-MD-231 cells expressing GFP or exogenous HSF2 were used for wound healing assays to assess the rate of wound closure in cells treated with 10 ng/ml TGFβ-1 or untreated control cells. Images were captured at the beginning (0 h), after 4 hours (4 h), and after 6 hours (6 h) to tract the rate of wound closure between these cells.

5.4 HSF1 does not affect the downregulation of HSF2 during EMT

HSF1 has previously been shown modulate HSF2 expression partially via affecting HSF2 promoter activity, which was demonstrated to result in transcriptional repression of HSF2 (Park et al. 2015). Thus, it was of high importance to determine whether it has an impact on the expression of HSF2 during EMT. In this experiment, MDA-MB-231 cells were transfected with a plasmid encoding either a so-called scrambled (Scr) control shRNA molecule or an shRNA molecule targeting HSF1 (shHSF1). These cells were treated with 10 µl/ml of an EMT-inducing supplement, StemXvivo (XV), for 24 h in order to achieve activation of EMT. Additionally, some cell samples were retained as untreated controls (Ctrl). Subsequently, western blot was performed using antibodies that specifically bind to HSF1, and HSF2 proteins. In addition, an Hsc70 antibody was used to verify equal loading of proteins in each sample.

The results presented in Figure 20 show that the level of HSF1 expression in cells transfected with Scr plasmids was slightly increased following an XV-treatment (Figure 20. HSF1 Blot: Scr; Ctrl vs. XV). Whereas, cells expressing shHSF1 displayed downregulation of the HSF1 protein both in the XV and Ctrl samples (Figure 20. HSF1 Blot: shHSF1; Ctrl and XV). This was expected, since the shRNA in the plasmid is specifically designed to target HSF1 mRNA and result in its degradation. Regarding HSF2 expression, the western blot result showed that the protein level of HSF2 was decreased, both in Scr and shHSF1 cells, in response to the XV treatment, when compared to the untreated counterparts (Figure 20. HSF2 Blot: Scr and shHSF1; Ctrl vs. XV). Despite the status of HSF1 expression a similar downregulation of HSF2 was observed in response to EMT stimuli, hence implying that HSF1 does not modulate the expression of HSF2 during EMT.

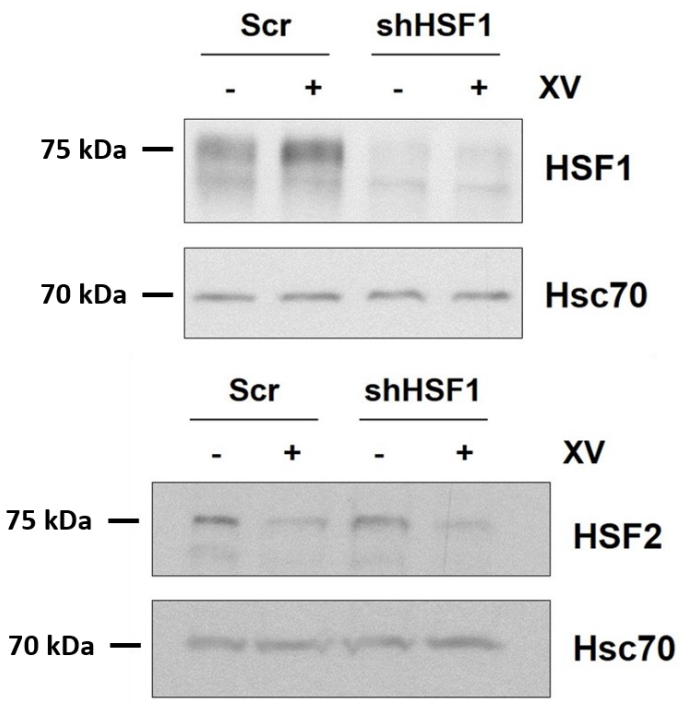

Figure 20. Representative western blot of HSF1 and HSF2 expression in MDA-MB-231 cells expressing Scr or shHSF1 plasmids during EMT stimuli and control conditions. The expression of HSF1 and HSF2 was examined in cells treated with StemXvivo (XV) for 24 h as well as in untreated control cells. MDA-MB-231 cells were transfected either with a Scramble (Scr) plasmid, which functioned as a control, or with an shHSF1 plasmid to obtain cells lacking endogenous HSF1. The level of protein expression was analyzed by immunoblotting using antibodies to specifically detect HSF1 and HSF2 proteins. In addition, an Hsc70 antibody was used to verify equal loading of proteins. Kilodaltons (kDa) indicate protein size.

6 Discussion

HSFs are transcription factors that initiate the HSR upon exposure to proteotoxic stress. However, these transcription factors also function in a variety of other cellular processes as well as during pathological conditions by regulating distinct transcriptional programs. Recently, several members of the HSF family have been demonstrated to display a function in cancer progression. A key process contributing to the invasion capacity of cancer cells is EMT, which can be induced by e.g. the TGFβ signaling pathway. One important member of the HSF family is HSF2, whose activity has recently been revealed to be modulated by active TGFβ signaling. Moreover, HSF2 has been implicated to display an inducing effect on malignant transformation in some forms of cancer, whereas a suppressive regulatory effect have been suggested for instance in prostate cancer progression (Björk et al. 2016). During the circumstances where HSF2 displays a suppressive effect on malignant transformation, its major regulatory activity has been implicated to be involved in the EMT process. In light of these findings, the major purpose of my thesis was to characterize what is the driving force regulating the transcriptional activity of HSF2 upon EMT and whether the expression of HSF2 impacts the cellular invasion capacity in a triple-negative breast cancer cell line during EMT.

6.1 The 5'UTR post-transcriptionally downregulates HSF2 during EMT in an HSF1-independet fashion

Plasmids encoding an HSF2 promoter region and a luciferase reporter gene were used in order to determine which part of the HSF2 promotor regulates HSF2 expression during EMT. Since I had to generate these plasmids myself, the size of each generated plasmid was verified by separating the DNA on a 1% agarose gel, which allowed estimation of construct sizes. Each construct was demonstrated to be of correct size as presented in Figure 16. As previously described, site-directed mutagenesis was used to correct three distinct point mutations in the pHSF2-2.5kb construct. It remains unclear whether these mutations are present in the HEK-293 genomic DNA, which was used as templated DNA to generate the initial constructs. However, in order to verify this, one would need to sequence this particular region in the genomic DNA of HEK-293 cells.

In the majority of HSF2-luciferase plasmids, the measured luciferase signal was decreased in response to an induced EMT, except for the plasmid where the 5'UTR of HSF2 was excluded, which displayed no change in the luciferase signal in response to EMT stimuli (Figure 17). These results suggest that the 5'UTR of HSF2 plays an important role in the post-transcriptional modulation of HSF2 upon EMT. The 5'UTR is a part of the gene that is transcribed into mRNA but is not translated into protein, and it is important for translation and post-translational modifications. Previous experiments in the Sistonen laboratory, conducted using an HSF2-1kb plasmid containing the 5'UTR, have shown that the luciferase signal is decreased already after a 6-hour TGFβ treatment, indicating that the process is not strictly time-dependent. Furthermore, my results are supported by previous research showing that the expression of HSFs, especially HSF1, is regulated in some cancers by miRNAs targeting the 5'UTR (Vivinus et al. 2001; Liang et al. 2018). Post-transcriptional regulation has also been reported for HSF2, illustrated by a study where a miRNA, called miR-18, was discovered to downregulate HSF2 expression during spermatogenesis, and the protein expression of HSF2 was in turn increased upon miR-18 inhibition (Björk et al. 2010). Taken together, it is interesting to speculate that a similar mechanism of miRNA binding to the 5'UTR of HSF2 would be responsible for the downregulation of HSF2 expression during EMT. Based on an miRNA-BLAST search (miRBase) potential miRNA targets binding to the 5'UTR of HSF2 are has-miR-4787-5p, has-miR-10400-5p, and has-miR-1237-5p. All of these miRNAs have been identified in unbiased genome-wide screens, and to date their functions are unknown. This type of regulation mechanism of HSF2 expression during EMT would also make sense as numerous studies have reported that the activity of transcription factors is in several different processes regulated by miRNAs binding to the 5'UTR sequence (Pandey & Picard, 2009; Caggiano et al. 2017; Guan et al. 2017; Li et al. 2017; Wongfieng et al. 2017; Shu et al. 2018). It would therefore be interesting to transfect cells expressing the HSF2-luciferase plasmids with commercially constructed siRNAs of miR-4787, miR-10400, and miR-12347. If the expression of HSF2 is modulated via this mechanism, these miRNAs should be able to mimic the TGFβ-treatment and induce downregulation of HSF2 during control conditions.

It is also possible that the molecule binding to the 5'UTR of HSF2 is a protein. In this case a feasible approach to determine what protein targets the 5'UTR could be to

utilize immunoprecipitation followed by mass-spectrometric analysis. In this method a specific nucleotide sequence, in my case the 5'UTR of HSF2, would be coupled to biotin. When this biotin-coupled nucleotide sequence is incubated in lysates, originating from cells undergoing EMT, the proteins will bind to the target sequence and the complex can be isolated with immunoprecipitation, in which biotin-specific antibodies are used. Subsequently, in order to identify the bound protein, a mass-spectrometric analysis could be utilized to identify the binding partner.

The positive controls, MMP9 and SNAI2, showed induction in the luciferase signals in response to EMT stimuli (Figure 17: pMM9 and pSNAI2), indicating increased gene transcription during EMT, which was expected. Originally, only one positive control plasmid was generated, but this plasmid did not show an induction in the luciferase activity after a 24-hour TGFβ treatment. Hence there was a need to generate an additional plasmid, where another EMT-responsive promoter region was driving the luciferase gene expression. However, this plasmid did not either show an induction in the luciferase signal after a 24-hour TGFβ treatment. The treatment time was originally set to 24 h since previous qRT-PCR experiments performed in the Sistonen laboratory had shown an induction in the mRNA levels of these genes after a 24-hour TGFβ treatment. Once shorter treatment times, 4 h and 8 h, were tested, an induced luciferase signal was displayed by each positive control in response to EMT stimuli. Since the functionality of a shorter treatment time was not discovered until the late phase of my study, I only had time to perform two biological repeats for these positive controls, thus for MMP9 and SNAI2 the n was 2, while the other samples had three biological repeats. A possible reason why the 24-hour TGFβ treatment did not result in an induced luciferase activity could be due to fast gene transcription or rapid turnover for luciferase. The luciferase reporter assay is a time-sensitive method, and is highly dependent on protein kinetics, rapid transcription and protein turnover could therefore result in the degradation of the luciferase protein before an induction is evident. Furthermore, the plasmid DNA lacks introns and histones, meaning that no RNA-splicing events or DNA reorganization by histone-modifying complexes are required, and it is likely that these features contribute to a fast transcription of the plasmid DNA. Concomitantly, the faster the gene is transcribed and translated into protein, the faster the protein is susceptible for degradation, yet in its defined turnover

time. However, further experiments would be required for optimization since the kinetics for MMP9 and SNAI2 constructs are unknown.

In future studies, one alternative to determine the kinetics for these controls would be to chemically inhibit the proteasome by utilizing commercially available proteasome inhibitors, e.g. bortezomib or MG132. Proteasome inhibitors prevent the activity of a proteolytic complex, which is responsible for degrading ubiquitylated proteins, thereby preventing degradation of a large set of proteins, as more than 80% of proteins are degraded by this complex (Kubiczkova et al. 2014). In this way the effect of protein turnover could be minimized. This method could improve the kinetics of the assay and toxicity would not be a major issue, since proteasome inhibition is not detrimental to cells within a short, 4-6 h, treatment period. Also, previous research has reported the use of varying sizes of the MMP9 and SNAI2 promoter in EMT-involved studies, confirming that the positive controls should work but require additional optimization (Liau et al. 2006; Bai et al. 2017; Mishra et al. 2017).

The results also showed that the luciferase activity for the empty pSTARR-luciferase vector was not significantly changed in response to EMT stimuli (Figure 17: pSTARR). A slight induction in the luciferase signal was observed after treatment, but this increase was not significant and, importantly, the signal was not decreased in any of the biological replicas. The observed minor transcriptional induction indicates that the transcription was driven by the origin of replication, since the plasmid was lacking a promoter. The origin of replication can function as a weak promoter and initiate gene transcription, thus resulting in a low level of basal transcription that is always detected (Muerdter et al. 2018).

Moreover, cells that were both expressing and lacking HSF1 were used to analyze HSF2 protein levels in the presence and absence of XV, which induces EMT. Regardless of the HSF1 expression status, the HSF2 protein levels were decreased in a similar manner upon EMT stimuli, indicating that HSF1 does not affect HSF2 expression during EMT (Figure 20. HSF2 Blot: Scr and shHSF1; XV). Although the exact mechanism modulating HSF2 activity remains to be elucidated, these results collectively suggest that the 5'UTR is important for the post-transcriptional downregulation of HSF2 during EMT and that HSF2 is modulated during this process by a mechanism, which is likely to be independent of HSF1. An additional approach to investigate the role of HSF2 in EMT would be to perform RNA-sequencing. This

method provides information about the entire transcriptome, revealing which genes are active and to what extent they are expressed, offering a more comprehensive insight to the biological status of the cell and how this status is altered during EMT.

6.2 HSF2 inhibits the cellular invasion capacity during EMT

The impact of HSF2 on the invasion capacity of MDA-MB-231 cells was assessed in the presence and absence of TGFβ. Considering that the cells overexpressing HSF2 displayed slow migration both in the presence and absence of EMT stimuli, the results indicate that HSF2 suppresses the cellular invasion capacity of MDA-MB-231 cells upon EMT (Figure 18: HSF2 Ctrl and HSF2 TGFβ). This was also directly observed in Figure 19, where the migration capacity of cells expressing exogenous HSF2 appeared to be similar despite the treatment (Figure 19: HSF2 Ctrl vs. HSF2 TGFβ). This is the first time that HSF2 has been identified to suppress cell invasion, demonstrating a novel role of HSF2 as a potential inhibitor of EMT. These results are also supported by the findings of Björk and co-workers, who discovered that HSF2 expression is decreased in prostate cancer as the cancer cells become more invasive (Björk et al. 2016). Although breast cancer cells were used in my study, these results collectively support the notion that HSF2 is downregulated as the cancer progression proceeds and cells become more invasive. My results are also interesting considering that HSF1 has been show to promote EMT (Zhao et al. 2011; Schieber & Chandel, 2013; Liu et al. 2016), raising the possibility that HSF1 and HSF2 display opposite functions during EMT. Data supporting this idea has been provided by genome-wide screens showing that even though these transcription factors share some common target genes, they also regulate a set of distinct genes (Vihervaara et al. 2013; Mahat et al. 2016). It is thereby interesting to speculate that HSF1 and HSF2 would regulate distinct gene programs also during EMT and that HSF2 could drive a transcriptional program that has to be inhibited in order for EMT to progress. Furthermore, previous research has also identified other TFs as inhibitors of EMT. For instance, p63, which belongs to the family of p53 transcription factors, was shown to inhibit EMT, as its depletion promoted EMT and the effect could be reverted by rescuing the p63 expression (Lindsay et al. 2011). Thus, p63 and HSF2 might have similar EMT-inhibiting roles. A hypothetical model of the function of HSF2 in EMT is depicted in Figure 21. The migration capacity of cells expressing GFP was induced in response to the treatment (Figure 18: GFP TGFβ), which was expected and further supported by

the observation in Figure 19. This is supported by prior studies stating that TGFβ increases the migration capacity of cells, verifying that my results are in accordance with previous reports (Romagnoli et al. 2012; Pang et al. 2016).

Breast cancer cells can be divided into luminal, HER2-positive, and triple-negative breast cancer cells on the basis of specific biomarkers. MDA-MB-231 cells, which were used in this experiment, are triple-negative breast cancer cells. Thus, it would be interesting to repeat the wound healing assay utilizing another type of breast cancer cell line to study whether HSF2 would similarly affect the invasion capacity of these cells during EMT. Additionally, as the presence of HSF2 was observed to impair the migration rate, it would be important to include samples where HSF2 is depleted, which I hypothesize would increase the migration capacity.

Yet another interesting approach for further research would be to investigate how the expression of HSF2 is affected in the reverse process called MET. To this date, only a handful of papers have been published where the MET process has been successfully induced in cells via hormones or chemical treatment (Zeisberg et al. 2005; Na et al. 2009; Chen et al. 2013; Ware et al. 2017; Watanabe et al. 2019). The conditions in which MET is induced are difficult to replicate *in vitro*, but successful MET-induction has been reported in sarcoma cells, fibroblasts, and melanoma cells (Zeisberg et al. 2005; Na et al. 2009; Ware et al. 2017; Watanabe et al. 2019). By inducing MET utilizing one of these cell types, I would expect an increase in the level of HSF2, which indicates that the mechanisms that quench HSF2 expression during EMT are removed once the cells shift toward an epithelial state.

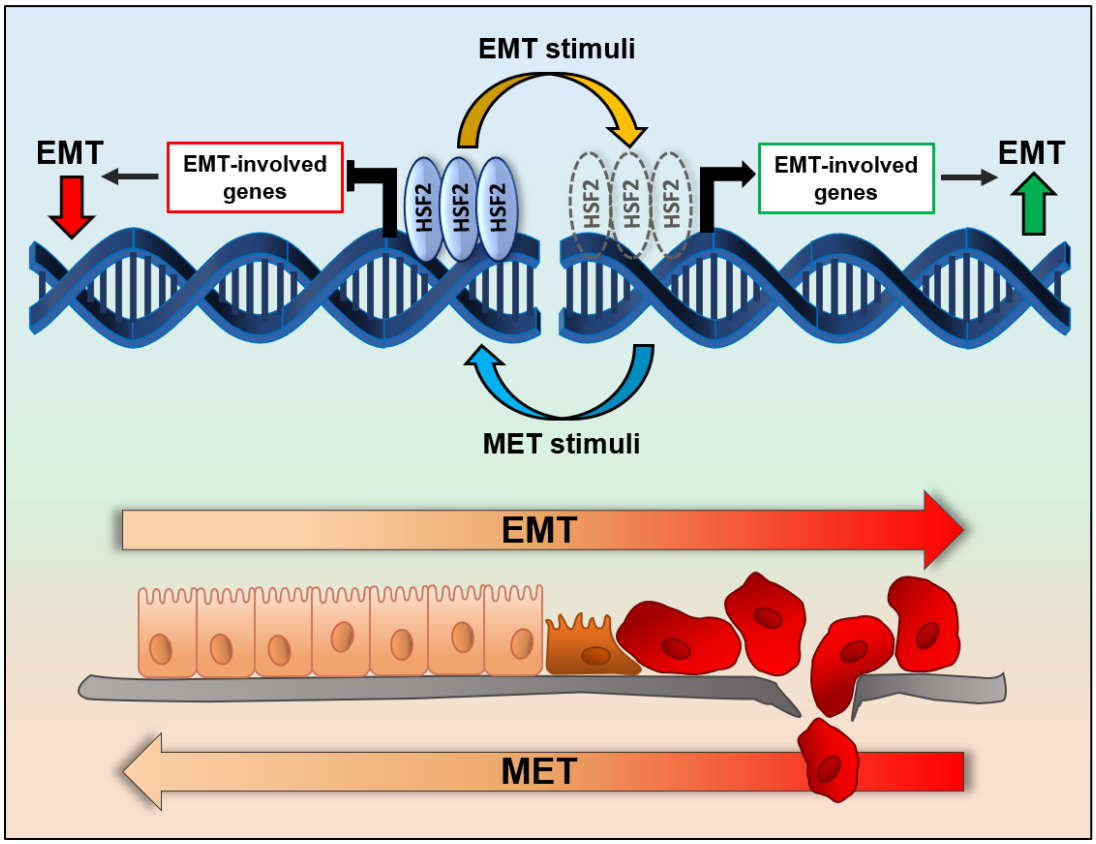

Figure 21. A hypothetical model demonstrating the function of HSF2 during EMT. The presence of HSF2, illustrated as DNA-bound trimers, suppresses the induction of EMT-involved genes leading to the inhibition of the EMT process (left side). Upon EMT stimuli (orange arrow) the expression of HSF2 is downregulated, which allows active transcription of EMT-involved genes, since they are no longer suppressed by the presence of HSF2, subsequently inducing the EMT process (right side). Whereas upon MET stimuli (blue arrow), the expression of HSF2 is rescued and the transcription of EMT-involved genes is in turn repressed. The displayed cellular phenotypes are indicated below to illustrate the switch from the epithelial state (light orange cells) to the mesenchymal state (red cells) during EMT, as well as the reversion from the mesenchymal state to the epithelial state via MET.

6.3 Concluding remarks

The main objectives of this thesis were to characterize how HSF2 is regulated upon EMT and to determine whether HSF2 impacts cellular characteristics during EMT. The obtained results showed that, surprisingly, the 5'UTR of HSF2 was important for the post-transcriptional downregulation of HSF2 during active EMT. The results also indicated that the modulation of HSF2 activity during EMT is driven by a mechanism that is likely to be independent of HSF1. Furthermore, this study identified a novel function of HSF2 in inhibiting the invasion capacity of cells during EMT. Collectively, these results indicate that HSF2 plays an important role in EMT, and it is tempting to speculate that a specific HSF2-EMT-inhibiting signature, similar to that of the HSF1-CaSig identified for HSF1 in cancer, would be regulating the EMT process. It remains to be elucidated whether the migration-inhibiting effect of HSF2 is regulated via specific gene networks or by another mechanism. In conclusion, this study emphasizes the importance of HSF2 in the context of cell invasion and cancer, and highlights the need for comprehensive research to obtain a better understanding of the underlying mechanisms regulating malignant transformation, and thereby allowing the improvement of therapeutic approaches against cancer.

7 Swedish summary

Funktionen av HSF2 vid epitel-mesenkymal övergång

7.1 Introduktion

I det västerländska samhället är cancer en av de ledande dödsorsakerna med miljoner nya fall som diagnostiseras årligen. Epitel-mesenkymal övergång (EMT) är ett av de huvudsakliga fenomenen som bidrar till invasionskapaciteten hos cancerceller. EMT är ett normalt biologiskt program involverat i utvecklingen av embryon och organ samt i sårläkningsprocessen. Under EMT skapar cellerna distinkta migrationsegenskaper genom förändringar i signalräckor, som i sin tur påverkar transkriptionsfaktorernas förmåga att styra uttrycket av gener, vilka reglerar cellens rörelser. Dessa förändringar resulterar i ett skift i den cellulära fenotypen, som tillåter epitelceller att anta en mer mesenkymal morfologi och därmed erhålla en ökning i den cellulära invasionskapaciteten. Förändringen i den cellulära fenotypen bidrar till förändringar i cell-cell- och cell-matriskontakter, organisering av cytoskelettproteiner och cellpolariteten. En viktig signalräcka som aktiverar EMT, kallas för transformerande tillväxtfaktor beta (TGFβ), och aktiveringen av denna signalräcka har tidigare visats påverka utvecklingen av cancer. Ett viktigt delområde inom cancerforskning är att karakterisera samverkan mellan olika signalräckor, som kan öka på cellens förmåga att överleva. En viktig signalräcka, som hjälper cellen att överleva proteinskadande stress, kallas för värmechockresponsen (eng. heat shock response, HSR). Aktivering av HSR styrs av transkriptionsfaktorer som kallas för värmechockfaktorer (eng. heat shock factor, HSF), vars aktivering leder till ökad transkription av gener som kodar värmechockproteiner (eng. heat shock protein, HSP). HSP:n är molekylära chaperoner, som stabiliserar andra proteiners struktur. Människan har flera olika HSF:er, varav värmechockfaktor 2 (eng. heat shock factor 2, HSF2) är en av de viktigaste som modulerar HSR. Tidigare studier antyder att HSF2 kan hämma utvecklingen av cancer, främst prostatacancer (Björk et al. 2016). Utöver dessa resultat visar opublicerade resultat från Sistonens laboratorium att i cancer styr TGFβ-signalräckan proteinuttrycket av HSF2, vilket antyder att det finns ett samband mellan HSF2 och EMT. Utgående från dessa resultat var ändamålet med min forskning att bestämma om HSF2 kan påverka EMT-processen.

7.2 Forskningsmål

Tidigare studier har visat att uttrycket av HSF2 minskar i respons till aktiveringen av TGFβ-signalräckan. Dessutom spelar HSF2 en viktig roll i flera olika typer av cancer som bröstcancer. Utgående från dessa resultat var huvudmålet med denna avhandling att karakterisera HSF2s funktion i EMT. Mina forskningsmål var därmed att:

1. Bestämma vilken del av HSF2-promotorn styr uttrycket av HSF2 under EMT.
2. Bestämma om HSF2 påverkar den cellulära invasionsförmågan vid EMT.
3. Bestämma om HSF1 bidrar till nedregleringen av HSF2 uttrycket vid EMT.

7.3 Material och metoder

7.3.1 Cellodling och behandlingar

En transformerad human bröstepitelcellinje, MDA-MB-231, användes som modellsystem i denna studie. Cellerna odlades i DMEM (eng. Dulbecco's Modified Eagle Medium, Biowest) innehållande 5 % fetalt kalvserum (Biowest), 2,5 mM glutamin (Biowest), 50 U/ml penicillin och 50 µg/µl streptomycin. Cellerna inkuberades vid 37 °C i 5 % CO_2 under odlingen.

För att inducera EMT behandlades cellerna med ett speciellt behandlingsmedium innehållande 2 % serum och 10 ng/ml TGFβ-1 eller 10 µl/ml StemXvivo (XV), vilket innehåller flera ämnen som inducerar EMT, i 4 eller 24 timmar. En del av cellerna utgjorde kontrollceller, vilka behandlades med behandlingsmedium som saknade de EMT-inducerande ämnen.

7.3.2 Kloning

Kloning är en metod som används för att införa en önskad DNA-sekvens in i en vektor. Metoden baserar sig på användningen av en vektor, som linjäriseras på ett bestämt ställe med hjälp av PCR, varefter ett In-Fusion-enzym används för att införa ett önskat fragment på denna plats. Vektorn linjäriseras och amplifieras i en PCR-reaktion med hjälp av framåtriktade och bakåtriktade primrar. Gensekvensen som placeras in i vektorn amplifieras med hjälp av en PCR-reaktion, i vilken primrar med 15 stycken basparsöverhäng används. Därmed erhåller PCR-produkten korta överhäng, som är komplementära med den linjäriserade vektorn. Den studerade

gensekvensen blandas med en liten mängd av vektorn, varefter en kommersiell reagensblandning, 5x In-Fusion HD Enzyme Premix (Takara Bio), används för att införa gensekvensen av intresse in i vektorn via homolog rekombination.

Kloning användes i denna studie för att utreda vilken del av HSF2-promotorn styr uttrycket av HSF2 under EMT. För detta ändamål framställdes plasmider där olika delar av HSF2-promotorn placerades vid gensekvensen som kodar luciferas-enzymet. Dessutom skapades två kontrollplasmider, i vilka promotorn för SNAI2 och MMP9 placerades vid gensekvensen som kodar luciferas-enzymet. Kontrollplasmiderna borde inducera uttrycket av luciferas under EMT, eftersom tidigare studier har visat att dessa gensekvenser induceras under EMT.

7.3.3 Transfektion av celler

För att transfektera celler med de specifika plasmiderna användes Neon ^{TM} Transfection System (Thermo Fisher Scientific). För varje transfektion suspenderades 2,2 miljoner MDA-MB-231 celler i R-buffert och 15 µg plasmid tillsattes i cellsuspensionen. Därefter transfekterades cellerna med en 100 µl transfektionspipett, som placerades i en transfektionskyvett innehållande 3 ml E2-buffert. MDA-MB-231-celler transfekterades enligt inställningarna som anges i Tabell 2. De transfekterade cellerna placerades på nya cellodlingsplattor tillsammans med odlingsmediet och de fick återhämta sig i 48 timmar, varefter en del behandlades med EMT-inducerande ämnen och användes för luciferas-raportöranalysen. I varje transfektion tillsattes 5 µg av en plasmid som innehåller gensekvensen som kodar för β-galaktosidas, vilket möjliggör normaliseringen av genuttrycket vid analysen av luciferasaktiviteten.

För att bestämma om HSF2 påverkar cellernas invasionsförmåga, användes celler som kontinuerligt uttrycker exogent HSF2 även under EMT. För detta syfte transfekterades MDA-MB-231 celler med plasmider vars gensekvens kodar för exogent HSF2. För kontrolltillståndet transfekterades celler med plasmider som kodar för grönt fluorescerande protein (eng. green fluorescent protein, GFP).

Western blot-analys användes för att jag skulle kunna bestämma om HSF1 påverkar nedregleringen av HSF2 under EMT. Därmed behövdes celler som inte uttrycker endogent HSF1. Således transfekterades celler med en plasmid som innehåller en gensekvens som kodar för en kort hårnåls-RNA-molekyl (eng. short hairpin RNA,

shRNA) riktad mot HSF1 (shHSF1). För kontrollprov transfekterades cellerna med en plasmid som kodar för en shRNA-molekyl innehållande omblandade sekvenser (eng. scrambled, Scr).

7.3.4 Luciferas-raportöranalys

Luciferas-raportöranalys är en metod som används för att indirekt mäta transkription. Analysen baserar sig på användningen av en plasmid, som innehåller en promotorsekvens som driver uttrycket av en luciferasgen. Denna gen kodar för ett 61 kDa enzym som kan oxidera dess substrat, D-luciferin, då Mg^{2+}, O_2 och adenosintrifosfat (ATP) är tillgängliga. Oxideringreaktionen leder till produktionen av ljus, som kan kvantitativt mätas med en maskin. Genom att kvantifiera mängden producerat ljus kan nivån av luciferas indirekt bestämmas. Dessutom används en annan raportöranalys, β-galaktosidas, för att normalisera genuttrycket i proven som användes under luciferas-raportöranalysen.

Passiv lysisbuffert användes för att lysera cellproven som användes för analysen. För varje prov pipetterades 3 µl lysat i tre brunnar i en 96-brunnars Packard-platta. Slutligen tillsattes 90 µl av luciferassubstratlösning, BriteLite Plus (Perkin Elmer), i varje brunn. Luciferasaktiviteten mättes sedan med hjälp av Hidex Sense Microplate Reader-maskinen (Hidex) med följande inställning: luminescens IR cutoff 1 s. Erhållna mätvärden normaliserades med β-galaktosidasraportöranalysen varefter de analyserades i Microsoft Excel.

7.3.5 Sårläkningsanalys

Sårläkningsanalys (eng. wound healing assay) användes i detta experiment för att bestämma om HSF2 påverkar migrationskapaciteten i MDA-MB-231-celler vid EMT. Celler som uttryckte antingen exogent HSF2 eller GFP, odlades i sex brunnar av en 12-brunns odlingsplatta. Cellodlingsmediet aspirerades och cellerna tvättades med 1x PBS. Sedan behandlades en uppsättning av celler med behandlingsmedium innehållande 10 ng/ml TGFβ-1 för 3 timmar och en annan uppsättning av celler behandlades endast med behandlingsmedium.

Efter 3 timmars behandling skapades en repa i cellagret med en 10 µl pipettspets, vilket imiterade ett sår. Cellplattans lock ersattes därefter med ett speciellt lock som möjliggjorde gasutbyte i avbildningsmaskinen. Sedan placerades cellodlingsplattan i

Cell-IQ-maskinen (Chip-Man Technologies), och sårläkningsprocessen filmades vid tre olika positioner i såret i varje brunn med ett tidsintervall på 5 minuter i 24 timmar vid 37 °C. Efter att cellmigrationsprocessen filmats, analyserades data med hjälp av bildanalysprogrammet ImageJ och programmet GraphPad Prism användes för den statistiska analysen.

7.3.6 Western blot

Western blot är en metod som kombinerar flera tekniker som möjliggör detektionen av ett specifikt protein. Metoden inkluderar natriumdodecylsulfatpolyakrylamidgelelektrofores (SDS-PAGE), överföring av proteiner till ett nitrocellulosamembran och immunblotting för att identifiera proteinet av intresse med hjälp av specifika antikroppar. Western blot användes för att bestämma om HSF1 påverkar uttrycket av HSF2 vid EMT. Transfekterade celler, som uttryckte antingen Scr eller shHSFl, behandlades med XV i 24 timmar. Sedan användes Western blot för att detektera HSF1, HSF2 och Hsc70 i proverna under kontrollförhållanden och EMT.

7.4 Resultat och diskussion

7.4.1 5’UTR reglerar uttrycket av HSF2 under EMT

Resultaten från luciferas-raportöranalysen visade att cellerna, som uttryckte plasmider innehållande HSF2-promotorn med 5’UTR, uppvisade en signifikant minskning i uttrycket av luciferas under EMT. Däremot var uttrycket av luciferas oförändrat i celler som uttryckte HSF2-promotorkonstrukt utan 5’UTR. Cellerna som uttryckte plasmiderna med promotorregioner från SNAI2 samt MMP9 visade en ökning i luciferas-uttrycket efter behandlingen. Dessa resultat antyder på att 5'UTR-delen av HSF2 är viktig i regleringen av HSF2-genuttrycket och krävs för att nedreglera HSF2 under EMT. Tidigare studier har visat att HSF-genuttrycket kan regleras av mikro-RNA-molekyler (eng. micro RNA, miR), som binder 5’UTR-delen (Vivinus et al. 2001; Björk et al. 2010; Liang et al. 2018). Därmed kan samma process reglera uttrycket av HSF2 vid EMT. För att studera detta i framtida experiment, skulle jag transfektera celler med plasmider som kodar för sh-miR som specifikt binder till 5’UTR av HSF2 och utföra en ny luciferas-raportöranalys.

7.4.2. HSF2 förhindrar den cellulära invasionsförmågan under EMT

Resultaten från analysen av sårläkningen visade att cellerna som uttryckte exogent HSF2, uppvisade samma sårläkningshastighet under både kontrollförhållanden och EMT. Däremot visade cellerna som uttryckte GFP, att behandlingen som inducerade EMT, ökade på sårläkningshastigheten. Detta tyder på att HSF2-uttrycket signifikant förhindrar den cellulära invasionskapaciteten vid EMT. Resultaten från sårläkningsanalysen stöder forskningsresultatet av Björk och kollegor, som visade att HSF2 kan inhibera prostatacancer (Björk et al. 2016). Tidigare studier har dessutom visat att ett ökat HSF1-uttryck inducerar EMT i levercancerceller (Liu et al. 2016) och äggstockscancerceller (Powell et al. 2016). Detta betyder att HSF2 har en motsatt funktion i jämförelse till HSF1 vid EMT. I framtiden vore det intressant att upprepa sårläkningsanalysen med en annan bröstcancercellinje. Därtill skulle jag nedreglera uttrycket av endogent HSF2 för att studera hur det påverkar invasionsförmågan i cellerna.

7.4.3 HSF1 styr inte nedregleringen av HSF2-uttrycket under EMT

Resultaten från western blot-analysen visade att HSF1-uttrycket i cellerna transfekterade med Scr-plasmider ökade lite efter XV-behandlingen. Cellerna som uttryckte shHSF1 visade en nedreglering av HSF1-proteinet både i XV-behandlade och i kontrollproven. Då man jämförde proteinuttrycket för HSF2 under kontroll och EMT, visade det sig att uttrycket av HSF2 minskade under XV-behandlingen. Resultaten indikerar att uttrycket av HSF2 under EMT inte påverkas av HSF1. Däremot regleras HSF2-uttrycket vid EMT av en distinkt mekanism, som troligtvis är oberoende av HSF1. Western blot är en metod som används för att analysera proteinuttrycket, däremot vore det intressant att mäta den relativa mRNA-mängden för att studera ifall HSF1 påverkar HSF2-uttrycket på mRNA-nivån.

7.4.4 Slutsatser

Denna avhandling belyser en viktig roll som HSF2 har i cancerutveckling, utöver dess traditionella roll i aktivering av HSR. Detta framhäver behovet av ytterligare forskning för att utreda värmechockfaktorernas funktion i varierande biologiska processer samt patologiska tillstånd, speciellt cancer. Därtill ger avhandlingen för första gången en

inblick i att HSF2 fungerar som en hämmare av EMT-processen och kan därmed inhibera migrationskapaciteten hos celler.

References

Abane, R., & Mezger, V. (2010). Roles of heat shock factors in gametogenesis and development. *FEBS Journal, 277*(20), 4150-4172.

Ahlskog, J. K., Björk, J. K., Elsing, A. N., Aspelin, C., Kallio, M., Roos-Mattjus, P., & Sistonen, L. (2010). Anaphase-promoting complex/cyclosome participates in the acute response to protein-damaging stress. *Molecular and Cellular Biology*, *30*(24), 5608–5620.

Aigner, K., Dampier, B., Descovich, L., Mikula, M., Sultan, A., Schreiber, M., Mikulits, W., Brabletz, T., Strand, D., Obrist, P., Sommergruber, W., Schweifer, N., Wernitznig, A., Beug, H., Foisner, R., & Eger, A. (2007). The transcription factor ZEB1 (deltaEF1) promotes tumour cell dedifferentiation by repressing master regulators of epithelial polarity. *Oncogene*, *26*(49), 6979–6988.

Amin, J., Ananthan, J., & Voellmy, R. (1988). Key features of heat shock regulatory elements. *Molecular and Cellular Biology*, *8*(9), 3761–3769.

Anckar, J., Hietakangas, V., Denessiouk, K., Thiele, D. J., Johnson, M. S., & Sistonen, L. (2006). Inhibition of DNA binding by differential sumoylation of heat shock factors. *Molecular and Cellular Biology*, *26*(3), 955–964.

Asano, Y., Kawase, T., Okabe, A., Tsutsumi, S., Ichikawa, H., Tatebe, S., Kitabayashi, I., Tashiro, F., Namiki, H., Kondo, T., Semba, K., Aburatani, H., Taya, Y., Nakagama, H., & Ohki, R. (2016). IER5 generates a novel hypo-phosphorylated active form of HSF1 and contributes to tumorigenesis. *Scientific Reports*, *6*, 19174.

Aybar, M. J., Nieto, M. A., & Mayor, R. (2003). Snail precedes slug in the genetic cascade required for the specification and migration of the Xenopus neural crest. *Development, 130*(3), 483–494.

Bae, G. Y., Hong, S. K., Park, J. R., Kwon, O. S., Kim, K. T., Koo, J., Oh, E., & Cha, H. J. (2016). Chronic TGFβ stimulation promotes the metastatic potential of lung cancer cells by Snail protein stabilization through integrin β3-Akt-GSK3β signaling. *Oncotarget*, *7*(18), 25366–25376.

Balsamo, J., Arregui, C., Leung, T., & Lilien, J. (1998). The nonreceptor protein tyrosine phosphatase PTP1B binds to the cytoplasmic domain of N-cadherin and regulates the cadherin-actin linkage. *The Journal of Cell Biology*, *143*(2), 523–532.

Batlle, E., & Clevers, H. (2017). Cancer stem cells revisited. *Nature Medicine, 23*(10), 1124–1134.

Batlle, E., Sancho, E., Francí, C., Domínguez, D., Monfar, M., Baulida, J., & García De Herreros, A. (2000). The transcription factor snail is a repressor of E- cadherin gene expression in epithelial tumour cells. *Nature Cell Biology, 2*(2), 84–89.

Beerling, E., Seinstra, D., de Wit, E., Kester, L., van der Velden, D., Maynard, C., Schäfer, R., van Diest, P., Voest, E., van Oudenaarden, A., Vrisekoop, N., & van Rheenen, J. (2016). Plasticity between Epithelial and Mesenchymal States Unlinks EMT from Metastasis-Enhancing Stem Cell Capacity. *Cell Reports*, *14*(10), 2281–2288.

Bertran, E., Crosas-Molist, E., Sancho, P., Caja, L., Lopez-Luque, J., Navarro, E., Egea, G., Lastra, R., Serrano, T., Ramos, E., & Fabregat, I. (2003). Overactivation of the TGF-β pathway confers a mesenchymal-like phenotype and CXCR4-dependent migratory properties to liver tumor cells. *Hepatology, 58*(6), 2032–2044.

Bierie, B., & Moses, H. L. (2006). TGF-β and cancer. *Cytokine Growth Factor Review, 17(1-2)*, 29–40.

Björk, J. K., Ahonen, I., Mirtti, T., Erickson, A., Rannikko, A., Bützow, A., Nordling, S., Lundin, J., Lundin, M., Sistonen, L., Nees, M., & Åkerfelt, M. (2018). Increased HSF1 expression predicts shorter disease-specific survival of prostate cancer patients following radical prostatectomy. *Oncotarget*, *9*(58), 31200–31213.

Björk, J. K., Åkerfelt, M., Joutsen, J., Puustinen, M. C., Cheng, F., Sistonen, L., & Nees, M. (2016). Heat-shock factor 2 is a suppressor of prostate cancer invasion. *Oncogene*, *35*(14), 1770–1784.

Björk, J. K., Sandqvist, A., Elsing, A. N., Kotaja, N., & Sistonen, L. (2010). miR-18, a member of Oncomir-1, targets heat shock transcription factor 2 in spermatogenesis. *Development*, *137*(19), 3177-3184.

Blanco, M. J., Moreno-Bueno, G., Sarrio, D., Locascio, A., Cano, A., Palacios, J., & Nieto, M. A. (2002). Correlation of Snail expression with histological grade and lymph node status in breast carcinomas. *Oncogene, 21*(20), 3241–3246.

Blokzijl, A., Dahlqvist, C., Reissmann, E., Falk, A., Moliner, A., Lendahl, U., & Ibáñez, C. F. (2003). Cross-talk between the Notch and TGF-beta signaling pathways mediated by interaction of the Notch intracellular domain with Smad3. *The Journal of Cell Biology*, *163*(4), 723–728.

Brasier, A.R., & Ron, D. (1992). Luciferase reporter gene assay in mammalian cells. *Methods in Enzymology,* 216, 386–397.

Bray, S. J. (2016). Notch signalling in context. *Nature Reviews Molecular Cell Biology, 17*(11), 722–735.

Brüser, L., & Bogdan, S. (2017). Adherens Junctions on the Move-Membrane Trafficking of E-Cadherin. *Cold Spring Harbor Perspectives in Biology*, *9*(3), a029140.

Budzyński, M. A., & Sistonen, L. (2017). Versatile Functions of Heat Shock Factors: It Is Not All About Stress. *Current Immunology Reviews*, *13*.

Caggiano, R., Cattaneo, F., Moltedo, O., Esposito, G., Perrino, C., Trimarco, B., Ammendola, R., & Faraonio, R. (2017). miR-128 Is Implicated in Stress Responses by Targeting MAFG in Skeletal Muscle Cells. *Oxidative Medicine and Cellular Longevity*, 9308310.

Campanella, C., Pace, A., Caruso Bavisotto, C., Marzullo, P., Marino Gammazza, A., Buscemi, S., & Palumbo Piccionello, A. (2018). Heat Shock Proteins in Alzheimer's Disease: Role and Targeting. *International Journal of Molecular Sciences*, *19*(9), 2603.

Cano, A., Pérez-Moreno, M. A., Rodrigo, I., Locascio, A., Blanco, M. J., del Barrio, M. G., Portillo, F., & Nieto, M. A. (2000). The transcription factor snail controls epithelial-mesenchymal transitions by repressing E-cadherin expression. *Nature Cell Biology, 2*(2), 76–83.

Cantelli, G., Crosas-Molist, E., Georgouli, M., & Sanz-Moreno, V. (2017). TGFB-induced transcription in cancer. *Seminars in Cancer Biology*, *42*, 60–69.

Carpenter, R. L., Paw, I., Dewhirst, M. W., & Lo, H. W. (2015). Akt phosphorylates and activates HSF-1 independent of heat shock, leading to Slug overexpression and epithelial-mesenchymal transition (EMT) of HER2-overexpressing breast cancer cells. *Oncogene*, *34*(5), 546–557.

Chang, Y., Östling, P., Åkerfelt, M., Trouillet, D., Rallu, M., Gitton, Y., El Fatimy, R., Fardeau, V., Le Crom, S., Morange, M., Sistonen, L., & Mezger, V. (2006). Role of heat-shock factor 2 in cerebral cortex formation and as a regulator of p35 expression. *Genes & Development*, *20*(7), 836–847.

Chen, R., Liliental, J. E., Kowalski, P. E., Lu, Q., Cohen, S. N. (2011). Regulation of transcription of hypoxia-inducible factor-1α (HIF-1α) by heat shock factors HSF2 and HSF4. *Oncogene*, *30*(22), 2570-2580.

Chen, Y., Wang, K., & Leach, R. (2013). 5-Aza-dC treatment induces mesenchymal-to-epithelial transition in 1st trimester trophoblast cell line HTR8/SVneo. *Biochemical and Biophysical Research Communications*, *432*(1), 116–122.

Christians, E., Davis, A., Thomas, S., & Benjamin, I. (2000). Maternal effect of Hsf1 on reproductive success. *Nature*, *407*(6805), 693-694.

Chu, B., Soncin, F., Price, B. D., Stevenson, M. A., & Calderwood, S. K. (1996). Sequential phosphorylation by mitogen-activated protein kinase and glycogen synthase kinase 3 represses transcriptional activation by heat shock factor-1. *The Journal of Biological Chemistry, 271*(48), 30847-30857.

Chu, B., Zhong, R., Soncin, F., Stevenson, M. A., & Calderwood, S. K. (1998). Transcriptional activity of heat shock factor 1 at 37 degrees C is repressed through phosphorylation on two distinct serine residues by glycogen synthase kinase 3 and protein kinases Calpha and Czeta. *The Journal of Biological Chemistry, 273*(29), 18640-18646.

Citri, A., Kochupurakkal, B. S., & Yarden, Y. (2004). The achilles heel of ErbB-2/HER2: regulation by the Hsp90 chaperone machine and potential for pharmacological intervention. *Cell Cycle, 3*(1), 51-60.

Clark, J. C., Thomas, D. M., Choong, P. F., & Dass, C. R. (2007). RECK-a newly discovered inhibitor of metastasis with prognostic significance in multiple forms of cancer. *Cancer Metastasis Rev*iews, *26*(3-4), 675-683.

Clay, M. R., & Halloran, M. C. (2014). Cadherin 6 promotes neural crest cell detachment via F-actin regulation and influences active Rho distribution during epithelial-to-mesenchymal transition. *Development*, *141*(12), 2506–2515.

Clevers, H. (2006). Wnt/beta- catenin signaling in development and disease. *Cell 127*(3), 469–480.

Cotto, J. J., Kline, M., & Morimoto, R. I. (1996). Activation of heat shock factor 1 DNA binding precedes stress-induced serine phosphorylation. Evidence for a multistep pathway of regulation. *The Journal of Biological Chemistry, 271*(1), 3355-8.

Cui, J., Tian, H., & Chen, G. (2015). Upregulation of nuclear heat shock factor 1 contributes to tumor angiogenesis and poor survival in patients with non-small cell lung cancer. *The Annals of Thoracic Surgery, 100*(2), 465-472.

Dai, C., Whitesell, L., Rogers, A. B., & Lindquist, S. (2007). Heat shock factor 1 is a powerful multifaceted modifier of carcinogenesis. *Cell*, *130*(6), 1005–1018.

Davoli, T., & de Lange T. (2011). The causes and consequences of polyploidy in normal development and cancer. *Annual Review of Cell and Developmental Biology*, *27*, 585-610.

de Sousa e Melo, F., Kurtova, A. V., Harnoss, J. M., Kljavin, N., Hoeck, J. D., Hung, J., Anderson, J. E., Storm, E. E., Modrusan, Z., Koeppen, H., Dijkgraaf, G. J., Piskol, R., & de Sauvage, F. J. (2017). A distinct role for Lgr5+ stem cells in primary and metastatic colon cancer. *Nature, 543*(7647), 676–680.

Derynck, R., & Miyazono, K. (2017). The Biology of the TGF-β Family. *New York, NY, USA: Cold Spring Harbor Laboratory Press,* 1164.

Derynck, R., Akhurst, R. J., & Balmain, A. (2001). TGF-beta signaling in tumor suppression and cancer progression. *Nature Genetics, 29*(2), 117–129.

Derynck, R., Muthusamy, B. P., & Saeteurn, K. Y. (2014). Signaling pathway cooperation in TGF-β-induced epithelial-mesenchymal transition. *Current Opinion in Cell Biology*, *31*, 56–66.

Dongre, A., & Weinberg, R. A. (2019). New insights into the mechanisms of epithelial-mesenchymal transition and implications of cancer. *Nature Reviews. Molecular Cell Biology, 20*(2), 69-84.

El Fatimy, R., Miozzo, F., Le Mouël, A., Abane, R., Schwendimann, L., Sabéran-Djoneidi, D., de Thonel, A., Massaoudi, I., Paslaru, L., Hashimoto-Torii, K., Christians, E., Rakic, P., Gressens, P., & Mezger, V. (2014). Heat shock factor 2 is a stress-responsive mediator of neuronal migration defects in models of fetal alcohol syndrome. *EMBO Molecular Medicine*, *6*(8), 1043–1061.

Elbashir, S. M., Lendeckel, W., & Tuschl, T. (2001). RNA interference is mediated by 21- and 22-nucleotide RNAs. *Genes & Development*, *15*(2), 188–200.

Fan, F., & Wood, K. V. (2007). Bioluminescent assays for high-throughput screening. *Assay and Drug Development Technologies, 5*(1):127-136.

Feng, H., Wang, S., Guo, L., Punekar, A. S., Ladenstein, R., Wang, D. C., & Liu, W. (2016). MD simulation of high-resolution X-ray structures reveals post-translational modification dependent conformational changes in HSF-DNA interaction. *Protein & Cell*, *7*(12), 916–920.

Fiorenza, M. T., Farkas, T., Dissing, M., Kolding, D., & Zimarino, V. (1995). Complex expression of murine heat shock transcription factors. *Nucleic Acids Research*, *23*(3), 467–474.

Forsythe, J. A., Jiang, B. H., Iyer, N. V., Agani, F., Leung, S. W., Koos, R. D., & Semenza, G. L. (1996). Activation of vascular endothelial growth factor gene transcription by hypoxia-inducible factor 1. *Molecular and Cellular Biology*, *16*(9), 4604–4613.

Franco, D. L., Mainez, J., Vega, S., Sancho, P., Murillo, M. M., de Frutos, C. A., del Castillo, G., López-Blau, C., Fabregat, I., & Nieto, M. A. (2010). Snail1 suppresses TGF-beta-induced apoptosis and is sufficient to trigger EMT in hepatocytes. *Journal of Cell Science, 123*(Pt 20), 3467–3477.

Fujimoto, M., & Nakai, A. (2010). The heat shock factor family and adaptation to proteotoxic stress. *The FEBS Journal, 277*(20), 4112– 4125.

Fujimoto, M., Izu, H., Seki, K., Fukuda, K., Nishida, T., Yamada, S., Kato, K., Yonemura, S., Inouye, S., & Nakai, A. (2004). HSF4 is required for normal cell growth and differentiation during mouse lens development. *The EMBO Journal*, *23*(21), 4297–4306.

Fujimoto, M., Takaki, E., Takii, R., Tan, K., Prakasam, R., Hayashida, N., Iemura, S., Natsume, T., & Nakai, A. (2012). RPA assists HSF1 access to nucleosomal DNA by recruiting histone chaperone FACT. *Molecular Cell, 48*(2), 182-194.

Garcia-Castro, M. I., Marcelle, C. & Bronner-Fraser, M. (2002). Ectodermal Wnt function as a neural crest inducer. *Science, 297*(5582), 848–851.

Gómez, A. V., Galleguillos, D., Maass, J. C., Battaglioli, E., Kukuljan, M., & Andrés, M. E. (2008). CoREST represses the heat shock response mediated by HSF1. *Molecular Cell, 31*(2), 222-31.

Gomez-Pastor, R., Burchfiel, E. T., & Thiele, D. J. (2018). Regulation of heat shock transcription factors and their roles in physiology and disease. *Nature Reviews Molecular Cell Biology*, *19*(1), 4–19.

Gomez-Pastor, R., Burchfiel, E. T., Neef, D. W., Jaeger, A. M., Cabiscol, E., McKinstry, S. U., Doss, A., Aballay, A., Lo, D. C., Akimov, S. S., Ross, C. A., Eroglu, C., & Thiele, D. J. (2017). Abnormal degradation of the neuronal stress-protective transcription factor HSF1 in Huntington's disease. *Nature Communications*, *8*, 14405.

Gonzalez, D. M., & Medici, D. (2014). Signaling mechanisms of the epithelial-mesenchymal transition. *Science Signaling*, *7*(344), re8.

González-Mariscal, L., Betanzos, A., Nava, P., & Jaramillo, B. E. (2003). Tight junction proteins. *Progress in Biophysics and Molecular Biology, 81*(1), 1-44.

Grada, A., Otero-Vinas, M., Prieto-Castrillo, F., Obagi, Z., & Falanga V. (2017). Research techniques made simple: analysis of collective cell migration using the wound healing assay. *Journal of Investigative Dermatology, 137*(2), e11-e16.

Gravdal, K., Halvorsen, O. J., Haukaas, S. A., & Akslen, L. A. (2007). A switch from E-cadherin to N-cadherin expression indicates epithelial to mesenchymal transition and is of strong and independent importance for the progress of prostate cancer. *Clinical Cancer Research, 13*(23), 7003–7011.

Green, M., Schuetz, T. J., Sullivan, E. K., & Kingston, R. E. (1995). A heat shock-responsive domain of human HSF1 that regulates transcription activation domain function. *Molecular and Cellular Biology*, *15*(6), 3354–3362.

Greenburg, G., & Hay, E. D. (1982). Epithelia suspended in collagen gels can lose polarity and express characteristics of migrating mesenchymal cells. *The Journal of Cell Biology*, *95*(1), 333–339.

Guan, B., Wu, K., Zeng, J., Xu, S., Mu, L., Gao, Y., Wang, K., Ma, Z., Tian, J., Shi, Q., Guo, P., Wang, X., He, D., & Du, Y. (2017). Tumor-suppressive microRNA-218 inhibits tumor angiogenesis via targeting the mTOR component RICTOR in prostate cancer. *Oncotarget, 8*(5), 8162–8172.

Guettouche, T., Boellmann, F., Lane, W. S., & Voellmy, R. (2005). Analysis of phosphorylation of human heat shock factor 1 in cells experiencing a stress. *BMC Biochemistry*, *6*, 4.

Guisbert, E., Czyz, D. M., Richter, K., McMullen, P. D., & Morimoto, R. I. (2013). Identification of a tissue-selective heat shock response regulatory network. *PLoS genetics*, *9*(4), e1003466.

Guo, W., Keckesova, Z., Donaher, J. L., Shibue, T., Tischler, V., Reinhardt, F., Itzkovitz, S., Noske, A., Zürrer-Härdi, U., Bell, G., Tam, W. L., Mani, S. A., van Oudenaarden, A., & Weinberg, R. A. (2012). Slug and Sox9 cooperatively determine the mammary stem cell state. *Cell*, *148*(5), 1015–1028.

Guo, Y. J., Pan, W. W., Liu, S. B., Shen, Z. F., Xu, Y., & Hu, L. L. (2020). ERK/MAPK signalling pathway and tumorigenesis. *Experimental and Therapeutic Medicine*, *19*(3), 1997–2007.

Hanrahan, K., O'Neill, A., Prencipe, M., Bugler, J., Murphy, L., Fabre, A., Puhr, M., Culig, Z., Murphy, K., & Watson, R. W. (2017). The role of epithelial-mesenchymal transition drivers ZEB1 and ZEB2 in mediating docetaxel-resistant prostate cancer. *Molecular Oncology*, *11*(3), 251–265.

Heimberger, T., Andrulis, M., Riedel, S., Stühmer, T., Schraud, H., Beilhack, A., Bumm, T., Bogen, B., Einsele, H., Bargou, R. C., & Chatterjee, M. (2013). The heat shock transcription factor 1 as a potential new therapeutic target in multiple myeloma. *British Journal of Haematology, 160*(4):465-76.

Heldin, C. H., Vanlandewijck, M., & Moustakas, A. (2012). Regulation of EMT by TGFbeta in cancer. *FEBS Letters, 586*(14), 1959–1970.

Hendriks, I. A., & Vertegaal, A. C. (2016). A comprehensive compilation of SUMO proteomics. *Nature Reviews Molecular Cell Biology, 17*(9), 581-595.

Herranz, N., Pasini, D., Díaz, V. M., Francí, C., Gutierrez, A., Dave, N., Escrivà, M., Hernandez-Muñoz, I., Di Croce, L., Helin, K., García de Herreros, A., & Peiró, S. (2008). Polycomb complex 2 is required for E-cadherin repression by the Snail1 transcription factor. *Molecular and Cellular Biology*, *28*(15), 4772–4781.

Hietakangas, V., Ahlskog, J. K., Jakobsson, A. M., Hellesuo, M., Sahlberg, N. M., Holmberg, C. I., Mikhailov, A., Palvimo, J. J., Pirkkala, L., & Sistonen, L. (2003). Phosphorylation of serine 303 is a prerequisite for the stress-inducible SUMO modification of heat shock factor 1. *Molecular and Cellular Biology*, *23*(8), 2953–2968.

Hietakangas, V., Anckar, J., Blomster, H. A., Fujimoto, M., Palvimo, J. J., Nakai, A., & Sistonen, L. (2006). PDSM, a motif for phosphorylation-dependent SUMO modification. *Proceedings of the National Academy of Sciences of the United States of America*, *103*(1), 45–50.

Hill, L., Browne, G., & Tulchinsky, E. (2013). ZEB/miR-200 feedback loop: at the crossroads of signal transduction in cancer. *International Journal of Cancer, 132*(4), 745-754.

Himanen, S. V., & Sistonen, L. (2019). New insights into transcriptional reprogramming during cellular stress. *Journal of Cell Science, 132*(21), pii: jcs238402.

Homma, S., Jin, X., Wang, G., Tu, N., Min, J., Yanasak, N., & Mivechi, N. F. (2007). Demyelination, astrogliosis, and accumulation of ubiquitinated proteins, hallmarks of CNS disease in hsf1-deficient mice. *The Journal of Neuroscience: the Official Journal of the Society for Neuroscience*, *27*(30), 7974–7986.

Hong, Y., Rogers, R., Matunis, M. J., Mayhew, C. N., Goodson, M. L., Park-Sarge, O. K., & Sarge, K. D. (2001). Regulation of heat shock transcription factor 1 by stress-induced SUMO-1 modification. *The Journal of Biological Chemistry, 276*(43), 40263-40267.

Hooper, P. L., Durham, H. D., Török, Z., Hooper, P. L., Crul, T., & Vígh, L. (2016). The central role of heat shock factor 1 in synaptic fidelity and memory consolidation. *Cell Stress & Chaperones*, *21*(5), 745–753.

Hu, Y., & Mivechi, N. F. (2006). Association and regulation of heat shock transcription factor 4b with both extracellular signal-regulated kinase mitogen-activated protein kinase and dual-specificity tyrosine phosphatase DUSP26. *Molecular and Cellular Biology*, *26*(8), 3282–3294.

Inouye, S., Izu, H., Takaki, E., Suzuki H., Shirai, M., Yokota, Y., Ichikawa, H., Fujimoto, M., & Nakai, A. (2004). Impaired IgG production in mice deficient for heat shock transcription factor 1. *The Journal of Biological Chemistry, 279*(37), 38701-38709.

Jacobs, A. T., & Marnett, L. J. (2009). HSF1-mediated BAG3 expression attenuates apoptosis in 4-hydroxynonenal-treated colon cancer cells via stabilization of anti-apoptotic Bcl-2 proteins. *The Journal of biological chemistry*, *284*(14), 9176–9183.

Jaeger, A. M., Makley, L. N., Gestwicki, J. E., & Thiele, D. J. (2014). Genomic heat shock element sequences drive cooperative human heat shock factor 1 DNA binding and selectivity. *The Journal of Biological Chemistry*, *289*(44), 30459–30469.

Jedlicka, P., Mortin, M. A., & Wu, C. (1997). Multiple functions of Drosophila heat shock transcription factor in vivo. *The EMBO journal*, *16*(9), 2452–2462.

Jennbacken, K., Tešan, T., Wang, W., Gustavsson, H., Damber, J. E., & Welen, K. (2010). N-cadherin increases after androgen deprivation and is associated with metastasis in prostate cancer. *Endocrine-Related Cancer, 17*(2), 469–479.

Jiang B. (2017). Aerobic glycolysis and high level of lactate in cancer metabolism and microenvironment. *Genes & diseases*, *4*(1), 25–27.

Jin, X., Eroglu, B., Cho, W., Yamaguchi, Y., Moskophidis, D., & Mivechi, N. F. (2012). Inactivation of heat shock factor Hsf4 induces cellular senescence and suppresses tumorigenesis in vivo. *Molecular Cancer Research : MCR*, *10*(4), 523–534.

Jin, X., Eroglu, B., Moskophidis, D., & Mivechi, N. F. (2011). Targeted deletion of Hsf1, 2, and 4 genes in mice. *Methods in molecular biology (Clifton, N.J.)*, *787*, 1–20.

Jin, X., Moskophidis, D., & Mivechi, N. F. (2011). Heat shock transcription factor 1 is a key determinant of HCC development by regulating hepatic steatosis and metabolic syndrome. *Cell Metabolism*, *14*(1), 91–103.

Joseph, J. V., Conroy, S., Tomar, T., Eggens-Meijer, E., Bhat, K., Copray, S., Walenkamp, A. M., Boddeke, E., Balasubramanyian, V., Wagemakers, M., den Dunnen, W. F., & Kruyt, F. A. (2014). TGF-β is an inducer of ZEB1-dependent mesenchymal transdifferentiation in glioblastoma that is associated with tumor invasion. *Cell Death & Disease*, *5*(10), e1443.

Joutsen, J., & Sistonen, L. (2019). Tailoring of proteostasis networks with heat shock factors. *Cold Spring Harbor Perspectives in Biology, 11*(4), pii:a034066.

Joutsen, J., Da Silva, A. J., Luoto, J. C., Budzynski, M. A., Nylund, A. S., de Thonel, A., Concordet, J. P., Mezger, V., Sabéran-Djoneidi, D., Henriksson, E., & Sistonen, L. (2020). Heat shock factor 2 protects against proteotoxicity by maintaining cell-cell adhesion. *Cell Reports, 30*(20), 583-597.

Kallio, M., Chang, Y., Manuel, M., Alastalo, T. P., Rallu, M., Gitton, Y., Pirkkala, L., Loones, M. T., Paslaru, L., Larney, S., Hiard, S., Morange, M., Sistonen, L., & Mezger, V. (2002). Brain abnormalities, defective meiotic chromosome synapsis and female subfertility in HSF2 null mice. *The EMBO Journal*, *21*(11), 2591–2601.

Kalluri, R., & Weinberg, R. A. (2009). The basics of epithelial-mesenchymal transition. *The Journal of clinical investigation*, *119*(6), 1420–1428.

Kang, S. W., You, S., Wong, E. A., & El Halawani, M. E. (2002). Normalization of transfection efficiency using the beta-lactamase gene of the pGL3 luciferase vector in primary anterior pituitary cells. *Biotechniques, 33*(2), 326-8, 330.

Kline, M. P., & Morimoto, R. I. (1997). Repression of the heat shock factor 1 transcriptional activation domain is modulated by constitutive phosphorylation. *Molecular and Cellular Biology*, *17*(4), 2107–2115.

Klunder, L. J., Faber, K. N., Dijkstra, G., & van IJzendoorn, S. (2017). Mechanisms of Cell Polarity-Controlled Epithelial Homeostasis and Immunity in the Intestine. *Cold Spring Harbor Perspectives in Biology*, *9*(7), a027888.

Kopan, R. (2002). Notch: a membrane- bound transcription factor. *Journal of Cell Science, 115*(Pt 6), 1095–1097.

Kourtis, N., Lazaris, C., Hockemeyer, K., Balandrán, J. C., Jimenez, A. R., Mullenders, J., Gong, Y., Trimarchi, T., Bhatt, K., Hu, H., Shrestha, L., Ambesi-Impiombato, A., Kelliher, M., Paietta, E., Chiosis, G., Guzman, M. L., Ferrando, A. A., Tsirigos, A., & Aifantis, I. (2018). Oncogenic hijacking of the stress response machinery in T cell acute lymphoblastic leukemia. *Nature medicine*, *24*(8), 1157–1166.

Kourtis, N., Moubarak, R. S., Aranda-Orgilles, B., Lui, K., Aydin, I. T., Trimarchi, T., Darvishian, F., Salvaggio, C., Zhong, J., Bhatt, K., Chen, E. I., Celebi, J. T., Lazaris, C., Tsirigos, A., Osman, I., Hernando, E., & Aifantis, I. (2015). FBXW7 modulates cellular stress response and metastatic potential through HSF1 post-translational modification. *Nature cell biology*, *17*(3), 322–332.

Krebs, A. M., Mitschke, J., Lasierra Losada, M., Schmalhofer, O., Boerries, M., Busch, H., Boettcher, M., Mougiakakos, D., Reichardt, W., Bronsert, P., Brunton, V. G., Pilarsky, C., Winkler, T. H., Brabletz, S., Stemmler, M. P., & Brabletz, T. (2017). The EMT-activator Zeb1 is a key factor for cell plasticity and promotes metastasis in pancreatic cancer. *Nature Cell Biology, 19*(5), 518–529.

Kreis, T. E., & Birchmeier, W. (1980). Stress fiber sarcomeres of fibroblasts are contractile. *Cell.* 22(2 Pt 2), 555-561.

Kubiczkova, L., Pour, L., Sedlarikova, L., Hajek, R., & Sevcikova, S. (2014). Proteasome inhibitors - molecular basis and current perspectives in multiple myeloma. *Journal of cellular and molecular medicine*, *18*(6), 947–961.

Lamouille, S., Xu, J., & Derynck, R. (2014). Molecular mechanisms of epithelial-mesenchymal transition. *Nature reviews. Molecular cell biology*, *15*(3), 178–196.

Lampe, P. D., & Lau, A. F. (2004). The effects of connexin phosphorylation on gap junctional communication. *The International Journal of Biochemistry & Cell Biology*, *36*(7), 1171–1186.

Le Breton, L., & Mayer, M. P. (2016). A model for handling cell stress. *eLife*, *5*, e22850.

Lee, J. L., & Streuli, C. H. (2014). Integrins and epithelial cell polarity. *Journal of Cell Science*, *127*(Pt 15), 3217–3225.

Li, J., Chauve, L., Phelps, G., Brielmann, R. M., & Morimoto, R. I. (2016). E2F coregulates an essential HSF developmental program that is distinct from the heat-shock response. *Genes & Development*, *30*(18), 2062–2075.

Li, J., Song, P., Zhu, L., Aziz, N., Zhou, Q., Zhang, Y., Xu, W., Feng, L., Chen, D., Wang, X., & Jin, H. (2017). Synthetic lethality of glutaminolysis inhibition, autophagy inactivation and asparagine depletion in colon cancer. *Oncotarget*, *8*(26), 42664–42672.

Li, J., Wang, J., Yue, H., & Lu, X. (2019). SNAI2 3'untranslated region promotes the invasion of ovarian cancer cells by inducing MARCKS expression. *Journal of Cancer, 10*(11), 2480–2487.

Li, P., Sheng, C., Huang, L., Zhang, H., Huang, L., Cheng, Z., & Zhu, Q. (2014). MiR-183/-96/-182 cluster is up-regulated in most breast cancers and increases cell proliferation and migration. *Breast Cancer Research : BCR*, *16*(6), 473.

Li, S., Ma, W., Fei, T., Lou, Q., Zhang, Y., Cui, X., Qin, X., Zhang, J., Liu, G., Dong, Z., Ma, Y., Song, Z., & Hu, Y. (2014). Upregulation of heat shock factor 1 transcription activity is associated with hepatocellular carcinoma progression. *Molecular Medicine Reports*, *10*(5), 2313–2321.

Li, Y., Xu, D., Bao, C., Zhang, Y., Chen, D., Zhao, F., Ding, J., Liang, L., Wang, Q., Liu, L., Li, J., Yao, M., Huang, S., & He, X. (2015). MicroRNA-135b, a HSF1 target, promotes tumor invasion and metastasis by regulating RECK and EVI5 in hepatocellular carcinoma. *Oncotarget*, *6*(4), 2421–2433.

Li, Z., Lan, X., Han, R., Wang, J., Huang, Y., Sun, J., Guo, W., & Chen, H. (2017). miR-2478 inhibits TGFβ1 expression by targeting the transcriptional activation region downstream of the TGFβ1 promoter in dairy goats. *Scientific Reports, 7*, 42627.

Liao, Y., Xue, Y., Zhang, L., Feng, X., Liu, W., & Zhang, G. (2015). Higher heat shock factor 1 expression in tumor stroma predicts poor prognosis in esophageal squamous cell carcinoma patients. *Journal of Translational Medicine*, *13*, 338.

Liau, S. S., Jazag, A., & Whang, E. E. (2006). HMGA1 is a determinant of cellular invasiveness and in vivo metastatic potential in pancreatic adenocarcinoma. *Cancer Research, 66*(24), 11613-11622.

Lim, J. & Thiery, J. P. (2012). Epithelial–mesenchymal transitions: insights from development. *Development, 139*(19), 3471–3486.

Lindsay, J., McDade, S. S., Pickard, A., McCloskey, K. D., & McCance, D. J. (2011). Role of DeltaNp63gamma in epithelial to mesenchymal transition. *The Journal of Biological Chemistry, 286*(5), 3915–3924.

Liu, C. Y., Lin, H. H., Tang, M. J., & Wang, Y. K. (2015). Vimentin contributes to epithelial-mesenchymal transition cancer cell mechanics by mediating cytoskeletal organization and focal adhesion maturation. *Oncotarget*, *6*(18), 15966–15983.

Liu, D., Sun, L., Qin, X., Liu, T., Zhang, S., Liu, Y., Li, S., & Guo, K. (2016). HSF1 promotes the inhibition of EMT-associated migration by low glucose via directly regulating Snail1 expression in HCC cells. *Discovery Medicine,* 22(120), 87-96.

Liu, J., Ruan, B., You, N., Huang, Q., Liu, W., Dang, Z., Xu, W., Zhou, T., Ji, R., Cao, Y., Li, X., Wang, D., Tao, K., & Dou, K. (2013). Downregulation of miR-200a induces EMT phenotypes and CSC-like signatures through targeting the β-catenin pathway in hepatic oval cells. *PloS one*, *8*(11), e79409.

Liu, P., Wakamiya, M., Shea, M. J., Albrecht, U., Behringer, R. R., & Bradley, A. (1999). Requirement for Wnt3 in vertebrate axis formation. *Nature Genetics, 22*(4), 361–365.

Loh, C. Y., Chai, J. Y., Tang, T. F., Wong, W. F., Sethi, G., Shanmugam, M. K., Chong, P. P., & Looi, C. Y. (2019). The E-Cadherin and N-Cadherin Switch in Epithelial-to-Mesenchymal Transition: Signaling, Therapeutic Implications, and Challenges. *Cells*, *8*(10), 1118.

Loomans, H. A., & Andl, C. D. (2014). Intertwining of Activin A and TGFβ Signaling: Dual Roles in Cancer Progression and Cancer Cell Invasion. *Cancers*, *7*(1), 70–91.

Ma, F., Li, W., Liu, C., Li, W., Yu, H., Lei, B., Ren, Y., Li, Z., Pang, D., & Qian, C. (2017). MiR-23a promotes TGF-β1-induced EMT and tumor metastasis in breast cancer cells by directly targeting CDH1 and activating Wnt/β-catenin signaling. *Oncotarget*, *8*(41), 69538–69550.

Ma, P., Tang, W. G., Hu, J. W., Hao, Y., Xiong, L. K., Wang, M. M., Liu, H., Bo, W. H., & Yu, K. H. (2020). HSP4 triggers epithelial-mesenchymal transition and promotes motility capacities of hepatocellular carcinoma cells via activating AKT. *Liver International,* doi: 10.1111/liv.14410 [Epub ahead of print].

Mahabir, R., Tanino, M., Elmansuri, A., Wang, L., Kimura, T., Itoh, T., Ohba, Y., Nishihara, H., Shirato, H., Tsuda, M., & Tanaka, S. (2014). Sustained elevation of Snail promotes glial-mesenchymal transition after irradiation in malignant glioma. *Neuro-Oncology*, *16*(5), 671–685.

Mahat, D. B., Salamanca, H. H., Duarte, F. M., Danko, C. G., & Lis, J. T. (2016). Mammalian Heat Shock Response and Mechanisms Underlying Its Genome-wide Transcriptional Regulation. *Molecular Cell*, *62*(1), 63–78.

Mahmood, M. Q., Ward, C., Muller, H. K., Sohal, S. S., & Walters, E. H. (2017). Epithelial mesenchymal transition (EMT) and non- small cell lung cancer (NSCLC): a mutual association with airway disease. *Medical Oncology, 34*(3), 45.

Martínez-Alvarez, C., Blanco, M. J., Pérez, R., Rabadán, M. A., Aparicio, M., Resel, E., Martínez, T., & Nieto, M. A. (2004). Snail family members and cell survival in physiological and pathological cleft palates. *Developmental Biology, 265*(1), 207–218.

Massagué J. (2008). TGFbeta in Cancer. *Cell*, *134*(2), 215–230.

Massagué J. (2012). TGFβ signalling in context. *Nature reviews. Molecular cell biology*, *13*(10), 616–630.

Mathew, A., Mathur, S. K., & Morimoto, R. I. (1998). Heat shock response and protein degradation: regulation of HSF2 by the ubiquitin-proteasome pathway. *Molecular and Cellular Biology*, *18*(9), 5091–5098.

Mendillo, M. L., Santagata, S., Koeva, M., Bell, G. W., Hu, R., Tamimi, R. M., Fraenkel, E., Ince, T. A., Whitesell, L., & Lindquist, S. (2012). HSF1 drives a transcriptional program distinct from heat shock to support highly malignant human cancers. *Cell*, *150*(3), 549–562.

Meng, X., Chen, X., Lu, P., Ma, W., Yue, D., Song, L., & Fan, Q. (2017). miR-202 promotes cell apoptosis in esophageal squamous cell carcinoma by targeting HSF2. *Oncology Research, 25*(2), 215-223.

Metcalf, D. (2003). The unsolved enigmas of leukemia inhibitory factor. *Stem Cells, 21*(1), 5-14.

Min, J. N., Huang, L., Zimonjic, D. B., Moskophidis, D., & Mivechi, N. F. (2007). Selective suppression of lymphomas by functional loss of Hsf1 in a p53-deficient mouse model for spontaneous tumors. *Oncogene, 26*(35), 5086-5097.

Mise, N., Savai, R., Yu, H., Schwarz, J., Kaminski, N., & Eickelberg, O. (2012). Zyxin is a transforming growth factor-β (TGF-β)/Smad3 target gene that regulates lung cancer cell motility via integrin α5β1. *The Journal of biological chemistry*, *287*(37), 31393–31405.

Mishra, V. K., Subramaniam, M., Kari, V., Pitel, K. S., Baumgart, S. J., Naylor, R. M., Nagarajan, S., Wegwitz, F., Ellenrieder, V., Hawse, J. R., & Johnsen, S. A. (2017). Krüppel-like Transcription Factor KLF10 Suppresses TGFβ-Induced Epithelial-to-Mesenchymal Transition via a Negative Feedback Mechanism. *Cancer Research, 77*(9), 2387–2400.

Miyoshi, A., Kitajima, Y., Kido, S., Shimonishi, T., Matsuyama, S., Kitahara, K., & Miyazaki, K. (2005). Snail accelerates cancer invasion by upregulating MMP expression and is associated with poor prognosis of hepatocellular carcinoma. *British journal of cancer*, *92*(2), 252–258.

Miyoshi, A., Kitajima, Y., Sumi, K., Sato, K., Hagiwara, A., Koga, Y., & Miyazaki, K. (2004). Snail and SIP1 increase cancer invasion by upregulating MMP family in hepatocellular carcinoma cells. *British journal of cancer*, *90*(6), 1265–1273.

Moses H.L., Yang E.Y., & Pietenpol J.A. (1990). TGF-beta stimulation and inhibition of cell proliferation: new mechanistic insights. *Cell, 63*(2), 245–247.

Muerdter, F., Boryń, Ł. M., Woodfin, A. R., Neumayr, C., Rath, M., Zabidi, M. A., Pagani, M., Haberle, V., Kazmar, T., Catarino, R. R., Schernhuber, K., Arnold, C. D., & Stark, A. (2018). Resolving systematic errors in widely used enhancer activity assays in human cells. *Nature Methods, 15*(2), 141–149.

Mustafa, D. A., Sieuwerts, A. M., Zheng, P. P., & Kros, J. M. (2010). Overexpression of Colligin 2 in Glioma Vasculature is Associated with Overexpression of Heat Shock Factor 2. *Gene regulation and systems biology*, *4*, 103–107.

Na, Y. R., Seok, S. H., Kim, D. J., Han, J. H., Kim, T. H., Jung, H., Lee, B. H., & Park, J. H. (2009). Bone morphogenetic protein 7 induces mesenchymal-to-epithelial transition in melanoma cells, leading to inhibition of metastasis. *Cancer Science, 100*(11), 2218-2225.

Nakai, A., & Morimoto, R. I. (1993). Characterization of a novel chicken heat shock transcription factor, heat shock factor 3, suggests a new regulatory pathway. *Molecular and cellular biology*, *13*(4), 1983–1997.

Nakai, A., Tanabe, M., Kawazoe, Y., Inazawa, J., Morimoto, R. I., & Nagata, K. (1997). HSF4, a new member of the human heat shock factor family which lacks properties of a transcriptional activator. *Molecular and cellular biology*, *17*(1), 469–481.

Natsuizaka, M., Whelan, K. A., Kagawa, S., Tanaka, K., Giroux, V., Chandramouleeswaran, P. M., Long, A., Sahu, V., Darling, D. S., Que, J., Yang, Y., Katz, J. P., Wileyto, E. P., Basu, D., Kita, Y., Natsugoe, S., Naganuma, S., Klein-Szanto, A. J., Diehl, J. A., Bass, A. J., … Nakagawa, H. (2017). Interplay between Notch1 and Notch3 promotes EMT and tumor initiation in squamous cell carcinoma. *Nature communications*, *8*(1), 1758.

Neef, D. W., Jaeger, A. M., & Thiele, D. J. (2011). Heat shock transcription factor 1 as a therapeutic target in neurodegenerative diseases. *Nature reviews. Drug Discovery*, *10*(12), 930–944.

Neumann, E., Schaefer-Ridder, M., Wang, Y., & Hofschneider, P. H. (1982). Gene transfer into mouse lyoma cells by electroporation in high electric fields. *EMBO Journal, 1*(7), 841-845.

Nielsen, D. A., Chou, J., MacKrell, A. J., Casadaban, M. J., & Steiner, D. F. (1983). Expression of a preproinsulin-beta-galactosidase gene fusion in mammalian cells. *Proceedings of the National Academy of Sciences of the United States of America*, *80*(17), 5198–5202.

Nieto, M. A. (2009). Epithelial–mesenchymal transitions in development and disease: old views and new perspectives. *The International Journal of Developmental Biology, 53*(8-10), 1541–1547.

Nieto, M. A., Huang, R. Y., Jackson, R. A., & Thiery, J. P. (2016). EMT: 2016. *Cell, 166*(1), 21–45.

Nishida, N., Yano, H., Nishida, T., Kamura, T., & Kojiro, M. (2006). Angiogenesis in cancer. *Vascular health and risk management*, *2*(3), 213–219.

Ocaña, O. H., Córcoles, R., Fabra, A., Moreno-Bueno, G., Acloque, H., Vega, S., Barrallo-Gimeno, A., Cano, A., & Nieto, M. A. (2012). Metastatic colonization requires the repression of the epithelial–mesenchymal transition inducer Prrx1. *Cancer Cell, 22*(6), 709–724.

Ocejo-Garcia, M., Baokbah, T. A., Ashurst, H. L., Cowlishaw, D., Soomro, I., Coulson, J. M., & Woll, P. J. (2005). Roles for USF-2 in lung cancer proliferation and bronchial carcinogenesis. *The Journal of Pathology, 206*(2), 151-159.

Oda, H., Tsukita, S., & Takeichi, M. (1998). Dynamic behavior of the cadherin- based cell- cell adhesion system during Drosophila gastrulation. *Developmental Biology, 203*(2), 435–450.

Osborne, B. A., & Minter, L. M. (2007). Notch signalling during peripheral T cell activation and differentiation. *Nature Reviews Immunology, 7*(1), 64–75.

Pandey, D. P., & Picard, D. (2009). miR-22 inhibits estrogen signaling by directly targeting the estrogen receptor alpha mRNA. *Molecular and Cellular Ciology, 29*(13), 3783–3790.

Pang, M. F., Georgoudaki, A. M., Lambut, L., Johansson, J., Tabor, V., Hagikura, K., Jin, Y., Jansson, M., Alexander, J. S., Nelson, C. M., Jakobsson, L., Betsholtz, C., Sund, M., Karlsson, M. C., & Fuxe, J. (2016). TGF-β1-induced EMT promotes targeted migration of breast cancer cells through the lymphatic system by the activation of CCR7/CCL21-mediated chemotaxis. *Oncogene*, *35*(6), 748–760.

Park, S. M., Kim, S. A., & Ahn, S. G. (2015). HSF2 autoregulates its own transcription. *International Journal of Molecular Medicine, 36*(4), 1173-1179.

Parker, C. S., & Topol, J. (1984). A Drosophila RNA polymerase II transcription factor contains a promoter-region-specific DNA-binding activity. *Cell, 36*(2), 357-369.

Parvani, J. G., Gujrati, M. D., Mack, M. A., Schiemann, W. P., & Lu, Z. R. (2015). Silencing β3 Integrin by Targeted ECO/siRNA Nanoparticles Inhibits EMT and Metastasis of Triple-Negative Breast Cancer. *Cancer research*, *75*(11), 2316–2325.

Pattabiraman, D. R., Bierie, B., Kober, K. I., Thiru, P., Krall, J. A., Zill, C., Reinhardt, F., Tam, W. L., & Weinberg, R. A. (2016). Activation of PKA leads to mesenchymal-to-epithelial transition and loss of tumor-initiating ability. *Science (New York, N.Y.)*, *351*(6277), aad3680.

Pei, D., Shu, X., Gassama-Diagne, A., & Thiery, J. P. (2019). Mesenchymal-epithelial transition in development and reprogramming. *Nature Cell Biology, 21*(1), 44-53.

Peteranderl, R., Rabenstein, M., Shin, Y. K., Liu, C. W., Wemmer, D. E., King, D. S., & Nelson, H. C. (1999). Biochemical and biophysical characterization of the trimerization domain from the heat shock transcription factor. *Biochemistry, 38*(12), 3559-3569.

Powell, C. D., Paullin, T. R., Aoisa, C., Menzie, C. J., Ubaldini, A., & Westerheide, S. D. (2016). The Heat Shock Transcription Factor HSF1 Induces Ovarian Cancer Epithelial-Mesenchymal Transition in a 3D Spheroid Growth Model. *PloS one*, *11*(12), e0168389.

Powers, M. V., & Workman, P. (2007). Inhibitors of the heat shock response: biology and pharmacology. *FEBS Letters*, *581*(19), 3758-3769.

Prudkin, L., Liu, D. D., Ozburn, N. C., Sun, M., Behrens, C., Tang, X., Brown, K. C., Bekele, B. N., Moran, C., & Wistuba, I. I. (2009). Epithelial-to-mesenchymal transition in the development and progression of adenocarcinoma and squamous cell carcinoma of the lung. *Modern Pathology : an official journal of the United States and Canadian Academy of Pathology, Inc*, *22*(5), 668–678.

Pu, H., Horbinski, C., Hensley, P. J., Matuszak, E. A., Atkinson, T., & Kyprianou, N. (2014). PARP-1 regulates epithelial-mesenchymal transition (EMT) in prostate tumorigenesis. *Carcinogenesis*, *35*(11), 2592–2601.

Rabindran, S., Haroun, R., Clos, J., Wisniewski, J., & Wu, C. (1993). Regulation of heat shock factor trimer formation: role of a conserved leucine zipper. *Science, 259*(5092), 230-234.

Ramachandran, A., Vizán, P., Das, D., Chakravarty, P., Vogt, J., Rogers, K. W., Müller, P., Hinck, A. P., Sapkota, G. P., & Hill, C. S. (2018). TGF-β uses a novel mode of receptor activation to phosphorylate SMAD1/5 and induce epithelial-to-mesenchymal transition. *eLife*, *7*, e31756.

Raychaudhuri, S., Loew, C., Körner, R., Pinkert, S., Theis, M., Hayer-Hartl, M., Buchholz, F., & Hartl, F. U. (2014). Interplay of acetyltransferase EP300 and the proteasome system in regulating heat shock transcription factor 1. *Cell, 156*(5), 975-985.

Rhim, A. D., Mirek, E. T., Aiello, N. M., Maitra, A., Bailey, J. M., McAllister, F., Reichert, M., Beatty, G. L., Rustgi, A. K., Vonderheide, R. H., Leach, S. D., & Stanger, B. Z. (2012). EMT and dissemination precede pancreatic tumor formation. *Cell*, *148*(1-2), 349–361.

Ritossa, F. (1962). A new puffing pattern induced by temperature shock and DNP in Drosophila. *Experentia*, *18*, 571-573.

Romagnoli, M., Belguise, K., Yu, Z., Wang, X., Landesman-Bollag, E., Seldin, D. C., Chalbos, D., Barillé-Nion, S., Jézéquel, P., Seldin, M. L., & Sonenshein, G. E. (2012). Epithelial-to-mesenchymal transition induced by TGF-β1 is mediated by Blimp-1-dependent repression of BMP-5. *Cancer research*, *72*(23), 6268–6278.

Roskamp, K. W., Kozlyuk, N., Sengupta, S., Bierma, J. C., & Martin, R. W. (2019). Divalent cations and the divergence of βγ-crystallin function. *Biochemistry, 58*(45), 4505-4518.

Roth, B., Jayaratna, I., Sundi, D., Cheng, T., Melquist, J., Choi, W., Porten, S., Nitti, G., Navai, N., Wszolek, M., Guo, C., Czerniak, B., McConkey, D., & Dinney, C. (2017). Employing an orthotopic model to study the role of epithelial-mesenchymal transition in bladder cancer metastasis. *Oncotarget*, *8*(21), 34205–34222.

Sahai, E., Astsaturov, I., Cukierman, E., DeNardo, D. G., Egeblad, M., Evans, R. M., Fearon, D., Greten, F. R., Hingorani, S. R., Hunter, T., Hynes, R. O., Jain, R. K., Janowitz, T., Jorgensen, C., Kimmelman, A. C., Kolonin, M. G., Maki, R. G., Powers, R. S., Puré, E., Ramirez, D. C., … Werb, Z. (2020). A framework for advancing our understanding of cancer-associated fibroblasts. *Nature reviews. Cancer*, *20*(3), 174–186.

Salvo, E., Garasa, S., Dotor, J., Morales, X., Peláez, R., Altevogt, P., & Rouzaut, A. (2014). Combined targeting of TGF-β1 and integrin β3 impairs lymph node metastasis in a mouse model of non-small-cell lung cancer. *Molecular cancer*, *13*, 112.

Sánchez-Tilló, E., Lázaro, A., Torrent, R., Cuatrecasas, M., Vaquero, E. C., Castells, A., Engel, P., & Postigo, A. (2010). ZEB1 represses E- cadherin and induces an EMT by recruiting the SWI/SNF chromatin-remodeling protein BRG1. *Oncogene, 29*(24), 3490–3500.

Sandqvist, A., Björk, J. K., Åkerfelt, M., Chitikova, Z., Grichine, A., Vourc'h, C., Jolly, C., Salminen, T. A., Nymalm, Y., & Sistonen, L. (2009). Heterotrimerization of heat-shock factors 1 and 2 provides a transcriptional switch in response to distinct stimuli. *Molecular Biology of the Cell*, *20*(5), 1340–1347.

Sansregret, L., & Swanton, C. (2017). The Role of Aneuploidy in Cancer Evolution. *Cold Spring Harbor perspectives in medicine*, *7*(1), a028373.

Santagata, S., Hu, R., Lin, N. U., Mendillo, M. L., Collins, L. C., Hankinson, S. E., Schnitt, S. J., Whitesell, L., Tamimi, R. M., Lindquist, S., & Ince, T. A. (2011). High levels of nuclear heat-shock factor 1 (HSF1) are associated with poor prognosis in breast cancer. *Proceedings of the National Academy of Sciences of the United States of America*, *108*(45), 18378–18383.

Sarge, K. D., Murphy, S. P., & Morimoto, R. I. (1993). Activation of heat shock gene transcription by heat shock factor 1 involves oligomerization, acquisition of DNA-binding activity, and nuclear localization and can occur in the absence of stress. *Molecular and cellular biology*, *13*(3), 1392–1407.

Sarge, K. D., Park-Sarge, O. K., Kirby, J. D., Mayo, K. E., & Morimoto, R. I. (1994). Expression of heat shock factor 2 in mouse testis: potential role as a regulator of heat-shock protein gene expression during spermatogenesis. *Biology of Reproduction, 50*(6), 1334-1343.

Savagner, P. (2001). Leaving the neighborhood: molecular mechanisms involved during epithelial–mesenchymal transition. *Bioessays, 23*(10), 912–923.

Savagner, P., Kusewitt, D. F., Carver, E. A., Magnino, F., Choi, C., Gridley, T., & Hudson, L. G. (2005). Developmental transcription factor slug is required for effective re-epithelialization by adult keratinocytes. *Journal of Cellular Physiology, 202*(3), 858–866.

Schafer, G., Narasimha, M., Vogelsang, E., & Leptin, M. (2014). Cadherin switching during the formation and differentiation of the Drosophila mesoderm – implications for epithelial- to-mesenchymal transitions. *Journal of Cell Science, 127*(Pt 7), 1511–1522.

Scherz-Shouval, R., Santagata, S., Mendillo, M. L., Sholl, L. M., Ben-Aharon, I., Beck, A. H., Dias-Santagata, D., Koeva, M., Stemmer, S. M., Whitesell, L., & Lindquist, S. (2014). The reprogramming of tumor stroma by HSF1 is a potent enabler of malignancy. *Cell*, *158*(3), 564–578.

Schieber, M. S., & Chandel, N. S. (2013). ROS links glucose metabolism to breast cancer stem cell and EMT phenotype. *Cancer Cell,* 23(3), 265-267.

Schmidt, J. M., Panzilius, E., Bartsch, H. S., Irmler, M., Beckers, J., Kari, V., Linnemann, J. R., Dragoi, D., Hirschi, B., Kloos, U. J., Sass, S., Theis, F., Kahlert, S., Johnsen, S. A., Sotlar, K., & Scheel, C. H. (2015). Stem- cell-like properties and epithelial plasticity arise as stable traits after transient Twist1 activation. *Cell Reports, 10*(2), 131–139.

Schuetz, T. J., Gallo, G. J., Sheldon, L., Tempst, P., & Kingston, R. E. (1991). Isolation of a cDNA for HSF2: evidence for two heat shock factor genes in humans. *Proceedings of the National Academy of Sciences of the United States of America*, *88*(16), 6911–6915.

Schulz, R., Streller, F., Scheel, A. H., Rüschoff, J., Reinert, M. C., Dobbelstein, M., Marchenko, N. D., & Moll, U. M. (2014). HER2/ErbB2 activates HSF1 and thereby controls HSP90 clients including MIF in HER2-overexpressing breast cancer. *Cell death & disease*, *5*(1), e980.

Shah, S. P., Nooka, A. K., Jaye, D. L., Bahlis, N. J., Lonial, S., & Boise, L. H. (2016). Bortezomib-induced heat shock response protects multiple myeloma cells and is activated by heat shock factor 1 serine 326 phosphorylation. *Oncotarget*, *7*(37), 59727–59741.

Shapiro, L., Fannon, A. M., Kwong, P. D., Thompson, A., Lehmann, M. S., Grübel, G., Legrand, J. F., Als-Nielsen, J., Colman, D. R., & Hendrickson, W. A. (1995). Structural basis of cell-cell adhesion by cadherins. *Nature*, *374*(6520), 327–337.

Shi, X., Cui, B., Wang, Z., Weng, L., Xu, Z., Ma, J., Xu, G., Kong, X., & Hu, L. (2009). Removal of Hsf4 leads to cataract development in mice through down-regulation of gamma S-crystallin and Bfsp expression. *BMC molecular biology*, *10*, 10.

Shiota, M., Zardan, A., Takeuchi, A., Kumano, M., Beraldi, E., Naito, S., Zoubeidi, A., & Gleave, M. E. (2012). Clusterin mediates TGF-β-induced epithelialmesenchymal transition and metastasis via Twist1 in prostate cancer cells. *Cancer Research, 72*(20), 5261–5272.

Shoval, I., Ludwig, A., & Kalcheim, C. (2007). Antagonistic roles of full-length N-cadherin and its soluble BMP cleavage product in neural crest delamination. *Development, 134*(3), 491–501.

Shu, L., Zhang, Z., & Cai, Y. (2018). MicroRNA-204 inhibits cell migration and invasion in human cervical cancer by regulating transcription factor 12. *Oncology Letters, 15*(1), 161–166.

Simões-Costa, M., & Bronner, M. E. (2015). Establishing neural crest identity: a gene regulatory recipe. *Development (Cambridge, England)*, *142*(2), 242–257.

Singh, A., & Settleman, J. (2010). EMT, cancer stem cells and drug resistance: an emerging axis of evil in the war on cancer. *Oncogene*, *29*(34), 4741–4751.

Sistonen, L., Sarge, K. D., & Morimoto, R. I. (1994). Human heat shock factors 1 and 2 are differentially activated and can synergistically induce hsp70 gene transcription. *Molecular and Cellular Biology*, *14*(3), 2087–2099.

Somasundaram, T., & Bhat, S. P. (2004). Developmentally dictated expression of heat shock factors: exclusive expression of HSF4 in the postnatal lens and its specific interaction with alphaB-crystallin heat shock promoter. *The Journal of Biological Chemistry, 279*(43), 44497-44503.

Sorger, P. K., & Nelson, H. C. M. (1989). Trimerization of a yeast transcriptional activator via a coiled-coil motif. *Cell, 59*(5), 807-813.

Sorger, P. K., & Pelham, H. R. (1988). Yeast heat shock factor is an essential DNA-binding protein that exhibits temperature-dependent phosphorylation. *Cell, 54*(6), 855-864.

Spaderna, S., Schmalhofer, O., Wahlbuhl, M., Dimmler, A., Bauer, K., Sultan, A., Hlubek, F., Jung, A., Strand, D., Eger, A., Kirchner, T., Behrens, J., & Brabletz, T. (2008). The transcriptional repressor ZEB1 promotes metastasis and loss of cell polarity in cancer. *Cancer Research, 68*(2), 537–544.

Su, J., Zhang, A., Shi, Z., Ma, F., Pu, P., Wang, T., Zhang, J., Kang, C., & Zhang, Q. (2012). MicroRNA-200a suppresses the Wnt/β-catenin signaling pathway by interacting with β-catenin. *International Journal of Oncology, 40*(4), 1162–1170.

Sullivan, E. K., Weirich, C. S., Guyon, J. R., Sif, S., & Kingston, R. E. (2001). Transcriptional activation domains of human heat shock factor 1 recruit human SWI/SNF. *Molecular and cellular biology*, *21*(17), 5826–5837.

Takaki, E., Fujimoto, M., Sugahara, K., Nakahari, T., Yonemura, S., Tanaka, Y., Hayashida, N., Inouye, S., Takemoto, T., Yamashita, H., & Nakai, A. (2006). Maintenance of olfactory neurogenesis requires HSF1, a major heat shock transcription factor in mice. *The Journal of Biological Chemistry*, *281*(8), 4931-4937.

Takii, R., Fujimoto, M., Tan, K., Takaki, E., Hayashida, N., Nakato, R., Shirahige, K., & Nakai, A. (2015). ATF1 modulates the heat shock response by regulating the stress-inducible heat shock factor 1 transcription complex. *Molecular and Cellular Biology*, *35*(1), 11–25.

Tammela, T., Sanchez-Rivera, F. J., Cetinbas, N. M., Wu, K., Joshi, N. S., Helenius, K., Park, Y., Azimi, R., Kerper, N. R., Wesselhoeft, R. A., Gu, X., Schmidt, L., Cornwall-Brady, M., Yilmaz, Ö. H., Xue, W., Katajisto, P., Bhutkar, A., & Jacks, T. (2017). A Wnt-producing niche drives proliferative potential and progression in lung adenocarcinoma. *Nature*, *545*(7654), 355–359.

Tang, Y., Tang, Y., & Cheng, Y. S. (2017). miR-34a inhibits pancreatic cancer progression through Snail1-mediated epithelial-mesenchymal transition and the Notch signaling pathway. *Scientific Reports*, *7*, 38232.

Tateishi, Y., Ariyoshi, M., Igarashi, R., Hara, H., Mizuguchi, K., Seto, A., Nakai, A., Kokubo, T., Tochio, H., & Shirakawa, M. (2009). Molecular basis for SUMOylation-dependent regulation of DNA binding activity of heat shock factor 2. *The Journal of Biological Chemistry, 284*(4), 2435-47.

Tessari, A., Salata, E., Ferlin, A., Bartoloni, L., Slongo, M. L., & Foresta, C. (2004). Characterization of HSFY, a novel AZFb gene on the Y chromosome with a possible role in human spermatogenesis. *Molecular Human Reproduction, 10*(4), 253-258.

Thakur, N., Gudey, S. K., Marcusson, A., Fu, J. Y., Bergh, A., Heldin, C. H., & Landström, M. (2014). TGFβ-induced invasion of prostate cancer cells is promoted by c-Jun-dependent transcriptional activation of Snail1. *Cell cycle (Georgetown, Tex.)*, *13*(15), 2400–2414.

Thiery, J. P., Acloque, H., Huang, R. Y., & Nieto, M. A. (2009). Epithelial–mesenchymal transitions in development and disease. *Cell, 139*(5), 871–890.

Timmerman, L. A., Grego-Bessa, J., Raya, A., Bertrán, E., Pérez-Pomares, J. M., Díez, J., Aranda, S., Palomo, S., McCormick, F., Izpisúa-Belmonte, J. C., & de la Pompa, J. L. (2004). Notch promotes epithelial-mesenchymal transition during cardiac development and oncogenic transformation. *Genes & Development*, *18*(1), 99–115.

Tissiéres, A., Mitchell, H. K., & Tracy, U. M. (1974). Protein synthesis in salivary glands of Drosophila melanogaster: Relation to chromosome puffs. *Journal of Molecular Biology, 84*(3), 389-398.

Trepat, X., Chen, Z., & Jacobson, K. (2012). Cell migration. *Comprehensive Physiology*, *2*(4), 2369–2392.

Tsai, J. H., Donaher, J. L., Murphy, D. A., Chau, S., & Yang, J. (2012). Spatiotemporal regulation of epithelial-mesenchymal transition is essential for squamous cell carcinoma metastasis. *Cancer cell*, *22*(6), 725–736.

Tsukao, Y., Yamasaki, M., Miyazaki, Y., Makino, T., Takahashi, T., Kurokawa, Y., Miyata, H., Nakajima, K., Takiguchi, S., Mimori, K., Mori, M., & Doki, Y. (2017). Overexpression of heat-shock factor 1 is associated with a poor prognosis in esophageal squamous cell carcinoma. *Oncology Letters*, *13*(3), 1819–1825.

Uchida, S., Hara, K., Kobayashi, A., Fujimoto, M., Otsuki, K., Yamagata, H., Hobara, T., Abe, N., Higuchi, F., Shibata, T., Hasegawa, S., Kida, S., Nakai, A., & Watanabe, Y. (2011). Impaired hippocampal spinogenesis and neurogenesis and altered affective behavior in mice lacking heat shock factor 1. *Proceedings of the National Academy of Sciences of the United States of America*, *108*(4), 1681–1686.

van Bokhoven, A., Varella-Garcia, M., Korch, C., Johannes, W.U., Smith, E. E., Miller, H. L., Nordeen, S. K., Miller, G. J., & Lucia, M. S. (2003). Molecular characterization of human prostate carcinoma cell lines. *Prostate, 57*(3), 205-225.

Verma, R. P., & Hansch, C. (2007). Matrix metalloproteinases (MMPs): chemical-biological functions and (Q)SARs. *Bioorganic and Medicinal Chemistry, 15*(6), 2223-2268.

Vihervaara, A., Sergelius, C., Vasara, J., Blom, M. A., Elsing, A. N., Roos-Mattjus, P., & Sistonen, L. (2013). Transcriptional response to stress in the dynamic chromatin environment of cycling and mitotic cells. *Proceedings of the National Academy of Sciences of the United States of America*, *110*(36), E3388–E3397.

Vivinus, S., Baulande, S., van Zanten, M., Campbell, F., Topley, P., Ellis, J. H., Dessen, P., & Coste, H. (2001). An element within the 5' untranslated region of human Hsp70 mRNA which acts as a general enhancer of mRNA translation. *European Journal of Biochemistry, 268*(7):1908-17.

Vogelstein, B., Fearon, E. R., Kern, S. E., Hamilton, S. R., Preisinger, A. C., Nakamura, Y., White, R. (1989). Allelotype of colorectal carcinomas. *Science, 244*(4901), 207–211.

Vuister, G. W., Kim, S. J., Orosz, A., Marquardt, J., Wu, C., & Bax, A. (1994). Solution structure of the DNA-binding domain of Drosophila heat shock transcription factor. *Nature Structural Biology, 1*(9), 605-14.

Vydra, N., Janus, P., Toma-Jonik, A., Stokowy, T., Mrowiec, K., Korfanty, J., Długajczyk, A., Wojtaś, B., Gielniewski, B., & Widłak, W. (2019). 17*β*-Estradiol Activates HSF1 via MAPK Signaling in ER*α*-Positive Breast Cancer Cells. *Cancers*, *11*(10), 1533.

Wang, G., Ying, Z., Jin, X., Tu, N., Zhang, Y., Phillips, M., Moskophidis, D., & Mivechi, N. F. (2004). Essential requirement for both hsf1 and hsf2 transcriptional activity in spermatogenesis and male fertility. *Genesis, 38*(2), 66-80.

Wang, M., Ren, D., Guo, W., Huang, S., Wang, Z., Li, Q., Du, H., Song, L., & Peng, X. (2016). N-cadherin promotes epithelial-mesenchymal transition and cancer stem cell-like traits via ErbB signaling in prostate cancer cells. *International Journal of Oncology, 48*(2), 595–606.

Wang, Y., Theriault, J. R., He, H., Gong, J., & Calderwood, S. K. (2004). Expression of a dominant negative heat shock factor-1 construct inhibits aneuploidy in prostate carcinoma cells. *Journal of Biological Chemistry*, *279*(31), 32651-32659.

Ware, K. E., Gilja, S., Xu, S., Shetler, S., Jolly, M. K., Wang, X., Bartholf Dewitt, S., Hish, A. J., Jordan, S., Eward, W., Levine, H., Armstrong, A. J., & Somarelli, J. A. (2017). Induction of Mesenchymal-Epithelial Transitions in Sarcoma Cells. *Journal of visualized experiments : JoVE*, (122), 55520.

Watanabe, K., Liu, Y., Noguchi, S., Murray, M., Chang, J. C., Kishima, M., Nishimura, H., Hashimoto, K., Minoda, A., & Suzuki, H. (2019). OVOL2 induces mesenchymal-to-epithelial transition in fibroblasts and enhances cell-state reprogramming towards epithelial lineages. *Scientific Reports*, *9*(1), 6490.

Westerheide, S. D., Anckar, J., Stevens, S. M., Jr, Sistonen, L., & Morimoto, R. I. (2009). Stress-inducible regulation of heat shock factor 1 by the deacetylase SIRT1. *Science (New York, N.Y.)*, *323*(5917), 1063–1066.

Whitesell, L., & Lindquist, S. L. (2005). HSP90 and the chaperoning of cancer. *Nature Reviews Cancer, 5*(10), 761-772.

Wongfieng, W., Jumnainsong, A., Chamgramol, Y., Sripa, B., & Leelayuwat, C. (2017). 5'-UTR and 3'-UTR Regulation of MICB Expression in Human Cancer Cells by Novel microRNAs. *Genes*, *8*(9), 213.

Xi, C., Hu, Y., Buckhaults, P., Moskophidis, D., & Mivechi, N. F. (2012). Heat shock factor Hsf1 cooperates with ErbB2 (Her2/Neu) protein to promote mammary tumorigenesis and metastasis. *The Journal of biological chemistry*, *287*(42), 35646–35657.

Xiao, X., Zuo, X., Davis, A. A., McMillan, D. R., Curry, B. B., Richardson, J. A., & Benjamin, I. J. (1999). HSF1 is required for extra-embryonic development, postnatal growth and protection during inflammatory responses in mice. *The EMBO journal*, *18*(21), 5943–5952.

Xu, J., Lamouille, S., & Derynck, R. (2009). TGF-beta-induced epithelial to mesenchymal transition. *Cell Research*, *19*(2), 156–172.

Yan, X., Yan, L., Liu, S., Shan, Z., Tian, Y., & Jin, Z. (2015). N-Cadherin, a novel prognostic biomarker, drives malignant progression of colorectal cancer. *Molecular Medicine Reports, 12*(2), 2999–3006 (2015).

Yan, Y., Wang, Q., Yan, X. L., Zhang, Y., Li, W., Tang, F., Li, X., & Yang, P. (2015). miR-10a controls glioma migration and invasion through regulating epithelial-mesenchymal transition via EphA8. *FEBS Letters, 589*(6), 756-765.

Yang, L. N., Ning, Z. Y., Wang, L., Yan, X., & Meng, Z. Q. (2019). HSF2 regulates aerobic glycolysis by suppression of FBP1 in hepatocellular carcinoma. *American journal of cancer research*, *9*(8), 1607–1621.

Yang, Y., Jin, L., Zhang, J., Wang, J., Zhao, X., Wu, G., Yao, H., & Zhang, Z. (2017). High HSF4 expression is an independent indicator of poor overall survival and recurrence free survival in patients with primary colorectal cancer. *IUBMB Life, 69*(12), 956-961.

Yang, Y., Zhou, Y., Xiong, X., Huang, M., Ying, X., & Wang, M. (2018). ALG3 Is Activated by Heat Shock Factor 2 and Promotes Breast Cancer Growth. Medical science monitor : international medical journal of experimental and clinical research, 24, 3479–3487. https://doi.org/10.12659/MSM.907461

Yarden, Y., & Pines, G. (2012). The ERBB network: at last, cancer therapy meets systems biology. *Nature Reviews Cancer, 12*(8), 553-563.

Yasuda, K., Hirohashi, Y., Mariya, T., Murai, A., Tabuchi, Y., Kuroda, T., Kusumoto, H., Takaya, A., Yamamoto, E., Kubo, T., Nakatsugawa, M., Kanaseki, T., Tsukahara, T., Tamura, Y., Hirano, H., Hasegawa, T., Saito, T., Sato, N., & Torigoe, T. (2017). Phosphorylation of HSF1 at serine 326 residue is related to the maintenance of gynecologic cancer stem cells through expression of HSP27. *Oncotarget*, *8*(19), 31540–31553.

Ye, X., Tam, W. L., Shibue, T., Kaygusuz, Y., Reinhardt, F., Ng Eaton, E., & Weinberg, R. A. (2015). Distinct EMT programs control normal mammary stem cells and tumour-initiating cells. *Nature*, *525*(7568), 256–260.

Yuan, X., Wu, H., Han, N., Xu, H., Chu, Q., Yu, S., Chen, Y., & Wu, K. (2014). Notch signaling and EMT in non-small cell lung cancer: biological significance and therapeutic application. *Journal of Hematology & Oncology*, *7*, 87.

Zavadil, J., Cermak, L., Soto-Nieves, N., & Böttinger, E. P. (2004). Integration of TGF-beta/Smad and Jagged1/Notch signalling in epithelial-to-mesenchymal transition. *The EMBO journal*, *23*(5), 1155–1165.

Zeisberg, M., Shah, A. A., & Kalluri, R. (2005). Bone morphogenic protein-7 induces mesenchymal to epithelial transition in adult renal fibroblasts and facilitates regeneration of injured kidney. *The Journal of Bioogical Chemistry, 280*(9), 8094-8100.

Zelin, E., & Freeman, B. C. (2015). Lysine deacetylases regulate the heat shock response including the age-associated impairment of HSF1. *Journal of Molecular Biology*, *427*(7), 1644–1654.

Zhang, J. Q., Chen, S., Gu, J. N., Zhu, Y., Zhan, Q., Cheng, D. F., Chen, H., Deng, X. X., Shen, B. Y., & Peng, C. H. (2018). MicroRNA-300 promotes apoptosis and inhibits proliferation, migration, invasion and epithelial- mesenchymal transition via the Wnt/beta- catenin signaling pathway by targeting CUL4B in pancreatic cancer cells. *The Journal of Cellular Biochemistry, 119(*1), 1027–1040.

Zhao, Y., Liu, H., Liu, Z., Ding, Y., Ledoux, S. P., Wilson, G. L., Voellmy, R., Lin, Y., Lin, W., Nahta, R., Liu, B., Fodstad, O., Chen, J., Wu, Y., Price, J. E., & Tan, M. (2011). Overcoming trastuzumab resistance in breast cancer by targeting dysregulated glucose metabolism. *Cancer Research, 71*(13), 4585–4597.

Zhong, Y. H., Cheng, H. Z., Peng, H., Tang, S. C., & Wang, P. (2016). Heat shock factor 2 is associated with the occurrence of lung cancer by enhancing the expression of heat shock proteins. *Oncology letters*, *12*(6), 5106–5112.

Zhou, Z. J., Dai, Z., Zhou, S. L., Hu, Z. Q., Chen, Q., Zhao, Y. M., Shi, Y. H., Gao, Q., Wu, W. Z., Qiu, S. J., Zhou, J., & Fan, J. (2014). HNRNPAB induces epithelial- mesenchymal transition and promotes metastasis of hepatocellular carcinoma by transcriptionally activating SNAIL. *Cancer Research, 74*(10), 2750–2762.

Åkerfelt, M., Morimoto, R. I., & Sistonen, L. (2010). Heat shock factors: integrators of cell stress, development and lifespan. *Nature reviews. Molecular cell biology*, *11*(8), 545–555.

Åkerfelt, M., Trouillet, D., Mezger, V., & Sistonen L. (2007). Heat shock factors at a crossroad between stress and development. *Annals of the New York Academy of Sciences, 1113*, 15-27.

Supplementary 1

Recipe Attachment

3x Laemmlie Lysis Buffer

30%	Glycerol
187.5 mM	SDS
3%	Tris-HCl (pH 6.8)
0.015%	Bromophenol blue
3%	β-mercaptoethanol

ONPG Buffer

4 mg/ml	ONPG stock
1x	100x Mg^{+} buffer
0.1 M	Sodium phosphate buffer

10x SDS-PAGE Running Buffer

247.6 mM	Tris-Base
1.92 M	Glycine
0.1%	SDS

→ SDS added before use

5x Transfer Buffer

300.3 mM	Tris-Base
243.9 mM	Glycine
20%	Methanol

→ Methanol added before use

2x SDS-PAGE Gels

Lower gel (8%)	**Upper gel (4%)**	
3 ml	-	1.5 M Tris-Base (pH 8.8)
-	1.25 ml	0.5 M Tris-Base (pH 6.8)
0.06 ml	0.025 ml	20% SDS
3.2 ml	0.75 ml	30% Acrylamide/bis-acrylamide
5.8 ml	3 ml	MQ-H_2O
0.06 ml	0.02 ml	10% APS
0.006 ml	0.01 ml	TEMED

→ APS and TEMED added last

1x Agarose Gel (1%)

0.4 g	Agarose
40 ml	1x TBE
2 µl	Midori Green

10x TBE

108 g	Tris-Base
55 g	Boric acid
40 ml	EDTA (pH 8.0)